Biochemical and molecular characterization of nitrogen stress mediated lipid accumulation in *Scenedesmus quadricauda* CASA CC202

**Thesis submitted to AcSIR for the Award of
the Degree of
DOCTOR OF PHILOSOPHY
in Biological Sciences**

By

**SUJITHA B S
Reg. No: 10BB14A39008**

Under the guidance of

Dr. M. ARUMUGAM

**Microbial Processes and Technology Division
National Institute for Interdisciplinary Science and Technology
(Council of Scientific and Industrial Research)
Industrial Estate P.O., Thiruvananthapuram-695 019, Kerala, INDIA**

December 2019

Thiruvananthapuram

30-12-2019

Declaration

I **Sujitha B S** (AcSIR Registration No. 10BB14A39008) hereby declare that the work presented in this thesis entitled **"Biochemical and molecular characterization of nitrogen stress mediated lipid accumulation in *Scenedesmus quadricauda* CASA CC202"** is a bonafied record of the research work carried out by me under the guidance of and supervision of Dr. M. Arumugam at the CSIR- National Institute for Interdisciplinary Science and Technology, Thiruvananthapuram, Kerala, India. I also declare that all relevant suggestions made by the audience during the Pre-synopsis presentation and those recommended by the Doctoral Advisory Committee have been incorporated in the thesis. I also declare that the work incorporated in this thesis or any part of it has not been submitted for the award of any other degree, diploma, associateship or any other title or recognition.

Sujitha B S

(PhD Scholar)

Declaration

I hereby declare that the work presented in this thesis entitled **"Biochemical and molecular characterization of nitrogen stress mediated lipid accumulation in *Scenedesmus quadricauda* CASA CC202"** is a bonafied record of the research work carried out by my student **Ms. Sujitha B S** (AcSIR Registration No. 10BB14A39008), under my guidance and supervision, at the CSIR- National Institute for Interdisciplinary Science and Technology, Thiruvananthapuram, Kerala, India. I also declare that all suggestions made by the audience during the Pre-synopsis presentation and those recommended by the Doctoral Advisory Committee have been incorporated in the thesis. The work incorporated in this thesis or any part of it has not been submitted for the award of any other degree, diploma, associateship or any other title or recognition.

31/DEC/2019

Dr. M. Arumugam
Thesis Supervisor

Thiruvananthapuram
30 December 2019

National Institute for Interdisciplinary Science and Technology (NIIST)

Council of Scientific & Industrial Research (CSIR)
(Department of Scientific & Industrial Research, Ministry of S&T, Govt. of India)
Industrial Estate P.O., Trivandrum - 695 019
Kerala, INDIA

Dr. Muthu Arumugam, *PhD (IISc)*
Senior Scientist and Assistant Professor (AcSIR)
Microbial Processes and Technology Division

Tel:+91-471-2515 424
Fax:+91-471-24 91 712
Mobile:+91-9562026677
E-mail: *arumugam@niist.res.in*;
aasaimugam@gmail.com

30Dec, 2019

CERTIFICATE

This is to certify that the work incorporated in this Ph. D. thesis entitled **"Biochemical and molecular characterization of nitrogen stress mediated lipid accumulation in *Scenedesmus quadricauda* CASA CC202"** submitted by Ms. Sujitha B S to Academy of Scientific and Innovative Research (AcSIR) in fulfilment of the requirements for the award of the Degree of Doctor of Philosophy In Biological Sciences, embodies original research work under my guidance. We further certify that this work has not been submitted to any other University or Institution in part or full for the award of any degree or diploma. Research material obtained from other sources has been duly acknowledged in the thesis. Any text, illustration, table etc., used in the thesis from other sources, have been duly cited and acknowledged.

Sujitha B S
(PhD Scholar)

Dr. M. Arumugam
(Thesis Supervisor)

Thiruvananthapuram
30 December 2019

Dedicated to

My parents and Teachers

Acknowledgements

<div align="right">Sujitha B S</div>

Contents

List of Abbreviations

ABA	Abscisic acid
ATP	Adenosine Tri Phosphate
BBM	Bold Basal Medium
BLAST	Basic Local Alignment Search Tool
C/N	Carbon/ Nitrogen
cDNA	Complementary DNA
CDS	Coding Sequence
CEST	Chloroplast Protein Enhancing Stress Tolerance
Cob	Cytochrome b
COX	Cytochrome c Oxidase
CRS	Chloroplast Retrograde Signaling
DHA	Docosa Hexanoic Acid
DMSO	Dimethyl Sulphoxide
DNA	Deoxy Nucleic Acid
EDTA	Ethylene Diamine Tetra Acetic acid
ELISA	Enzyme Linked Immuno Sorbent Assay
EPA	Eicosa Pentanoic Acid
ESI	Electron Spray Ionization
FAME	Fatty Acid Methyl Ester
FITC	Fluorescein Isothiocyanate
GABA	Gamma Amino Butyric Acid
GC	Gas Chromatography
GTP	Guanosine Tri phosphate
H_2O_2	Hydrogen peroxide
HE	Homing Endonuclease
HRP	Horse Radish Peroxidase
IEA	International Energy Agency
IEF	Iso Electric Focussing
IPTG	Isopropyl β-D-1-thiogalactopyranoside
L/B ratio	Length/ Breadth ratio
LB	Luria Bertani
LCMS	Liquid Chromatography Mass Spectrometry
LDs	Lipid Droplets
LHE	LAGLIDADG Homing Endonuclease
MALDI -TOF	Matrix Assisted Laser Desorption /Ionization- Time of Flight
MDA	Malondialdehyde
MDM	Mitochondrial Dysfunction Motif
MLDP	Major Lipid Droplet Protein
mRNA	Messenger RNA
MRS	Mitochondrial Retrograde Signaling
MUFA	Monounsaturated fatty acid
MUSCLE	MUltiple Sequence Comparison by Log Expectation
N	Nitrogen
N^-	Nitrogen starved
NAD	Nicotinamide Adenine Dinucleotide
NADP	Nicotinamide Adenine Dinucleotide Phosphate
NADPH	Nicotinamide Adenine Dinucleotide Phosphate hydrogen

nBLAST	Nucleotide Basic Local Alignment Search Tool
NCBI	National Centre for Biotechnology and Information
NRR1	Nitrogen Response Regulator 1
$O_2^{\cdot-}$	Superoxide anion
OH^-	Hydroxyl ion
OPEC	Organization of Petroleum Exporting Countries
ORF	Open Reading Frame
PBS	Phosphate Buffer Saline
PDB	Protein Data Bank
PEG	Poly Ethylene Glycol
PIR	Protein Information Resources
PMF	Peptide Mass Fingerprinting
PMSF	Phenyl methyl sulfonyl fluoride
PUFA	Polyunsaturated fatty acid
RACK1	Receptor for Activated C Kinase 1
RBCL	Ribulose bis phosphate carboxylase
RCF	Rotation per centrifugal force
Rh123	Rhodamine 123
RNA	Ribosomal Nucleic Acid
ROS	Reactive Oxygen Species
RPL 23	Ribosomal Protein L23
rRNA	Ribosomal RNA
RT-PCR	Real Time Polymerase Chain Reaction
SAP	Stress Associated Protein
SDS PAGE	Sodium Dodecyl Sulphate Poly Acrylamide Gel Electrophoresis
SFA	Saturated fatty acid
SOD	Superoxide Dismutase
SQDG	Sulfoquinovosyl Diacyl glycerol
TAG	Tri Acyl Glycerol
TBA	Thio Barbituric Acid
TCA	Tri Chloro Acetic acid
TCA cycle	Tri Carboxylic Acid cycle
TEM	Transmission Electron Microscope
TFs	Transcription Factors
TRN	Transcriptional Regulatory Network
tRNA	Transfer RNA
2D PAGE	Two Dimensional Poly Acrylamide Gel Electrophoresis
$\Delta\psi_m$	Mitochondrial membrane Potential

List of Schemes

List of Tables

List of Figures

Synopsis

AcSIR	**Synopsis to be submitted to the Academy of Scientific and Innovative Research (AcSIR) for award of the degree of doctor of philosophy in Biological science.**
Name of the Candidate	Sujitha B. S.
Registration No.	10BB14A39008
Faculty	Biological Sciences
Laboratory	CSIR-National Institute for Interdisciplinary Science and Technology Thiruvananthapuram
Title of the thesis	"Biochemical and molecular characterization of nitrogen stress mediated lipid accumulation in *Scenedesmus quadricauda CASA CC202*"
Supervisor	Dr. M. Arumugam

Chapter.1: Introduction

Microalgae are unicellular photosynthetic autotrophs located in fresh and marine water bodies. They are gaining important attention globally as they are promising feed stock for third generation biofuel because of faster growth rate, short generation time, adaptive in harsh environmental conditions, do not compete for inputs required for agriculture or arable land. Several micro algal species which specifically produces essential polyunsaturated fatty acids, pigments like astaxanthin, carotenoid etc. and lipids in the form of triacylglycerol (TAG). *Scenedesmus quadricauda* is an oleaginous microalga which accumulates 18 percent of dry cell weight as lipid content. The lipid content can be enhanced by several strategies like nutrient deprivation (nitrogen, phosphorous, sulphur, iron, and heavy metals), altered pH, salinity, temperature etc. Nitrogen starvation is a practically feasible method, as it can be practiced in large scale cultivation. Also, nitrogen being an integral part of amino acid, limiting nitrogen will leads to rearrangement of the metabolism and many other molecular changes which leads to accumulation of neutral lipid (TAG) as energy reserve.

Rationale of the study

Scenedesmus quadricauda CASA CC202 tends to accumulate 2.27 fold lipid during nitrogen starvation (Anand and Arumugam, 2014). The experimental evidence showed that there is concomitant increase in lipid with decrease in protein and chlorophyll content. Biomass yield was also drastically reduced during the nitrogen stress induction. Here the cause is nitrogen stress and the effect is increased TAG accumulation with reduced biomass. The biochemical/metabolic and molecular changes which lead to increased lipid accumulation with reduced biomass in *Scenedesmus quadricauda* is obscure. And thus understanding the above phenomena in oleaginous microalgae forms

the rational of the present study which is outlined in four data chapters as described under. In order to understand such complex biological phenomena an integrated approach to analyze the biological events are required.

Chapter.2 deals with the morphological, biochemical and metabolic changes during nitrogen stress mediated lipid accumulation. The nitrogen stress induces ROS which leads to lipid accumulation and lipid droplet maturation; here the major protein involved in maturation is Major Lipid Droplet Protein (MLDP). It was visualized using MLDP specific antibody through immuno staining. The cell size enlarged by the accumulation The predominant ROS generated was H_2O_2, OH^-, $O_2^{.-}$ and in order to suppress the ROS antioxidant scavenging enzymes like peroxidase and catalase were quantified. The results showed that the inverse correlation between $O_2^{.-}$ and H_2O_2, also the OH^- and lipid peroxidation in terms of Malondialdehyde. The Metabolic changes mainly associated with the liberation of low molecular weight bio molecules and their levels during abiotic stress condition. The integrated targeted metabolic analysis was characterized by LC-MS analysis and the results showed stress related non proteinogenic amino acids and energy equivalents elevated during nitrogen starvation.

Chapter.3 describes about the molecular changes during nitrogen starvation. In order to study the proteins which are involved in nitrogen starvation mediated lipid accumulation. Total proteins were extracted from nitrogen sufficient (N+) and deficient (N-) *S. quadricauda*. SDS PAGE of N+ and N- revealed that there is difference in the protein profiling and further detailed protein pattern were obtained from 2 Dimensional PAGE. Ten differentially expressed protein (Nitrogen stress associated proteins –SAPs) spots were mapped and consistent four protein spot were subjected for MALDI-TOF MS analysis. The stress associated proteins (SAP 1-4) were identified as mitochondrial orf 151, ribosomal protein L23, envelope membrane protein (Chloroplast) and ATP synthase β-subunit of *Acutodesmus* (*Scenedesmus*) *obliquus* respectively. SAP 2 ie., ribosomal protein L23 was confirmed at gene level. Further, the differential expression quantification by RT PCR showed about 2.6 fold up regulation in nitrogen stressed *S. quadricauda* at 6h of incubation.

Chapter.4 followed the mapping of stress associated protein- LAGLIDADG homing endonuclease (SAP1). Here the SAP1 amplification was failed due to the sequence divergence between *S. obliquus* and *S.quadricauda*. In order to confirm that whole mitochondrial genome sequencing of *S. quadricauda* was done by Illumia NextSeq500 Paired-end sequencing. The phylogenetic tree showed divergence in sequence between *S. obliquus* and *S. quadricauda* even though they were in the same clade. The annotated 19 proteins were analyzed for the conserved domain search. Finally the ORF 42 of *S.quadricauda* is having the similar conserved motif as LAGLIDADG as in orf 151 of *S. obliquus*. This ORF 42 was confirmed as LAGLIDADG Homing endonuclease (LHE) at gene level. LHE was differentially expressed about 4.2 fold during 48 hour of nitrogen stress induction. Further the secondary protein structure was predicted by Swiss model and validated by Ramachandran plot. LHE of *S. quadricauda* act as a

homodimer and perform its endonuclease action. Thus the DNA binding residues of LHE was predicted by Predict protein software.

Chapter.5 addresses the sustaining of biomass yield by supplement Stress responsive hormone Abscisic acid (ABA). The demerit of nitrogen starvation was drastic biomass reduction with increased lipid accumulation. In order to prove that endogenous ABA level shoots up during nitrogen starvation it was quantified by competitive ELISA kit. The ABA level during nitrogen stress was found to be increased 4.1 fold than the control in 24 hour of incubation. If we exogenously supplement ABA, it will rescue the microalgae and there by sustaining the biomass yield during nitrogen starvation. For that we added 1-5µM concentration of ABA to the nitrogen stress induced *S. quadricauda*. The effect of ABA on growth showed that 2 µM ABA promotes growth and eventually the increased the biomass. The total lipid yield and photosynthetic pigment content were not increased by supplementing ABA. The fatty acid composition has altered by the supplementation of ABA as it prefers more conversion of saturated fatty acid from the poly unsaturated fatty acids (11.16%).

CHAPTER

1

Introduction and Review of literature

1.1. Introduction

Microalgal biomass is considered the most promising venue for food, feed and energy applications due to higher growth rate, short generation time, adaptability to environmental harsh conditions; do not compete with agricultural inputs and cultivability in non arable land. In order to meet energy requirements, oleaginous microalgae (oil-producing) are specifically cultivated in biofuel industry as they store lipids as triacylglycerol (TAG) under environmental harsh conditions. They produce lipid, starch, proteins, carotenoids as storage reserves during unfavourable conditions such as abiotic stress, pathogen attack etc. (Lim et al., 2012). Several stress conditions influence lipid accumulation in microalgae, which includes nutrient starvation, salinity, illumination and pH. Large amounts of Triacyl glycerol (TAG) synthesis is accompanied by considerable changes in lipid and fatty acid composition. This is mainly due to the different chemical or physical environmental stimuli under stress conditions (Hu *et al*., 2008).

Environmental harsh conditions; particularly nutrient deprivation of Nitrogen, Sulphur, Phosphorous, Iron, Silicon etc. was adapted to enhance the TAG production (Guarnieri et al., 2011; Cakmak et al., 2012). The TAG accumulation in microalgae is highly influenced by type and availability of nutrients. Also nutrient availability has a significant impact on growth, lipid and fatty acid composition of microalgae. Nitrogen being major nutrients, consumed first during microalgal growth and thus it becomes most important growth-limiting factor (Rodolfi et al., 2009; Dong et al., 2013; Blaby et al., 2013; Liu and Benning, 2013; Schmollinger et al., 2014). Under nitrogen starvation, cell division stops at the same time TAG accumulation increases which leads to the enlargeme'nt of cells. As a result TAG content in microalgal cells could increase twice and more. The maximum TAG accumulation is stimulated by the presence of organic carbon source while shifting C/N ratio toward carbon under nitrogen depleted condition. Also nitrogen starvation leads to reduction in protein content of the microalgal cells and increase in neutral lipid content (Msanna *et al*., 2012). Several researchers have reported that during nitrogen starvation the metabolic responses are considerably faster and that leads to increased accumulation of TAG within early hours of nitrogen stress induction than other stresses. As nitrogen is an

essential element, it plays an active role in the synthesis of protein, nucleic acids and chlorophyll synthesis (Goncalves et al., 2013, 2016).

The metabolic changes in nitrogen deficient algae are associated with the stress response and redirection of carbon to energy reserve as starch or lipid (Wase et al., 2014). The major changes include; termination of protein synthesis, degradation of chlorophylls and reduction in chloroplast membrane lipids (Wase et al., 2014; Allen et al., 2015). Several studies on TAG accumulation under nitrogen starvation implies three possible reasons (i) increased TAG biosynthesis from acyl-CoA, (ii) membrane lipid disintegration into free acyl moieties and finally TAG accumulation and (iii) elevated carbon flux towards glycerol-3-phosphate and acyl-CoA for synthesis of fatty acids (Goncalves *et al*., 2013; Fan *et al*., 2011, 2012; Miller *et al*., 2010). However, in algae the TAG synthesis may play a major role in the abiotic stress response, in addition to functioning as carbon and energy storage under environmental stress conditions (Hu et al., 2008). As already discussed the nitrogen starvation leads to increased TAG accumulation with a drastic reduction in biomass in microalgae. Here the cause is nitrogen stress and the effect is TAG accumulation and reduced biomass. Thus we are trying to address the stress responsive factors which are over expressed during nitrogen starvation by proteomic and metabolic perspectives.

Guarnieri et al, 2011 and Gao et al., 2013 had worked on the identification of the major triggering factor for the neutral lipid accumulation under nitrogen starvation. The shreds of evidences mainly points to the genes in fatty acid biosynthetic pathways, photosynthetic system and carbon metabolic pathways. But the real factor responsible for the activation of these lipid synthetic genes was not addressed. The stress responsive genes may be activating the genes of lipidomic, carbon and other metabolic pathways to neutral lipid accumulation. Clearly, this area is not explored well. Therefore it needs to be addressed in a global perspective. The monogenic approach will not lead a clear understanding of the reason for neutral lipid accumulation in microalgae during nitrogen starvation. The effective answers for the query covers different omics approaches like transcriptomics, proteomics, lipidomics and metabolomics which explains the key regulators and proteins involved in pile up of TAG under nitrogen starvation (Blaby et al., 2013; Boyle et al., 2012; Gargouri et al., 2015; Guarnieri et al., 2011; Miller et al., 2010; Park et al., 2015). The

transcription factor Nitrogen-responsive regulator-1 (NRR1), which has a crucial role in neutral lipid accumulation under nitrogen starvation because it is a putative transcriptional regulator that has a regulatory role with the expression of acyltransferase DGTT1 and the ammonium transporter AMT1D during nitrogen starvation in *Chlamydomonas*. In addition to that, the NRR1expression was specifically evidenced during nitrogen starvation, not in other stresses (Boyle et al., 2012).

When microalgae are exposed to nutrient deprivation like Nitrogen starvation, primarily the cell recognizes the stress condition and that is known as the stress response. The stress signalling molecules like Reactive Oxygen species (ROS), Ca^{2+}, Melatonin, Abscisic acid etc helps the cell to sense the unfavourable environment and will in turn activate signal transduction cascades to initiate a series of counter reactions which will lead to the phase of resistance or tolerance of the stressed cell. The major stress responses involve the induction of transcription factors, synthesis of signalling molecules and stress-responsive hormones etc. Nitrogen starvation in *Tetraselmis suecica* transcript analysis revealed an up-regulation of the transcript in signal transduction, stress and antioxidant responses and solute transport and a down-regulation of transcripts involved in photosynthesis, degradation of sugars and amino acid synthesis (Lauritano et al., 2019). ROS which are formed by redox reactions of the reactive forms of molecular Oxygen including H_2O_2, O_2^- or OH^- radicals during abiotic stress are recognized as signals to activate the defence response (Vranova et al., 2002) and also as a second messenger to activate several signalling cascades (Shi et al., 2017). The increased ROS accumulation during prolonged nitrogen starvation leads to oxidative damage and eventually promotes neutral lipid accumulation in *Dunaliella salina*. An increase in both ROS production and lipid peroxidation were observed under nitrogen starvation in association with increased lipid accumulation (Yilancioglu et al., 2014). Thus ROS have direct effects on neutral lipid accumulation in microalgae under nitrogen starvation.

Ca^{2+} is an intracellular second messenger and ubiquitous in nature. Its level rises rapidly and transiently in the cytoplasm and activates Ca^{2+} mediated signal transduction pathways. During Nitrogen starvation in *Chlorella sp.* C2 evidenced that the Ca^{2+} molecules were flooded into the cell through the Ca^{2+} channels, which was

activated by the nitrogen starvation. Also in order to confirm the increased Ca^{2+} channel activity induced neutral lipid accumulation they pre-treated the channels by blockers and determined the neutral lipid accumulation. The results showed that a decreased neutral lipid synthesis in nitrogen starved *Chlorella sp.* C2 (Chen et al., 2014). From these experiments it is clear that Ca^{2+} channels get activated and regulate Ca^{2+} homeostasis during nitrogen starvation and these eventually leads to TAG accumulation in microalgae. Another factor that elevated the lipid accumulation under nitrogen starvation was reported by Zhao et al., 2018 that is melatonin which accelerated induction of lipid biosynthesis in *Monoraphidium sp.* (Ding et al., 2018). Abscisic acid (ABA) is a stress-responsive hormone well studied in signaling, stress response and catabolism in *Arabidopsis thaliana* (Nagamune, et al., 2008; Hartung, 2010). It was reported that endogenous levels of ABA shoots up and released across the plasma membrane of algae and cyanobacteria under environmental harsh conditions. Saradhi et al., 2000; Yoshida, 2005 and Yasohida et al., 2003 evidenced that the enhanced level of ABA was observed during onset of stress in order to cope-with the stress by protecting the cells from photoinhibition and oxidative damage in *Chlamydomonas reinharditi*. Similarly, during nitrogen starvation the *Scenedesmus quadricauda* showed an elevated endogenous ABA level and exogenous supplementation also promotes the stress tolerance effect in *S. quadricauda* (Sulochana and Arumugam, 2016).

In addition to the above stress responsive factors individual organelles like chloroplast and mitochondria also involve in stress signaling by several ways. Chloroplast is the major organelles for phototrophs to synthesize sugars as they are the sites of photosynthesis. The plastids are one of the prototypes of chloroplast mainly found in plants and algae (Keeling et al., 2010). They are having a reduced genome of nearly 100 genes (Kleine et al., 2009a) and at the same time they also contain nearly 2000-3000 nuclear encoded proteins (Abdallah et al., 2000; Yu et al., 2008; Xu et al., 2019). The chloroplast gene expression machinery comprises a mixture of proteins encoded by chloroplast and nuclear genes. Thus chloroplast requires a stringent coordination of the expression of the two genomes (Woodson and Chory, 2008). This is governed by exchange of information between the nucleus and chloroplast (Xu et al., 2019). During retrograde signaling, chloroplasts give signal to the nucleus about their developmental and physiological status so that the nuclear

gene expression can be regulated (Bobik & Burch-Smith, 2015; Chan et al., 2016; Kleine and Leister, 2016). In Chloroplast Retrograde Signaling (CRS), the signals are involved mainly in tetrapyrrole biosynthesis, plastid gene expression and reactive oxygen species (Kleine et al., 2009b).

The role of chloroplast under abiotic stress is crucial as the intracellular signaling from chloroplast to the nucleus governs the stress responsiveness against the environmental harsh condition. Thus, communicating perturbations to the nucleus is crucial during exposure to abiotic stresses such as heat stress (Sun & Guo, 2016). There are a few proteomic studies have carried out for the identification of chloroplast stress responsive proteins in plants (Agarwal et al., 2009; Taylor et al., 2009). More than 40% of stress response protein is predicted to be present in the chloroplast under cold stress (Cui et al., 2005). Yokotani et al., 2010, revealed that CEST (Chloroplast protein Enhancing Stress Tolerance) protein induces tolerance to environmental stress like salinity, high temperature, drought and herbicide stress in rice. Abiotic stresses while inhibiting photosynthesis also induces abnormal energy flows in the chloroplast (Takahashi & Murata, 2008). Therefore excess energy from photo systems causes ROS generation and it lead into oxidative damage to the chloroplast. In order to tolerate the adverse effect of ROS several antioxidant systems get activated in the chloroplast. The stress response mechanisms of the chloroplast have been elucidated partially in plants but in microalgae it is not yet elucidated. The function of chloroplast proteins under abiotic stress open up a chapter of unknown roles of stress mediated lipid accumulation in microalgae.

Another vital organelle; the mitochondrion are the producers of ATP, regulators of ion homeostasis or redox state and ROS generation. The ATP, energy currency is synthesized by cellular respiration as it takes nutrients in from the cytoplasm and breaks down it into energy for other cellular functions. Mitochondria play a major role in adaptation to abiotic stresses, which are known to induce oxidative stress. According to Hill and Remmen, 2014, they play a crucial role in redox signaling by the generation of ROS. Mitochondria are directly involved in the metabolism of lipids and amino acids and transport of metabolites and proteins. Also microalgal mitochondria are believed to originate from an alpha-proteobacterial ancestor that was engulfed by a primitive eukaryotic host. The mitochondrial genes

were either transferred to nucleus or lost completely (Barbrook et al., 2010), thus exhibiting a limited number of genes in the genome.

During abiotic stress the perturbations of mitochondria activates a signaling phenomena called retrograde signaling. In retrograde signaling, signals from the chloroplast and mitochondria regulate the expression of nuclear genes encoding organellar proteins and other cellular proteins (Millar et al., 2001; Eckardt, 2011). Also the metabolites of photorespiration, nitrogen assimilation and sugar metabolism exchange the information into organelles and coordinate the stress induced metabolism (Millar et al., 2001). The over accumulation of these low molecular weight metabolites may act as a retrograde signal to adapt to the harsh environmental condition. Thus when the mitochondrial functions are affected it activates retrograde signaling to alter the mitochondrial gene expression under stress conditions such as nutrient deficiency, drought, cold, pathogen attack and limiting O_2 availability (Kmiecik et al., 2016). The ROS marker genes, heat shock proteins and proteins of alternative respiratory chain are involved in mitochondrial stress responses. All these mitochondrial stress response genes share a common motif called Mitochondrial - Dysfunction Motif (MDM), which is recognized by Transcription factors (TFs) such as ATAF1/2, NAC, NAM and WRKY families (De Clercq et al., 2013). Among these TFs, NAC TFs were released from the endoplasmic reticulum membrane in the presence of ROS, proposing that translocation of the TFs may be giving signal from mitochondria to nucleus (Ng et al., 2014).

With this background knowledge, we made an effort to answer the sequential biochemical events happen during lipid accumulation in microalgae under nitrogen starvation. Primarily, the morphological changes and lipid droplet accumulation were observed during nitrogen starvation followed by the biochemical changes and targeted metabolite analysis. In addition, the Stress Associated Proteins (SAPs) were mapped and identified. The major drawback of nitrogen stress associated lipid accumulation was the drastic reduction in biomass. Thus we are focussing to retain the biomass with the increased TAG accumulation to execute the nitrogen stress as a suitable strategy to enhance lipid accumulation in microalgae.

1.2. Rationale and Objectives of the study

Microalgae gaining lots of importance due to its many attractive futures however there are still technical challenges needs to be addressed. Microalgae when subjected to nitrogen starvation leads to neutral lipid accumulation. *Scenedesmus quadricauda* tends to accumulate 2.27 fold increases in lipid accumulation during nitrogen starvation. Microalgae accumulates more lipids in short time is one of the major advantages of nitrogen starvation. The present investigation aims to fill certain knowledge GAP in understanding the stress induced lipid accumulation and molecular changes in microalgae. This will serve as reference for best possible time for harvesting maximum algal biomass with enhanced lipid content and scientific base for better understanding of stress mediated lipid accumulation and, engineering of algal strains. Therefore the present study was proposed with the following objectives.

- Morphological and biochemical/metabolic changes of *Scenedesmus quadricauda* during nitrogen starvation.
- Mapping of nitrogen stress associated proteins – a) Ribosomal protein L23
- Mapping of nitrogen stress associated proteins- b) LAGLIDADG Homing Endonuclease
- Sustaining biomass level during nitrogen stress- role of stress responsive hormone Abscisic acid (ABA).

1.3. Review of Literature

Microalgae are prokaryotic or eukaryotic organisms that fix the atmospheric CO_2 and produce algal biomass were concerned as biodiesel fuel reserve. The fuel requirement studies shows that world population requires 50% more energy in 2030 (Sani et al., 2013). Currently the energy needs fulfilled by fossil fuels; is only about 80% of the world energy demand (Huang et al., 2012). In this context the microalgae are considered as a platform for sustainable energy resource. The necessity for alternative renewable energy sources increased during the last decades due to over exploitation of fossil fuels. The CO_2 emission upon combustion of these non renewable energy sources pollutes the atmosphere. Hence the microalgae are having importance as renewable and non pollutant energy sources rather than as CO_2 utilizers during photosynthesis. Microalgae are photosynthetic organisms that inhabit fresh water and marine ecosystems. They are gaining more attention for their ability to produce lipid, starch, proteins, carotenoids etc. as storage reserves for survival during unfavourable conditions; such as abiotic stress, pathogen attack etc. (Lim et al., 2012). In order to meet energy requirements the oil producing microalgae are specifically cultivated for biofuel industry as they store lipids as triacyl glycerol (TAG) under environmental harsh conditions. The microalgae have several advantages over other fuel crops, like adaptability, efficiency towards CO_2 usage, rapid biomass yield, and they do not compete for cultivable land (Falkowski et al., 1998; Parker et al., 2008;
Sheehan et al., 1998; Huesemann et al., 2009).

1.3.1. Microalgal Biomass productivity

Biomass is a renewable and sustainable source of energy which is developed from organic materials. The microalgal biomass is having several advantages such as being energy rich, and has structural resemblance with fossil fuels. Thus they are commercially important as precursors for biodiesel production. The fuel crops currently used as biomass are canola, soybeans, palm and Jatropha (Kulkarni and Dalai, 2006; Barnwal and Sharma, 2005). But they are also important as food and compete for arable lands. The major components of algal biomass are carbohydrates, proteins and lipids. Microalgae grow faster than terrestrial plants and their doubling

time is about 24 hours. And they double within 3.5 hours during the onset of log phase (Chiisti, 2007). Algal biomass productivity is high but with a relatively low lipid yield which is about 5-20% of dry cell weight.

1.3.2. Microalgae as potent source as biofuel feedstock

The salient features of the microalgal fuel includes high productivity, adaptation to waste water and its treatment, annual round production, CO_2 utilization, biochemical composition of algae and chemical composition of oil content. In addition to that they have advantage over plants as they do not need herbicides and pesticides (Brennan and Owende 2010). Also the simple structure simplifies the technical limitations of harvesting when comparing plants. Even though metabolic flexibility was one of the major advantages over oil crops because the biochemical composition of microalgae can be tuned to desired product (Tredici 2010). Finally these characteristics make algae with enormous market potential and as a sustainable energy source for the future.

1.3.3. Microalgae are source of nutraceuticals

Algae have been used as food, feed and medicines for various diseases (Richmond, 1990; Gao, 1998). Microalgae are photosynthetic organisms that produce biomass, rich in value added products such as lipids, carbohydrates, proteins, pigments and vitamins (Markou and Nerantzis, 2013) (Fig. 1.1). The microalgal strains that have more potential as food supplements and nutraceuticals are *Botryococcus*, *Anabaena*, *Nostoc*, *Chlamydomonas*, *Scenedesmus*, *Parietochloris*, *Synechococcus*, *Porphydium* etc. because they have the ability to produce necessary vitamins such as Retinol (A), Thiamine (B1), Riboflavin (B2), Niacin (B3), Pyridoxine (B6), Folic acid (B9), Cobalamin (B12), L-Ascorbic acid (C), Tocopherol (E) and Biotin (H) (Bishop and Zubeck, 2012). Along with these they are also reported to produce essential elements like Potassium, Zinc, Iodine, Selenium, Iron, Manganese, Copper, Phosphorus, Sodium, Nitrogen, Magnesium, Cobalt, Molybdenum, Sulphur and Calcium (Bishop and Zubeck, 2012). Also algae are potent producers of essential amino acids and omega 3 (docosahexaenoic acid, eicosapentaenoic acid) and omega 6 (Arachidonic acid) fatty acids (Fig. 1.1) (Simoons, 1991).
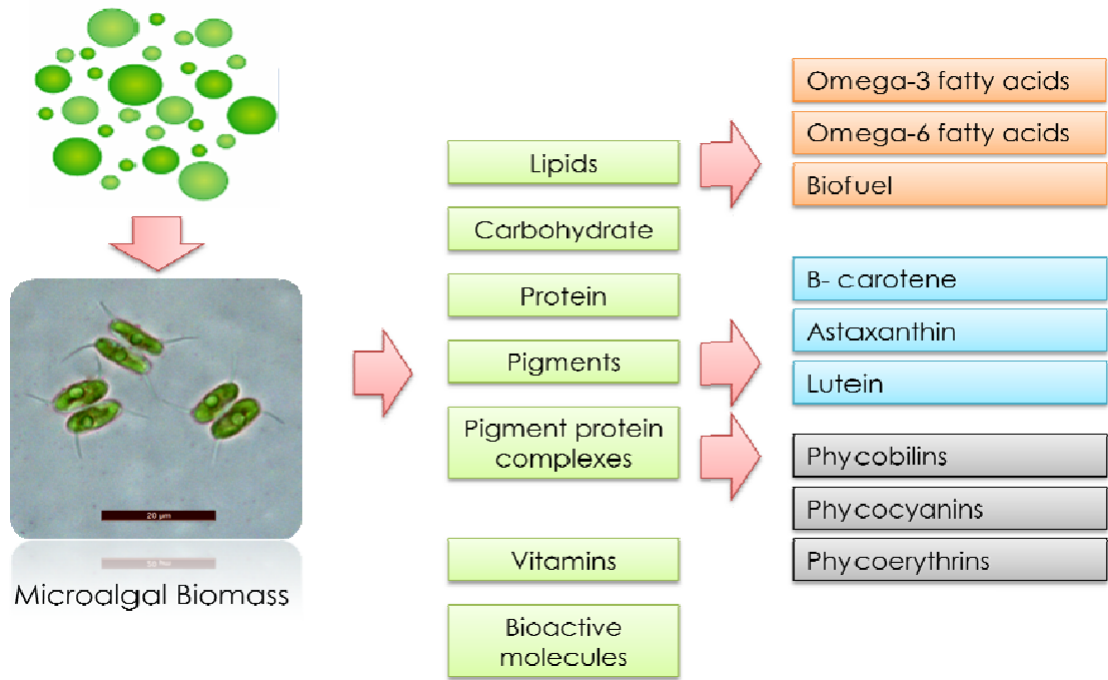
Figure.1.1: Microalgae: source of renewable energy and nutraceuticals

1.3.4. Lipid accumulation in microalgae under abiotic stress

Green algae descended from higher plants and share their metabolic mechanisms and photosynthetic pigments (Y u et al., 2011). Several microalgae produce large amounts of lipids in the form of tri acyl glycerol and it varies from species to species (Hu et al., 2008). Lipids act as structural co mponents of cell membrane in eukaryotic photosynthetic microalgae and also serve as energy storage co mpounds (Fuentes-Grunewald et al., 2013). Thus microalgae are promising lipid-producers having short generation time and are adapted to various environmental conditions (Mata et al., 2013), increased specific growth rate and photosynthetic efficiencies than fuel crops (Chisti 2007; Wu et al., 2013). Microalgal lipid content varies from about 1- 85% of dry weight but in unfavourable conditions it goes higher as 40% (Chisti 2007). The environmental factors which cause microalgae to accumulate more lipids are nutrient availability, temperature and irradiance (Takagi et al., 2006; Rao et al., 2007). The neutral lipid accumulation triggered by abiotic stress in green microalgae has been previously reported (Hu et al., 2008). The oil synthesized in microalgal cells are mostly in the form of cytoplasmic lipid bodies specifically as neutral lipid ie., triacyl

glycerol (TAG) in stress induced microalgae (Guschina and Harwood, 2006; Takagi et al., 2006; Battah et al., 2015) (Fig. 1.2). Similar effect was studied during salt stress in marine microalga *Dunaliella* (Takagi et al., 2006) and also in dinoflagellates (Mansour et al., 1999). The accumulation of TAG occurs due to the conversion of carbon to lipids but the conversion depends on microalgal strains. Also different algae have different mechanism to convert carbon flux to synthesize lipids from the carbohydrate pathway (Li et al., 2012).
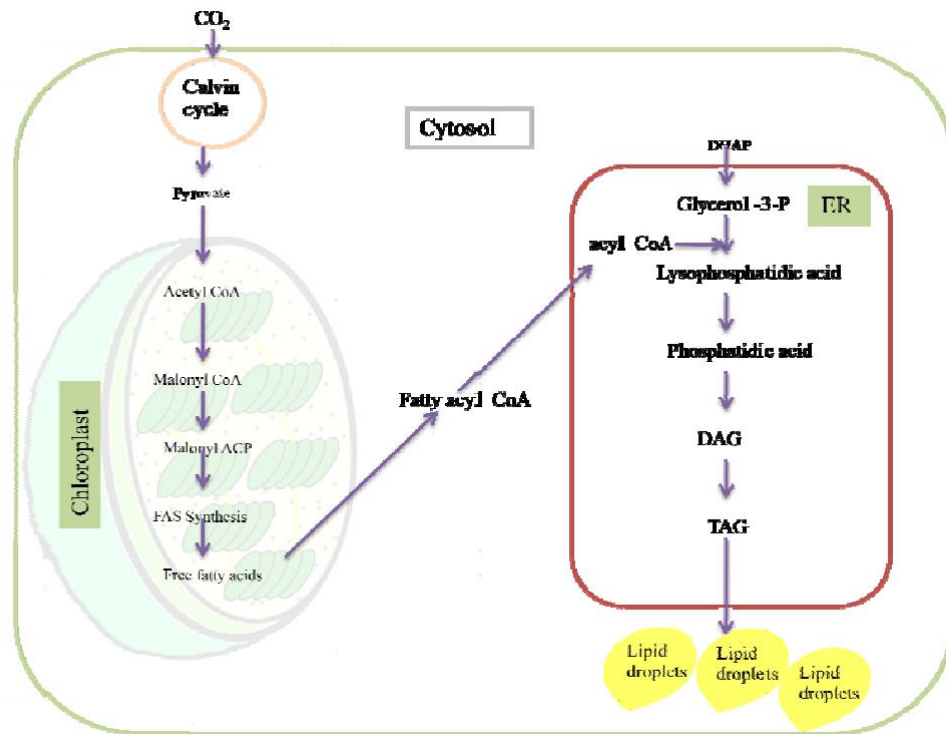
Fig. 1.2: Neutral lipid (TAG) synthesis in microalgae

1.3.5. Lipid enhancement in microalgae by Nutritional stress

The neutral lipid accumulation in oleaginous microalgae depends on strain and culture conditions. A potent strain can be devised to modify the neutral lipid composition by altering the nutrient composition of growth media. Nutrient limitation or deprivation was the commonly practised strategy for increasing lipid accumulation in several microalgal species (Lima et al., 2018). The advantage of nutrient manipulation is that it can be practically feasible for large scale cultivation. Microalgae when grown under nutritional stress conditions; alter their metabolism and biochemical composition. Thus an enhanced production of biofuels was attained by tuning with the nutrient conditions (Fig. 1.3).
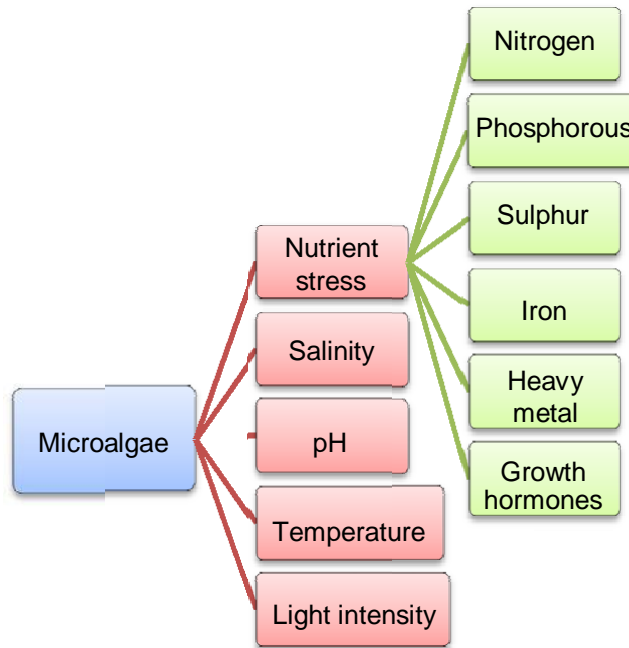
Fig.1.3: Strategies for lipid enhancement in microalgae

1.3.5.1. Manipulation of growth parameters

Changes in growth factors other than nutrients such as light intensity, temperature, pH and salinity, lead to enhanced lipid accumulation in microalgae.

1.3.5.1.1. Salinity

Microalgal cultivation using fresh water is a major concern when practicing large scale cultivation. Therefore, microalgae which can adapt to marine environment will be a good choice as an industrially potent strain. Salinity got attention as it created osmotic stress and eventually ROS generation with lipid accumulation in microalgae (Asulabh et al., 2012). The lipid content of *Chlorococcum* sp. was significantly increased during salinity stress (Harwati et al., 2012), *Botryococcus braunii* (Zhila et al., 2011), *Chlorella protothecoides* (Campenni et al., 2013) and *Nannochloropsis sp.* (Pal et al., 2011). *Dunaliella* cells accumulated about 70% of lipid content under high salt concentration (Takagi and Yoshida, 2006). When the diatom *Nitzschialaevis* was subjected to high salt concentrations, 71.3% of total EPA (Eicosapentanoic acid) was obtained (Chen et al., 2008).

1.3.5.1.2. pH

One of the environmental parameter which influences microalgal growth is pH. The optimum pH mainly lies between 7.0 to 9.0. pH fluctuation in growth medium of microalgae was reported to alter the lipid accumulation. For example, in *Chlorella* CHLOR1found out an increase in TAG accumulation during alkaline pH stress and it was not due to carbon or nitrogen limitation (Guckert and Cooksey, 1990). The environment of microalgal culture shows a varying pH range in day/night depending on photosynthesis and respiration. During the day, increased CO_2 level raise pH levels.

1.3.5.1.3. Light intensity

Being a photoautotrophic micro-organism, microalgae requires a light source for the normal growth and metabolism. Light intensity is a known parameter for the growth of microalgae. Light source and light intensity obtained by microalgae will affects the photosynthetic activity. Also different light intensities and wavelengths increase the TAG accumulation in microalgae. Particularly, under low light PUFA levels increases and high light enhances the level of saturated and monounsaturated fatty acids.

High light intensity induces oxidative damage of PUFA. Pal et al., 2011, evidenced that maximum lipid content was observed in *Nannochloropsis sp.* under 700 μmol photons $s^{-1}m^{-2}$ light intensity. Under higher light intensities, in *Pavlova lutheri* increased lipid content were associated with increase in both cell population and weight per cell profile (Carvalho and Malcata, 2005). The effect of different light intensities on algal lipid composition was successfully demonstrated in a detailed study on *Chlorella vulgaris* (Hassan et al., 2013). Thus the lipid productivity of different microalgae can be attenuated with high light stress. Similarly, there is increased lipid productivity in *C. vulgaris*, *Raphidocelis subcapitata*, *Mychonastes homosphaera* and *Scenedesmus* sp. under high light irradiance (Tang et al., 2011; J. Liu et al., 2012; Goncalves et al., 2013).

1.3.5.1.4. Temperature

Temperature has an essential role in growth and lipid composition of microalgae. Optimum temperature for growth and lipid content in microalgae varies

between species to species (Sibi et al., 2016). For example the optimum temperature for *Scenedesmus sp.* was found to be 20 °C (Xin et al., 2011). Converti et al., 2009, has reported that the lipid content increased from 7.9 to 14.9% at 20-25 °C temperature. According to Renaud et al., 2002, there is a shift in fatty acid composition by temperature i.e, at lower temperature, unsaturated fatty acid is found to be increased and saturated fatty acid content will be increased at higher temperature. The properties of algal biodiesel would also change during different climates and seasons and seasonal cultivation can be practiced for biodiesel production.

1.3.5.2. Nutritional stress

1.3.5.2.1. Phosphorous limitation

Phosphorous is an important microalgal growth component which actively takes part in cellular metabolism such as signal transduction, energy generation, nucleic acid synthesis, respiration and photosynthesis (Raghothama, 2000; El-Kassas, 2013; Singh et al., 2016). Phosphorous limitation results in enhanced lipid accumulation as evidenced in *Scenedesmus* sp. LX1 where 53 % increase in lipid content was observed (Xin et al., 2010). The fresh water microalga, *Scenedesmus obliquus* showed an increment in lipid content from 10 to 29.5 % during phosphorous starvation (Mandal and Mallick, 2009). Likewise lipid accumulation was observed in *Pavlova lutheri*, *Nannochloropsis* sp. and *Phaeodactylumtric ornutum* but there was a decrease in lipid content in *Tetraselmis* sp. and *Nannochloris atomus* during phosphorous limitation (Reitan et al., 1994; Rodolfi et al., 2009). The polyphosphate forms stored in nutrient sufficient condition was utilized in the phosphorous limited conditions as phosphorous reserves (Liang et al., 2013; Qi et al., 2013; Chu et al., 2014). Also the sequential effect of phosphorous deficiency induced reduction in membrane lipid was compromised by non-phosphorous glycolipids and sulpholipids. Liang et al., 2013 reported that maximum lipid content was found to be 23.60 % in *Chlorella* sp. at a concentration of 32 μM phosphorous.

1.3.5.2.2. Iron

Among the trace metals, iron is important for the normal metabolism and functioning of microalgae. Iron has a major role in photosynthetic electron transport chain and impairment in iron metabolism leads to a drastic reduction in CO_2 fixation

and nitrogen assimilation and alteration of lipid content in microalgae (Van Oijen et al., 2004; Liu et al., 2008; Buitenhuis and Geider, 2010; Cheng and He, 2014). Low iron concentration resulted in decreased chlorophyll concentration, which leads to low biomass and lipid content. *C. vulgaris* and *S. obliquus* when grown under iron deficient condition the lipid content increased up to 19.6 and 24.4 % (dry cell weight) with a reduction in biomass yield (Singh and Mallick, 2014).

1.3.5.2.3. Sulphur

Sulphur limitation altered fatty acid content and composition in *Chlamydomonas reinharditi* (Matthew et al., 2009). Under sulphur and phosphorous depletion in *C. reinhardtii*, decrease in sulfoquinovosyl diacyl glycerol (SQDG) and increase of two fold in phosphatidylglycerol (PG) was observed (Sato et al., 2000). Furthermore, Branyikova et al., 2011, reported that *Chlorella vulgaris* produced 50% more starch under sulphur-limiting conditions than under sulphur-replete conditions.

1.3.5.2.4. Silicon

Silicon is an important trace metal for diatoms as it influences cell metabolism and is a major component of diatom cell walls. According to Griffiths and Harrison, 2009 silicon limitation increased cellular lipid content in *Chaetoceros muelleri*, *Cyclotella cryptica*, and *Naviculas aprophila* as on average of above 24 – 41% of dry cell weight.

1.3.5.2.5. Plant Growth Regulators

Phytohormones are chemical messengers which actively take part in growth, metabolic processes, senescence and resistance to biotic and abiotic stresses of plants. They mainly comprise of five different classes like auxin, gibberellins, cytokinins, abscisic acid and ethylene (Han et al., 2018). According to several researchers the phytohormones particularly shoots up during stress conditions to induce cell defence mechanism for adapting the harsh environmental conditions. The research groups also evidenced that the exogenous supplementation of these phytohormones improves growth and lipid pattern of microalgae.

Wu et al., 2018, reported that Abscisic acid (ABA- 1mg/L), Salicylic acid (SA- 10mg/L) and Jasmonic acid (JA- 0.5mg/L) induced 1.5- 2 fold elevated lipid content in *Chlorella vulgaris* ZF strain than the controls. Similarly the supplementation of auxins, cytokinins, ABA, polyamines, brassinosteroids, JA and SA improved the adaptability to environmental stress tolerance to *Chlorella vulgaris*

(Bhola et al., 2011; Piotrowska-Niczyporuk et al., 2012). Enhanced lipid accumulation was observed in *Monoraphidium sp.* by the addition of melatonin (Li et al., 2017) and fluvic acid (Che et al., 2017). The increased level of phytohormones may induce cellular ROS production, gene expression and stress tolerance eventually leads to lipid accumulation (Che et al., 2017; Chu, 2017). Individually IAA (Indole Acetic Acid) promoted growth in *C. vulgaris* (50 ppm), *Nannochloropsis oceanica* (Udayan and Arumugam, 2017) and *Scenedesmus obliquus* (10^{-5} M) (Salama et al., 2014) as 11-19 times and 1.9 fold than the control respectively. Also exogenous ABA, stress responsive hormone suppressed the growth in *Haematococcus pluvialis* with elevated carotenoids by the exogenous supplementation (Kobayashi et al., 1997). The similar growth pattern was observed in other microalgae like *Coscinodiscus granii* (Kentzer and Mazur, 1991) and *Nannochloropsis oceanica* (Lu et al., 2014). When comparing this negative impact of ABA to fresh water microalga *Scenedesmus quadricauda*, the biomass concentration was sustained in nitrogen stressed condition rather a rapid decline in biomass (Sulochana and Arumugam, 2016). Ethylene well studied as a growth inhibitor but promoted growth depending upon the concentration supplemented. Exogenous ethylene in *H. pluvialis* increased astaxanthin production (Gao and Meng, 2007).

1.3.5.2.6. Nitrogen

The nitrogen in growth medium directly facilitates the growth of cell as it forms major back bone for the synthesis of proteins and nucleic acids (Li et al., 2008; Arumugam et al., 2013; Sulochana and Arumugam, 2016). Due to these peculiarities, nitrogen stress induction was widely practiced for enhanced lipid accumulation in microalgae. The nitrogen stress induction was performed in two stage cultivation processes; in the first stage the microalgae are grown in nitrogen sufficient media to obtain maximum cell density. Further in the second stage, the harvested biomass was subjected to nitrogen deficient or nitrogen limited media to induce nitrogen stress (Anand and Arumugam, 2015; Minhas et al., 2016; Sulochana and Arumugam, 2016; Zhu et al., 2016). Nitrogen stress can be induced by either complete removal (Nitrogen deprived) or by limiting the supply of nitrogen to the medium (Nitrogen limited) (Fig. 1.4). Either nitrogen limitation or deprivation proved to enhance the lipid accumulation in microalgae. Among the nutritional stress, most extensively followed strategy is nitrogen deprivation because it is directly related to the lipid

metabolism of microalgae and can yield more lipids within hours respect to other stresses (Table. 1.1).

The assimilable form of nitrogen sources like ammonium, nitrate, peptone and urea altered the biomass and neutral lipid accumulation in microalgae (Chen and Chen, 2006). Nitrogen stress induced *Nannochloropsis* sp., *Haematococcus pluvialis* shows lipid accumulation after 2 days with a sharp decline in chlorophyll content (Li et al.,2008; Rodolfi et al., 2009). Certain microalgae accumulate carbohydrates under nitrogen limitation. For example *Tetraselmis subcordiformis* accumulates fourfold carbohydrate than control during nitrogen limitation. Similarly *S. obliquus* CNW-N showed a 29% increase in carbohydrate content (Ho et al., 2012).

Microalgae	Lipid content (% dcw)	N stress Lipid (% dcw)	Reference
Neochloris oleoabundans	13	29	Adams et al., 2013
Scenedesmus dimorphus	9	20	Adams et al., 2013
Chlorella vulgaris	10	40	Adams et al., 2013
Monoraphidium sp.	36.68	44..4	Zhao et al., 2016
Ankistrodesmus falcatus	36.54	34.4	Alvarez-Diaz et al., 2014
Nannochloris sp.	31	51	Takagi et al., 2000
Chlorella sorokiniana	15	21	Adams et al., 2013
Chlorella oleofaciens	12	35	Adams et al., 2013
Scenedesmus naegleii	10	21	Adams et al., 2013

Table.1.1: Nitrogen stress induced lipid accumulation in microalgae
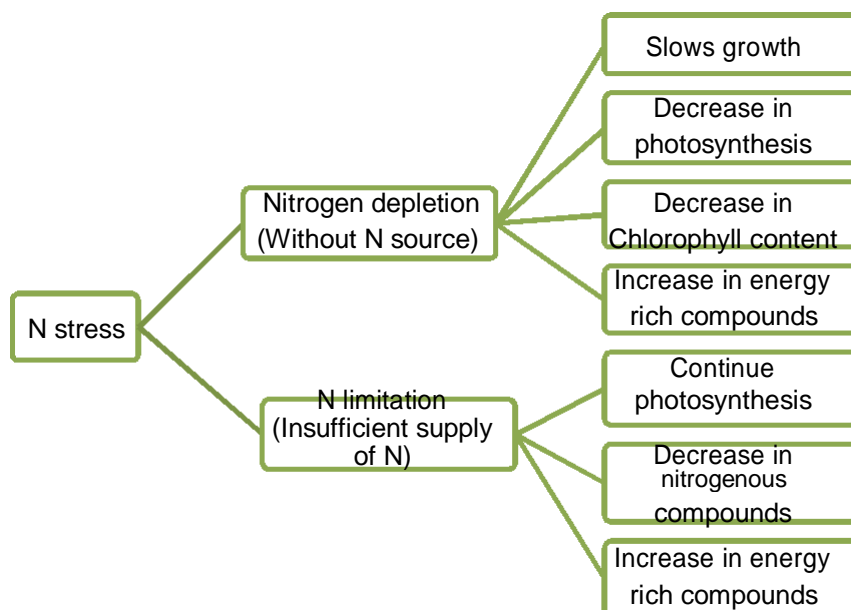
Fig.1.4: Different types of nitrogen stress induction in microalgae.

1.3.6. Nitrogen stress induced TAG accumulation in microalgae

1.3.6.1. Morphological variation during nitrogen starvation

Nitrogen starvation or other abiotic stresses can affect growth, morphology and metabolism of microalgae (Hockin et al., 2012; Pasaribu et al., 2015). The morphology of dinoflagellates changed due to lower temperature or nitrogen starvation (Jiang et al., 2014; Pasaribu et al., 2015; Pasaribu et al., 2016). *Symbiodinium sp.* when cultured under nitrogen deprivation, after 5 days of stress induction the cell walls became thickened and more number of lipid droplets were observed inside the cell by TEM analysis (Pasaribu et al., 2016). The fresh water microalgae *Scenedesmus quadricauda* changes its morphology to produce unicells and coenobia under various environmental conditions and in response to predators (Anand and Arumugam, 2015).

1.3.6.2. Biochemical changes under nitrogen stress

Microalgae accumulates TAG under nitrogen starvation is mainly due to increased synthesis of TAG and membrane lipid disintegration into TAG (Fan et al., 2011, 2012; Goncalves et al., 2013; Miller et al., 2010). Boyle et al., 2012, reported those three acyl transferase genes (DGAT1, DGTT1, and PDAT1) and a nitrogen response regulator (NRR1) are up regulated during nitrogen starvation. Several reports suggested that in some microalgae initial starch accumulation followed by TAG accumulation during nitrogen stress (Siaut et al., 2011).

At differential expression levels metabolites such as octadecanoic acid, triethanolamine, citric acid, citramalic acid, methionine, nicotianaminesx, trehalose, and sorbitol, showed increased levels during nitrogen stress. Similarly the ethanolamine and hydroxycitric acid were reported in increased levels with increased lipid yield in three different cyanobacteria (*Synechocystis* sp. PCC 6803, *Anabaena* sp. PCC 7120, and *Scenedesmus obliquus*) (Cheng et al., 2012). Metabolite level changes during stress conditions influences protein activities to stress responses. The proteome analysis of nitrogen starved *C. reinharditi* showed that activities of several key enzymes of rate limiting steps in glycolysis was increased and gluconeogenesis

were decreased (Wase et al., 2014). Also the ribosomal proteins were reduced to 40% or more during nitrogen stress. The down regulation of ribosomal proteins is an indicative of nitrogen stress responses (Wase et al., 2014).

1.3.6.3. Altered fatty acid composition due to nitrogen starvation

Nitrogen limitation is the feasible strategy to enhance lipid content in microalgae. Several microalgae species accumulate about 70% of dry cell weight (DCW) as lipid under nitrogen limitation (Rodolfi et al. 2008). Most of the studies revealed that nitrogen stress favours more of saturated fatty acids (SFA) and monounsaturated fatty acids (MUFA) (Hu, 2004; Rodolfi et al., 2009). *Phaeodactylum tricornutum* produced about 29 % neutral lipids with a fatty acid composition of oleic acid (up to 46.4%), linoleic acid (up to 8.8%) and linolenic (n-3) acid (up to 7.2%) (Fosse, 2016). The MUFA content were increased in *P. tricornutum* and there is no change in MUFA content of *Rhodopirellula baltica* under nitrogen limitation. In addition to this the PUFA content of *R. baltica* was increased, but in *P. tricornutum* showed about 40% reduction especially around 50 % reduced EPA levels under nitrogen stress (Fosse, 2016). From these evidences it is clear that the fatty acid composition vary depends on the type of nutrient limitation and algal strains.

1.3.6.4. Biomass loss and growth inhibition during nitrogen starvation

In order to maintain the C/N homeostasis there is a rechanneling of reduced carbon and lipid reserves leading into TAG accumulation under nitrogen stress (Breuer et al., 2012). At the same time the lipid droplets, carotenoid and carbohydrate content increases in microalgae. Also cell division stops, protein reduction chlorophyll degradation and biomass reduction were observed during nitrogen starvation (Cakmak et al., 2012). Thus limiting nutrients to the microalgae results in increased lipid yield with reduced biomass, this really affects the lipid productivity of the organism. Therefore one of the major bottlenecks of nitrogen limitation was the reduced biomass when cultivated in large scale. Even though biomass reduction is one of the major drawback but it will give more yield within short stress induced cultivation time. For example *Nannochloropsis* can withstand

for a few days in nitrogen stressed condition with increased TAG accumulation (Negi et al., 2016).

1.3.6.5. Strategies to enhance biomass production and lipid accumulation in microalgae

The neutral lipid accumulation in oleaginous microalgae depends on strain and culture conditions. A potent strain can be devised to modify the neutral lipid composition by altering the nutrient composition of growth media. The optimization of growth medium includes carbon source, nitrogen, phosphorous, vitamins and salts (Mata et al., 2010). Also the physical growth parameters and mode of culturing (heterotrophic, mixotrophic etc.,) can be optimized to enhance lipid production in microalgae (Rawat et al., 2013; Yeh and Chang, 2012). Hakalin et al., 2014 revealed that devised nutritional medium improved cell number and oil production in microalgae. Another strategy to improve biomass, cell number and lipid yield is by phytohormone supplementation. A lower concentration of abscisic acid is needed to sustain the biomass and lipid yield in nitrogen starved *S. quadricauda* (Sulochana and Arumugam, 2016). Conventional approaches focussed on optimization of nutrients and culture conditions, mixed microalgal-microbial consortia, genetic modification and improved photo-bioreactor (PBR) designs increases the biomass yield.

CHAPTER

2

Morphological and biochemical/metabolic changes of *Scenedesmus quadricauda* during nitrogen starvation

2.1. Introduction

Nitrogen stress in microalgae induces changes in internal biomolecular pattern and morphology. *Scenedesmus* is a pleomorphic strain which changes its morphology during nitrogen starvation as unicells or coenobia. As the microalga is having these peculiar characteristics the nitrogen stress-driven morphological changes have not completely studied in *S. quadricauda*.

When nitrogen stress is induced along with morphological changes several biochemical changes occurs in the microalga. Such biochemical changes represent the Reactive Oxygen Species (ROS) generation and antioxidant scavenger's elevation during nitrogen stress induction. The increased ROS accumulation during prolonged nitrogen starvation leads to oxidative damage and finally, it promotes neutral lipid accumulation in *Dunaliella salina*. Both increased ROS production and lipid peroxidation were observed under nitrogen starvation in association with increased lipid accumulation (Yilancioglu et al., 2014). To study the oxidative stress-induced lipid body accumulation in *S. quadricauda* the ROS and antioxidant enzymes were quantified.

The stress response genes may be activating the genes of lipidomic, carbon and other metabolic pathways leading to neutral lipid accumulation. Clearly, this area is not explored well. The major evidences for the query covers different omics approaches like transcriptomics, proteomics, lipidomics and metabolomics which explains the key regulators and proteins for TAG accumulation under nitrogen starvation (Park et al., 2015). The monogenic approach towards the study will not address the problem. Thus targeted stress metabolite analysis was followed during nitrogen starvation. The metabolic changes are mainly associated with the liberation of low molecular weight biomolecules and their levels during abiotic stress condition.

2.2. Materials and methods

2.2.1. Culturing and induction of nitrogen stress

Scenedesmus quadricauda CASA CC202 (Fig. 2.1) batch cultures were grown in flasks containing Bold Basal medium. The composition of media wherein (g/L): $NaNO_3$ - 25; $CaCl_2.2H_2O$ - 2.5; $MgSO_4.7H_2O$ - 7.5; K_2HPO_4 - 7.5 KH_2PO_4 -17.5; $NaCl$ - 2.5, trace elements are (mg/L) $FeCl_3.6H_2O$ - 97; $MnCl_2.4H_2O$ - 41; $ZnCl_2.6H_2O$ - 5; $CoCl_2.6H_2O$ - 2; $Na_2MoO_4.2H_2O$ - 0.75; Boric acid- 500, and the media also contain vitamins (g/L) Biotin-0.1; vitamin B12-1; Thiamine- 0.2. The pH of the media was adjusted to 6.8 – 7.0. The cultures were cultivated in an artificial growth chamber having a temperature of 25 °C with 14:10 hour light-dark period. The adherence of cells to the bottom of flasks was avoided by shaking twice per day. The nitrogen stress was

induced when the control (N^+) algal cultures reached log phase and the cells were harvested by centrifugation at 10000 rpm for 10 minutes. The pelleted cells were washed twice with distilled water and re-inoculated to the nitrogen starved (N^-) medium (Anand and Arumugam, 2015) (Scheme. 2.1).

Fig. 2.1: Microscopic images of *Scenedesmus quadricauda* CASA CC202. NCBI Genbank Acc.no.: KM250077, Culture Collection Acc. No.: CASA CC202.
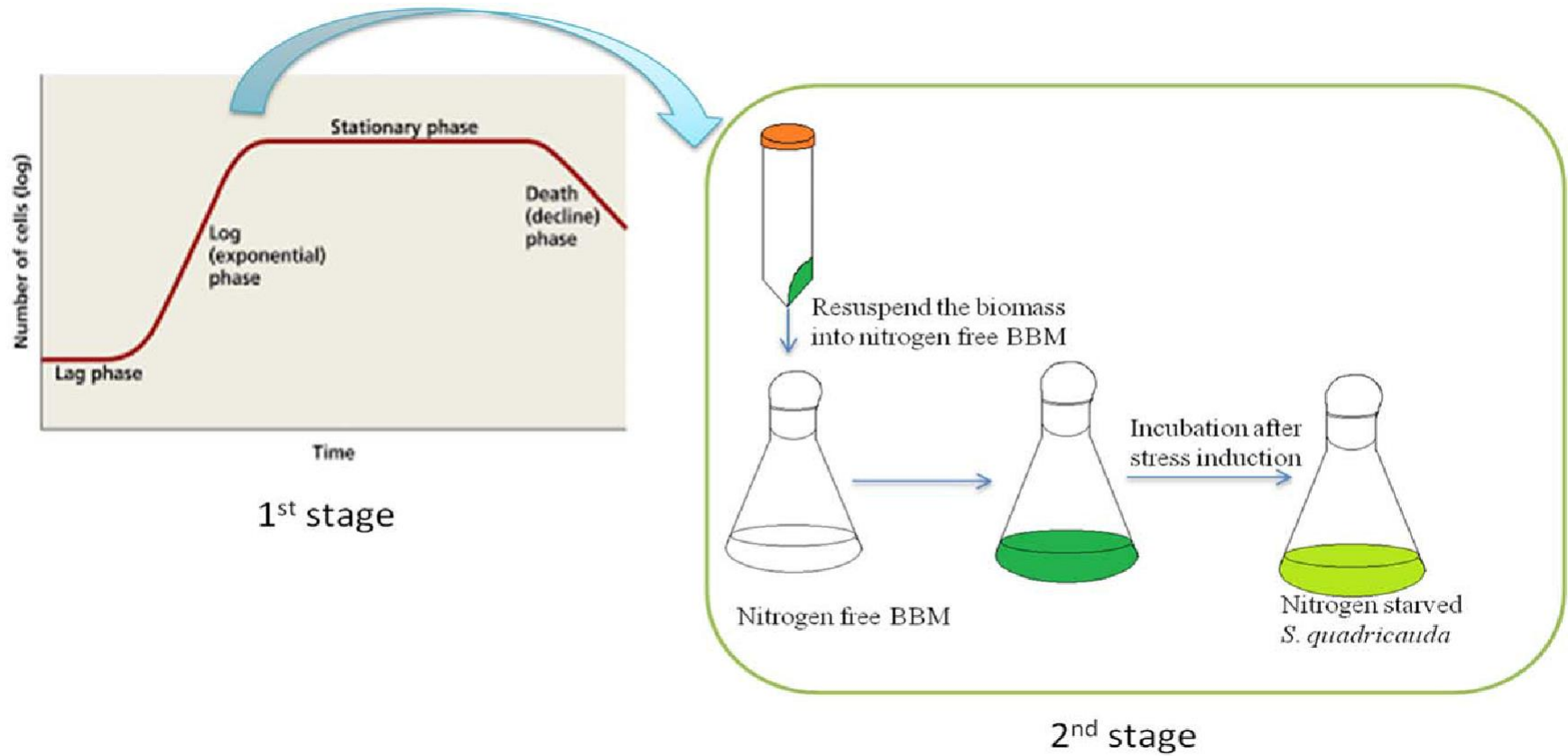
Scheme.2.1: Nitrogen stress induction in *S. quadricauda*. The culture was grown in two stage conditions, as it reaches maximum cell density in control (N+) represents first stage. In the second stage the cells were harvested and reinoculated into nitrogen starved (N-) medium.

2.2.2. Effect of nitrogen stress induction in growth and morphology of *S. quadricauda*

2.2.2.1. Growth - Cell number

The control and nitrogen stressed cultures were aseptically drawn in 0, 24, 48 and 72 hours of induction. The culture flasks were shaken well and 1ml of each sample was collected in a microcentrifuge tube. After that, the sample was vortexed and taken 100 µl and diluted with 900 µl sterile distilled water. The cell number was enumerated by a light microscope (Leica) using a haemocytometer and expressed in terms of 10^6 cells/ml.

2.2.2.2. Morphological variation

20 µl of the sample was dropped into a clean microscopic slide covered with a cover slip and the slide was allowed to stand for a few minutes. After that, the slide was observed under a light microscope (Leica). The individual cells length to breadth measurement was calculated by Leica application suite software.

2.2.2.3. Morphological variation in population of *S. quadricauda* by flow cytometry analysis

All the three experiments the sample of 1 ml taken from nitrogen stress induced and respective control in microcentrifuge tube. From that 100 µl sample was taken and diluted with 900 µl sterile distilled water and the pellet was obtained by centrifugation at 10000 rpm for 10 minutes. Then the pellet was collected and washed twice with phosphate buffer saline (PBS) (pH- 7.4). The washed pellet was fixed with 2.5% glutaraldehyde in PBS of 50 µl for 5 minutes. The pellet was then collected by centrifugation at 10000 rpm for 5 minutes and washed with 1 ml PBS and again pelleted by centrifugation. The washed pellet was resuspended in 1ml of Rhodamine 123 dye (1mg/ml ethanol stock) of 10 µl diluted with 990 µl of distilled water and incubated for 5 minutes at 20 °C. After incubation the excess dye was washed away by centrifugation and was resuspended pellet in 1 ml of PBS. Then the fluorescent intensity were analysed by flow cytometry BD FACS Aria^{TM} II excitation at 505 nm and emission at 534 nm using software BD FACS Diva^{TM}.

2.2.2.4. Ultra structure of nitrogen stressed *S. quadricauda* – Transmission Electron Microscopy (TEM)

The harvested algal cells were washed with phosphate buffer (pH 7.0) twice at 8000 rpm for 10 minutes. The algal cells were fixed in 2.5% glutaraldehyde and 4% paraformaldehyde in 0.1 M sodium phosphate buffer, pH 7.0 at 4°C for storing. After that the prefixed cells were washed with phosphate buffer, then the cells were placed on the (300-mesh) copper grid. The dropped sample in the grid was allowed to air dry, and then the samples were dehydrated in an acetone series of 60, 70, 80, 90 and 100% each. The algal sample should be prepared one day before to view TEM analysis. Make sure the instrument runs on >100 KV. The images were captured using High Resolution TEM (LaB6), Tecnai G2, T30S-TWIN (FEI).

2.2.2.5. Staining of lipid droplets using lipophilic dye

Nile red (9-diethylamino-5H-benzo [α]phenoxa-phenoxazine-5-one) is a sensitive method to stain lipids inside the cell. Nitrogen deprived and nitrogen rich algal cells were collected by centrifugation at 10000 rpm for 10 minutes. The algal samples were then washed twice with phosphate buffer (pH-7.0). Then 400µl of DMSO was added and incubated for one minute in an oven. After that 20µl of Nile red (SIGMA) solution (stock- 10mg/ml) was added and incubated for 10 minutes in dark. Then the image was captured by a fluorescent microscope BD Pathway 855 using the Attovision software at excitation and emission of 535nm and 575 nm respectively.

2.2.2.6. Immunostaining of Major lipid droplet protein in *S.quadricauda*

The algal cells were prefixed with 4% paraformaldehyde, subsequently, the fixed cells were suspended with sensitization solution composed of 0.1M Tris-7.5, 0.15M NaCl, 0.1% Triton X-100 for 30 min. Sensitised cells were washed two times with washing solution (0.1 M Tris-7.5 with 0.1% Triton X-100), in the same tube, MLDP polyclonal antibody was added in 1: 1000 dilution ratio, and incubated for 3 hrs in rocker at 4°C. Cells were washed three times with wash solution followed by incubation with secondary antibody, anti-rabbit antibody conjugated with FITC for 2 more hours. The cells were washed three times and suspended in 1x PBS and viewed under a confocal microscope.

2.2.3. Biochemical changes during nitrogen starvation

 2.2.3.1. Detection of mitochondrial membrane potential by flow cytometry

The algal cells were fixed with 2.5% glutaraldehyde in PBS of 50 µl for 5 minutes. The pellet was then collected by centrifugation at 10000 rpm for 5 minutes and washed with 1 ml PBS and again pelleted by centrifugation. The washed pellet was resuspended in 1ml of Rhodamine 123 dye (1mg/ml ethanol stock) of 10 µl diluted with 990 µl of distilled water and incubated for 5 minutes at 20 °C. After incubation the excess dye was washed away by centrifugation and was resuspended pellet in 1 ml of PBS. Then the fluorescent intensity were analysed by flow cytometry BD FACS Aria^{TM} II excitation at 505 nm and emission at 534 nm using software BD FACS Diva^{TM}. The protocol is detailly described in materials and methods of chapter 2 section 2.2.2.3.

2.2.3.2. Quantification of Reactive oxygen species and Antioxidant enzymes during nitrogen starvation

2.2.3.2.1. Measurement of H$_2$O$_2$

The control (N$^+$, culture grown in BBM for 12 days) and nitrogen starved (N$^-$) algal cells from three experimental replicates were harvested by centrifugation and resuspended in 0.1% w/v TCA solution for sonication. The total cell lysate was collected by centrifugation at 13000 rpm for 10 minutes. An aliquot of 0.5 ml of the supernatant was mixed with 0.5ml of 10 mM phosphate buffer (pH-7.0) and 1 ml of 1M potassium iodide. The absorbance of the solution was read at 390nm. The H$_2$O$_2$ concentration (µmol H$_2$O$_2$/gFW) in the sample was determined from a calibration curve prepared using the known concentrations of H$_2$O$_2$ (Velikova et al., 2000). The mean values of three independent of H$_2$O$_2$ concentration were plotted as a graph with standard deviation as an error bars.

2.2.3.2.2. Quantification of O$_2$$^{\cdot-}$

The control (N$^+$) and nitrogen starved (N$^-$) algal cells of three experimental replicates (n=3) were harvested by centrifugation, sonicated with 5 ml of 65 mM potassium phosphate buffer (pH-7.8), and centrifuged at 12000 rpm for 5 minutes. An aliquot of 1 ml of supernatant was mixed with 0.9 ml of mM potassium phosphate buffer (pH-7.8) and 0.1 ml of 10 mM hydroxyl ammonium chloride. After incubation at 25 °C for 20 minutes, 1 ml of 17 mM sulphanilic acid, and 1 ml of 7 mM α-

naphthylamine were added to the mixture. Further the tubes were incubated for 20 minutes and the absorbance of the solution was read at 530 nm. The mean values of three independent replicates of $O_2^{\cdot-}$ concentration were plotted as a graph with standard deviation as an error bars.Sodium nitrite was used to plot the standard curve from that the production of $O_2^{\cdot-}$ was calculated (Liu et al., 2010).

2.2.3.2.3. Measurement of OH⁻

The control (N^+) and nitrogen starved (N^-) algal cells of three experimental replicates (n=3) were harvested by centrifugation and sonicated with 2 ml of 50 mM potassium phosphate buffer (pH-7.0) and centrifuged at 12000 rpm for 5 minutes. There after 0.5 ml of supernatant was mixed with 0.5 ml of 50 mM potassium phosphate buffer (pH-7.0) containing 2.5 mM of 2-deoxy ribose. The tubes were kept at 35 °C in dark for 1 hour. After adding 1 ml of 1% TBA in 0.5 M sodium hydroxide and 1 ml of acetic acid, the mixture was boiled for 30 minutes and immediately cooled on ice. The absorbance of the solution was read at 532 nm and the OH⁻ content was expressed as absorbance units per gram of FW (Halliwell, 2006). The mean values of three independent replicates of OH⁻ concentration were plotted as a graph with standard deviation as an error bars.

2.2.3.2.4. Lipid peroxidation

Microalgal cells of three independent replicates from N^+ (12th day) and N^- (0, 24, 48, 72 hours) samples were harvested by centrifugation, homogenized in 2 ml of 80:20 (v/v) ethanol: water followed by centrifugation at 13000 rpm for 10 minutes. An aliquot of 1 ml of the supernatant was mixed with 1 ml of Thiobarbituric acid (TBA) solution comprising of 20% (w/v) TCA, 0.01% butylated hydroxytoluene and 0.65% TBA. Samples were then mixed vigorously then heated at 95 °C for 25 minutes and cooled. The contents were centrifuged at 13000 rpm for 10 minutes and the absorbance of the supernatant was read at 450, 532 and 660 nm (Hodges et al., 1999). The mean values of three independent replicates were plotted as a graph with standard deviation as an error bars.

$$\text{MDA (µmol/gFW)} = \frac{[\,6.45\times(A_{532}\text{-}A_{600})\,] - [\,0.56\times A_{450}\,]}{FW}$$

2.2.3.2.5. Estimation of antioxidant enzymes

2.2.3.2.5.1. Catalase assay

Catalase activity was determined using catalase calorimetric activity kit (Invitrogen). Nitrogen stressed and control algal pellet (100 mg) were collected by centrifugation at 8000 rpm for 10 minutes. Further the pellet was homogenized or sonicated in 1 ml of cold 1x assay buffer (as provided by the manufactures) per 100 mg of cells. Then the content was centrifuged at 10000 rpm for 15 minutes at 4 °C. Collect the supernatant and assay immediately, or store at ≤ -70 °C.

As dilution of standards for catalase assay was prepared as described by the manufactures instructions. In brief, one unit of catalase decomposes 1 μmol of H_2O_2 per minute at pH-7.0 and 25 °C. About 10 μl of catalase standards were added to one tube containing 190 μl 1x assay buffer and labelled as 5U/ml catalase. 100 μl of 1x assay buffer was added to each of 6 tubes labelled as follows: 2.5, 1.25, 0.625, 0.313, 0.156 and 0 U/ml catalase. Serial dilutions of the standard were prepared as described in the kit manual.

Accurately 25 μl of standards or diluted samples were added to the appropriate wells. Then added 25 μl of H_2O_2 reagent into each well and incubated for 30 minutes at room temperature. After that 25 μM of substrate was added into each well. Again added 25 μl of 1x Horse Radish Peroxidase (HRP) solution into each well and incubated for 15 minutes at room temperature, further the absorbance were read at 560 nm. Curve fitting software with a four parameter algorithm (Graph pad prism2) was used to generate the standard curve.

2.2.3.2.5.2. Peroxidase assay

The peroxidase activity was quantified using Peroxidase activity assay kit (SIGMA). As dilution of standards for peroxidase assay was prepared as described by the manufactures instructions. In brief, about 10 μl of the 12.5 mM H_2O_2 solution was diluted with 1,240 μl of assay buffer to prepare a 0.1 mM standard solution. Then 0, 10, 20, 30, 40, and 50 μL of the 0.1 mM standard solution was added into a 96 well plate, generating 0 (blank), 1, 2, 3, 4, and 5 nmole/well standards. Further the assay buffer was added to each well to bring the volume to 50 μl. To each standard curve well, 50 μl of the standard curve reaction mix was added. Each well were mixed well and incubated at room temperature for 5 minutes and absorbance was read at 570 nm.

About 10 mg of algal pellet was rapidly homogenized with 100–200 µl of assay buffer and centrifuged at 15,000 rpm for 10 minutes to remove insoluble materials. Then 50 µl of the master reaction mix was added to each sample and positive control well. The contents in the well were mixed well by pipetting and incubated the plate at 37 °C for 3 minutes, then the initial measurement was read at 570 nm (T initial). The plate was protected from light during the incubation. The measurements were taken until the value of the most active sample is greater than the value of the highest standard (Colorimetric – 5 nmole/well). The final measurement [(A$_{570}$) final] for calculating the enzyme activity would be the value before the most active sample is near or exceeds the end of the linear range of the standard curve. The time of the penultimate reading is T final.

The change in measurement from T initial to T final for samples was calculated.

$$\Delta A_{570} = (A_{570}) \text{ final} - (A_{570}) \text{ initial}$$

Compared the ∆measurement value (∆A$_{570}$) of each sample to the standard curve to determine the amount of H$_2$O$_2$ reduced during the assay between T initial and T final (B). The Peroxidase activity of a sample was determined by the following equation:

$$\text{Peroxidase Activity} = \frac{[B \times \text{Sample Dilution Factor}]}{(\text{Reaction Time}) \times V}$$

B = Amount (nmole) of H$_2$O$_2$ reduced between T initial and T

final Reaction Time = T final–T initial (minutes)

V = sample volume (mL) added to well

Peroxidase activity reported as nmole/min/mL = milliunit/mL, where one unit of peroxidase is defined as the amount of enzyme that reduces 1.0 µmole of H$_2$O$_2$ per minute at 37 °C. The mean values of three independent replicates were plotted as a graph with standard deviation as an error bars.

2.2.4. Targeted metabolite analysis by LC-MS

The nitrogen starved (N⁻) *S. quadricauda* cells were collected by centrifugation at 8000 rpm for 10 minutes at room temperature. The culture grown in the Bold Basal Medium for 12 days was used as a control. Metabolites were extracted

by homogenizing with liquid nitrogen in a prechilled sterile mortar and pestle. The samples then suspended with mixture of 1 ml of methanol: water (80:20). Subsequently the supernatant was collected by centrifugation at 8000 rpm for 10 minutes at 4 °C and the extracted metabolites were stored at -20°C for LC-MS analysis. The mobile phase used for LC- MS is mixture of triethylamine (A, 60%) and methanol (B, 40%) containing 0.1% formic acid adjusted to pH-4.2 and separated through a 1.9 μM C18 Shimadzu shim pack GISS column (Dimension 2.1×150mm). Column temperature was maintained at 4 °C and the temperature of the drying gas in ionization source was 300 °C. The gas flow was 10 L/min and the capillary voltage was 4KV and the detection was using electro spray ionization (ESI)-MS. The LC- MS 8045 (Shimadzu, Japan) chromatogram was analyzed and the results were plotted by a heat map. The mean values of two experimental results were calculated and the data were used for the heat map generation. The heat map was generated using heat mapper (an online tool to interpret the metabolomic analysis) (Babicki et al., 2016).

2.3. Results

2.3.1. Morphological changes during nitrogen starvation
2.3.1.1. Effect of nitrogen stress induction in growth and morphology of *S. quadricauda*
2.3.1.1.1. Growth – Cell number

The cell number is the primary parameter to examine the growth of an organism. When stress initiates the cell number is found to be decreasing as 26.5×10^6 cells within 24 hours than control (30.5×10^6 cells/ml). There is no fresh cell division happening as evident from Fig. 2.2 during nitrogen starved condition. Finally, a gradual decrease in cell number was observed in 48 and 72 hour of nitrogen stress induction from 24.5 to 23.5 $\times 10^6$ cells/ml when compared to the respective control (N^+) cells (34.5 to 39 $\times 10^6$ cell/ml) (Fig. 2.2).
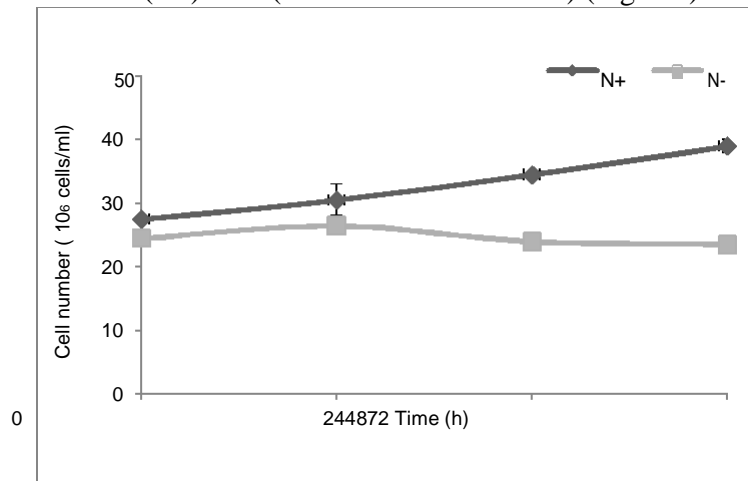
Fig. 2.2: Growth (Cell number) of *S. quadricauda* in control (N^+) and Nitrogen starved (N^-) condition.

2.3.1.1.2. Morphological variation

Nitrogen being an integral part of bio molecules such as proteins of an organism and thus it's deficiency in the medium affects the enzymes required for cell division and eventually the growth of microalgae. Morphological changes during nitrogen starvation are due to the cellular events. The nitrogen stress induced cells showed that there is an increment in cell size compared to control ie, N^+ cells (Fig. 2.3 a & b). Further each cell length breadth ratio was calculated. The length breadth ratio also suggested that there is an increment of 0.13 μm in nitrogen stressed (N^-) *S. quadricauda* (Fig. 2.3 b & c).
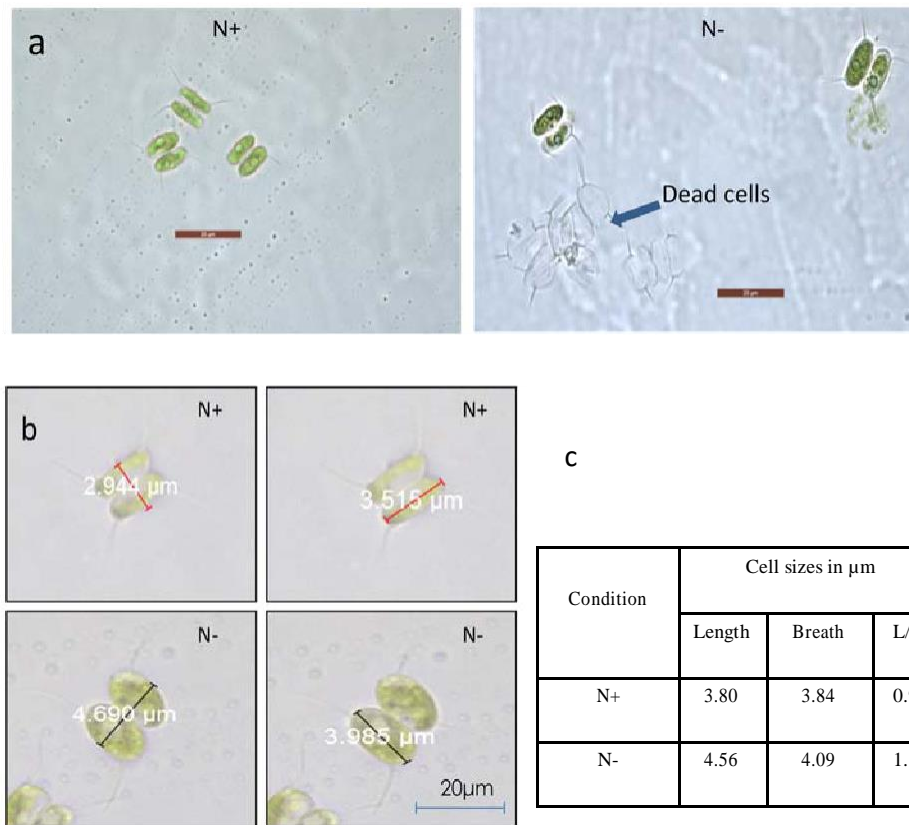
Fig. 2.3: a; Microscopic images of Control (N$^+$) and b; Nitrogen starved (N$^-$) *S. quadricauda*. b & c: Length and breadth ratio of Control (N$^+$) and Nitrogen starved (N$^-$) *S. quadricauda*.

2.3.1.1.3. Nitrogen stress induced morphological variation in population of *S. quadricauda*

The above experiments suggested that nitrogen starvation leads to morphological change in *S. quadricauda*. Morphological changes studied in certain number of cells under a microscope are not an appropriate way to represent in a population. Thus the variation in size of the cell due to nitrogen stress induction was studied in a population of *S. quadricauda*. The flow cytometry analysis showed cell enlargement occurs in the nitrogen stress induced cells than the control. The forward scatter analysis, the control cells were gated in such a way that large cells were presumed to represent 10% of the population and it compares to nitrogen stressed cells. The gated region represents the 'region of hypertrophy' (Fig. 2.4a). The population statistics of the cell enlargement showed that there is a 2.6 % cell size enlargement in nitrogen stress induced *S. quadricauda* (Fig.2. 4b).
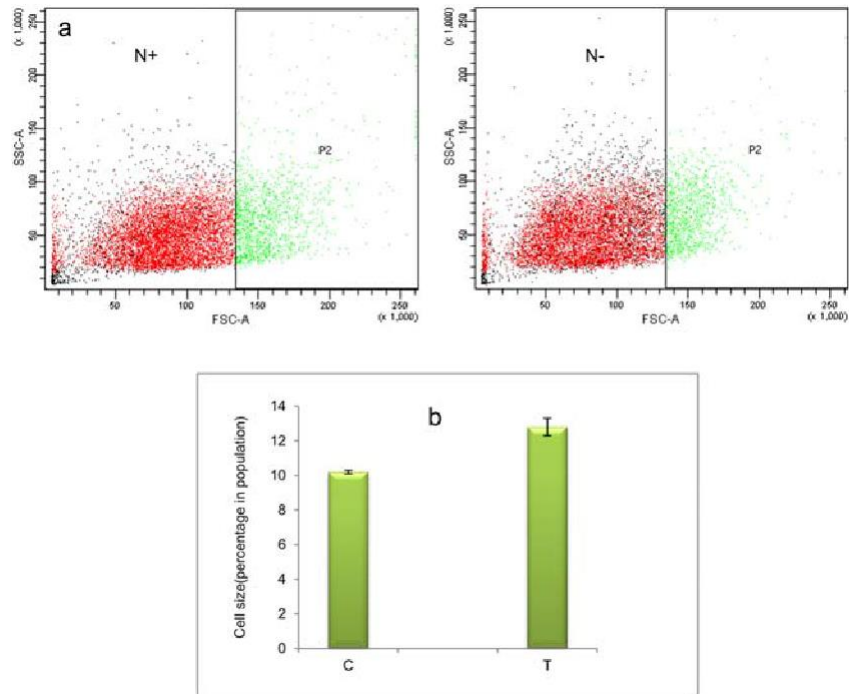
Fig. 2.4: Nitrogen stress induced cell enlargement in a population of *S. quadricauda*. a; Flow cytometry analysis of control (N$^+$) and nitrogen starved (N$^-$) *S. quadricauda,* b; Population statistics of enlarged cells during nitrogen starvation (T) and control *S. quadricauda*

2.3.1.1.4. Ultra structure of nitrogen stressed *S. quadricauda*- Transmission Electron Microscopy (TEM)

The cell size variation in nitrogen stress induction was confirmed in population of *S. quadricauda.* The reason for the cell enlargement had to be studied by internal organization of the cell during nitrogen starvation. Thus the ultra structure of the nitrogen stressed *S. quadricauda* was revealed by the TEM imaging. TEM images of control (N$^+$) and nitrogen starved (N$^-$) *S. quadricauda* reveals that there might be more number of lipid bodies in nitrogen starved cells (Fig. 2.5).
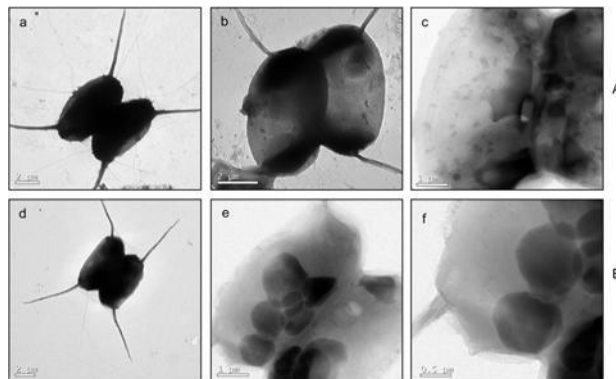
Fig.2.5: Transmission Electron Micrograph explains the ultra structure of A; control (N$^+$) and B; nitrogen starved (N$^-$) *S. quadricauda*.

2.3.1.1.5. Staining of lipid droplets in nitrogen stressed *S. quadricauda*

The TEM images showed there might be more oil droplets in nitrogen stressed cells. In order to confirm the lipid body accumulation Nile red staining was performed. The stained lipid bodies were observed in golden colour. The nitrogen stress induced *S. quadricauda* is having more number of oil droplets (Fig. 2.6) than the control.
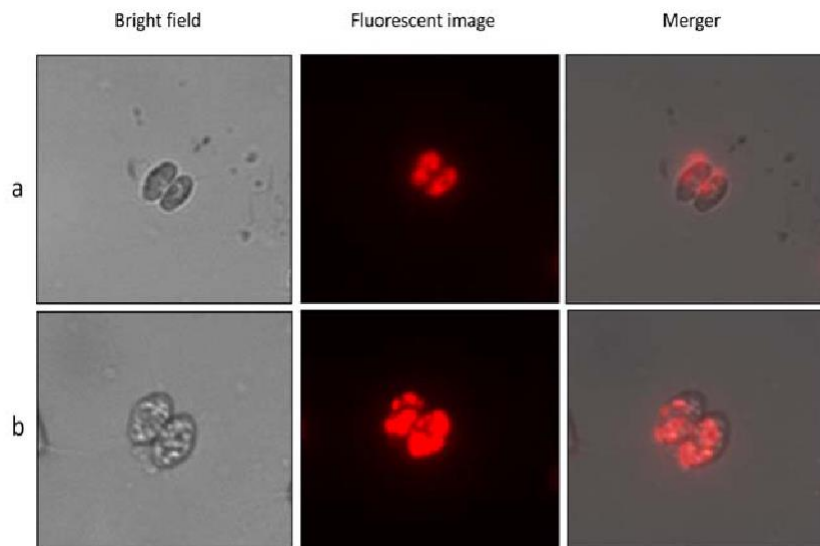
Fig. 2.6: Lipid droplet staining of a; control (N$^+$) and b; nitrogen starved (N$^-$) *S. quadricauda* by Nile red staining.

2.3.1.1.6. Detection of MLDP during nitrogen stress

Major Lipid Droplet Protein (MLDP), a major structural protein involved in lipid body synthesis. Not much information is available for *Scenedesmus quardicauda*, regarding the presence of MLDP and its abundance during the nitrogen starvation. Here we observed that *C. reinhardtii* MDLP polyclonal antibody (Huang et al., 2013) recognises and cross-reacts with the *S. quadricauda* MLDP, indicating the presence and conservation of MLDP like protein in green microalga linage (Fig. 2.7). Additionally, we also tested the relative abundance of MLDP in stress condition like nitrogen starvation; confocal imaging reveals the accumulation of MLDP in both the control and nitrogen stressed condition (Fig. 2.7).

| Bright field | FITC | Merger |
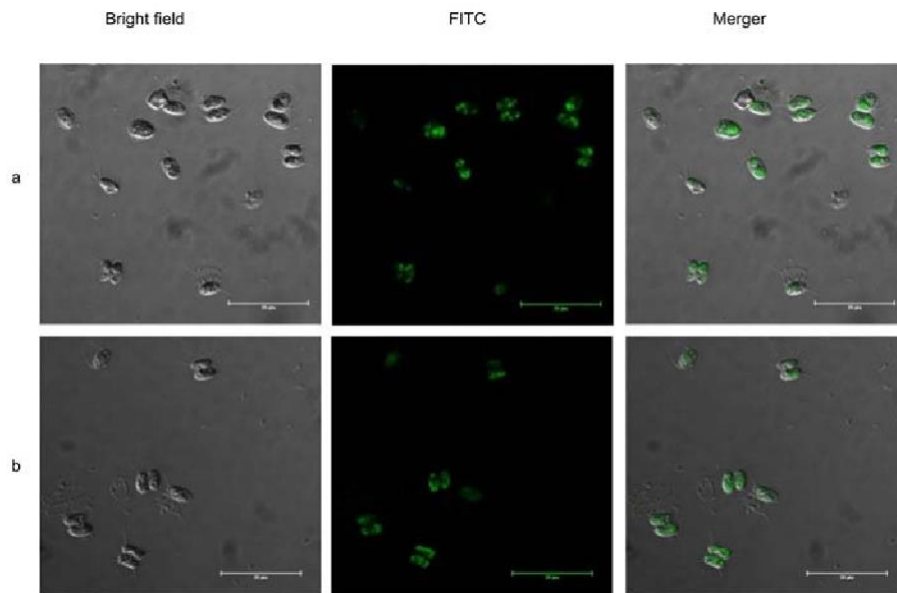
Fig. 2.7: Immuno stained images of major lipid droplet protein (MLDP) in a; control (N$^+$) and b; nitrogen starved (N$^-$) *S. quadricauda*. The green fluorescence shows the conserved MLDP presence in micro algal lineages.

2.3.2. Biochemical changes during nitrogen starvation

2.3.2.1. Changes in mitochondrial membrane potential during nitrogen starvation

Nitrogen stress induces perturbations in mitochondrial membrane potential ($\Delta\psi_m$), which is one of the signals to the mitochondria. The increased mitochondrial membrane potential is directly proportional to the increased fluorescence of Rhodamine 123 (Rh123). Also the increased mitochondrial membrane potential leads to elevated ROS generation and thus stress responses to the *S. quadricauda*. Here in *S. quadricauda* the rate of fluorescence of Rh 123 is increased during nitrogen stress. There is a 25% elevation of fluorescence emission in 24 hour nitrogen stress induced *S. quadricauda* when compared to nitrogen sufficient cells (Fig. 2.8). Also the 48 and 72 hour samples revealed an increased membrane potential during onset of nitrogen stress. Thus it implies that there is a fluctuation in mitochondrial membrane potential in the initial hours during nitrogen stress. As the stress progresses, increased ROS generation was observed in mitochondria and which lead to metabolic rearrangements.
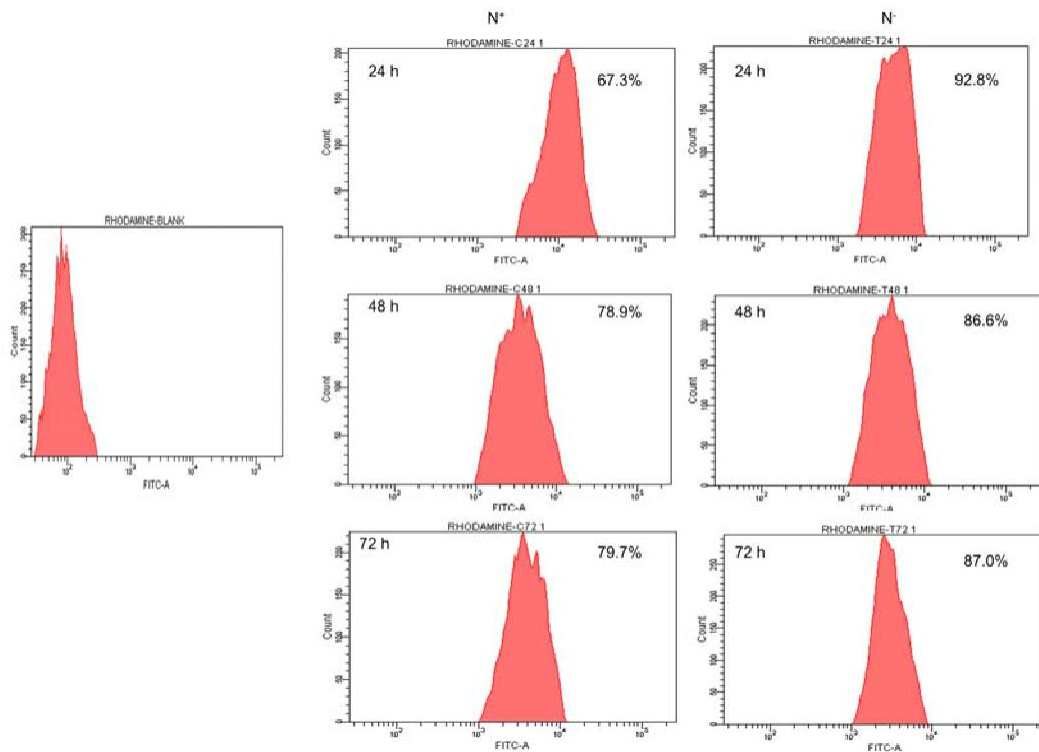
Fig. 2.8: Nitrogen stress induced changes in mitochondrial membrane potential of *S. quadricauda* by flow cytometry. Mitochondria were stained by Rhodamine123. Blank represents the auto fluorescence of *S.quadricauda*; N^+- control, N^- - Nitrogen starved *S. quadricauda* at 24 h, 48 h and 72 h.

2.3.2.2. Reactive Oxygen Species (ROS) generation during nitrogen stress mediated lipid accumulation

The mitochondria are the primary producers of ROS and also it depends on the metabolic state of mitochondrion during nitrogen stress. The increased production of Reactive oxygen species (ROS) is a sign of stress at a molecular level and the subsequent accumulation tends to oxidative damage. The concentration of H_2O_2 in the algal extract was plotted using a standard curve (Fig. 2.9a). The H_2O_2 accumulation during nitrogen stress induced *S. quadricauda* showed an elevated level at 24 and 48 hour of incubation around 7 µM and 11 µM respectively compared to control (0.17 µM) (Fig. 2.9b). The $O_2^{\cdot-}$ radical in the nitrogen stressed *S. quadricauda* showed around 3.09 µM on 24 hour of incubation and it was a lower concentration compared to nitrogen rich *S. quadricauda* where the $O_2^{\cdot-}$ concentration was about 7.13 µM (Fig. 2.10). Also the level of hydroxyl radical elevated during the initial hours of nitrogen stress induction (Fig. 2.11a).

Lipid peroxidation is the oxidative degradation of lipids. The free radicals steal electrons from the membrane lipids and cause severe cell damage. Lipid peroxidation was determined in terms of malondialdehyde (MDA) content in the cells. The MDA was elevated during the 72 hr of incubation and it was around 1.13 µM. The MDA content was lower during the initial hours of stress induction (Fig. 2.11b).
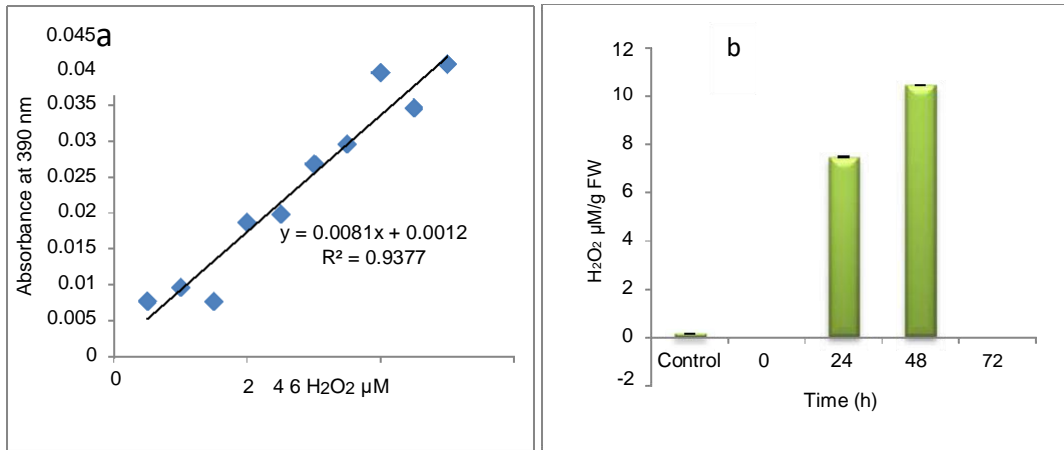
Fig. 2.9: a; Standard curve of H_2O_2, b: H_2O_2 generation during nitrogen stress induced (N^-) at 0, 24, 48 and 72 hour and the control (N^+) *S. quadricauda* at 12th day.
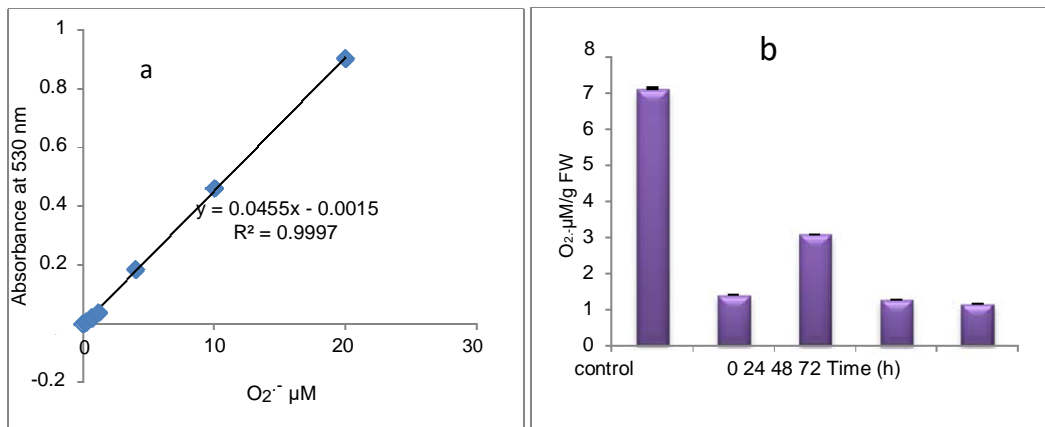
Fig. 2.10: a; Standard curve of $O_2^{.-}$, b: $O_2^{.-}$ generation during nitrogen stress induced *S. quadricauda* at 0, 24, 48 and 72 hour and the control (N^+) *S. quadricauda* at 12th day.
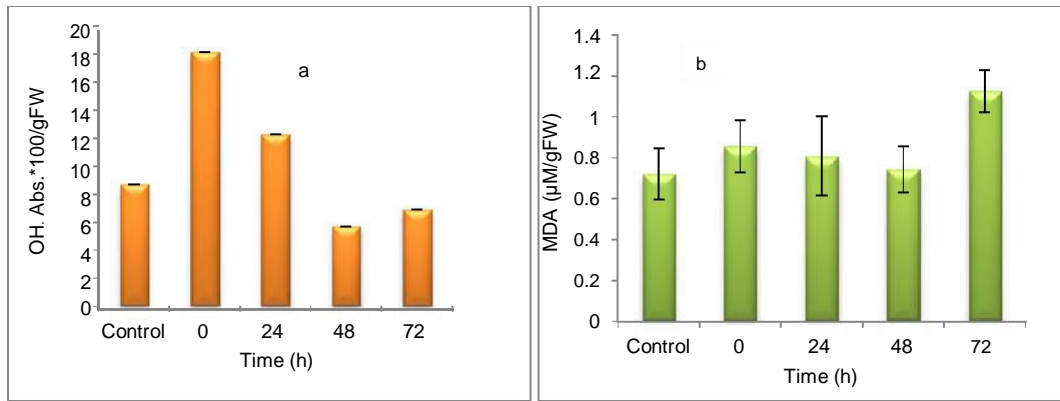
Fig. 2.11: a; OH⁻ generation in nitrogen stress induced (N⁻) and the control (N⁺) *S. quadricauda* at 12th day. b: Level of lipid peroxidation (MDA) under nitrogen stress induction in *S. quadricauda*.

2.3.2.3. Antagonistic antioxidant enzymes during nitrogen stress

2.3.2.3.1. Catalase activity in *S.quadricauda* under nitrogen stress

In order to clear off the highly reactive oxygen species, the free radical scavenging enzymes were also elevated during nitrogen stress induction. Catalase is the enzymes which speed up the conversion of H_2O_2 to water and oxygen. During nitrogen stress H_2O_2 generation was elevated at the same time the catalase activity was also found to be increased. The catalase activity was observed to be about 0.8 U/ml (Fig. 2.12b) and it was calculated according to the standard curve (Fig. 2.12a).
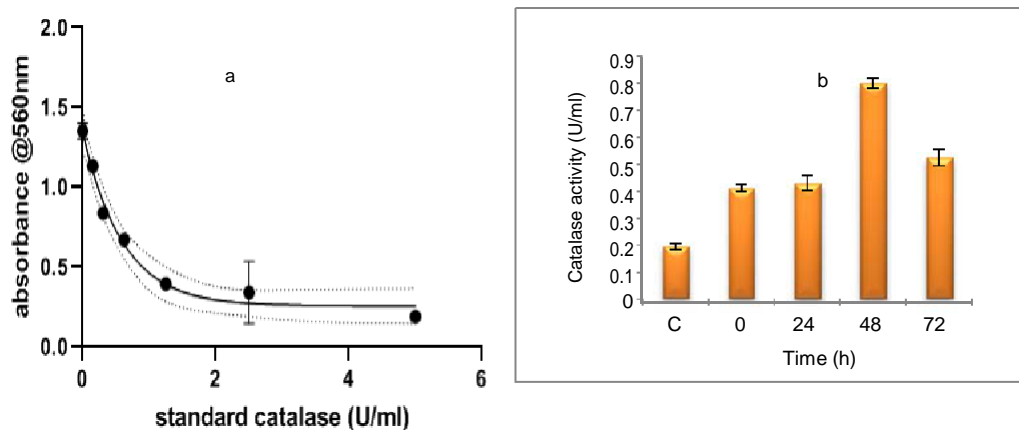
Fig. 2.12: a; Standard curve of Catalase activity on H_2O_2 and the curve was plotted using four parameter algorithm (Graph pad prism 2). b: Catalase activity in nitrogen stress induced (N⁻) and the control (N⁺) *S. quadricauda* at 12th day.

changes **2.3.2.3.2. Peroxidase activity in *S.quadricauda* under nitrogen stress**

The peroxidase is heme containing proteins which catalyzes the conversion of H_2O_2 into water and an activated donor molecule. It utilizes H_2O_2 from various organic and inorganic substrates. The peroxidase enzyme in *S. quadricauda* was observed as not an active participant for H_2O_2 oxidoreduction. As it was evidenced from Fig. 2.13b, there is a deviation in peroxidase activity at 48 hour of nitrogen stress induction (23.16 mU/ml) compared to control (20.22 mU/ml). The peroxidase activity was calculated using H_2O_2 as substrate (Fig. 2.13a)
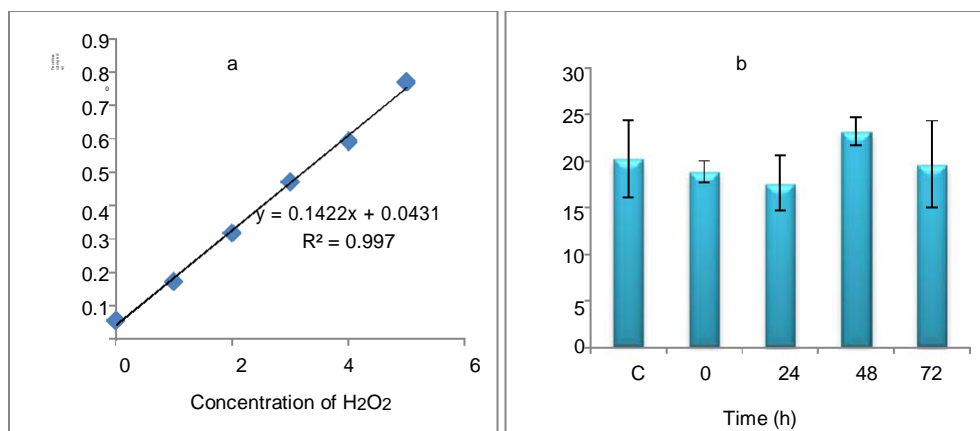
Fig. 2.13: a; Standard curve of Peroxidase activity on H_2O_2. b: Peroxidase activity in nitrogen stress induced (N⁻) and the control (N⁺) *S. quadricauda* at 12th day.

2.3.3. Metabolic changes during nitrogen starvation

2.3.3.1. Targeted stress metabolite analysis by LC-MS

During nitrogen stress there are several changes happening in the cell and the cellular events triggered by the stress finally leads to TAG accumulation. The monogenic approach for solution to the effect of nitrogen stress will not correlate to the cellular events. Thus an integrated approach was followed by several research groups to address the problem. Metabolomics is one of the omics study which helps to understand the metabolic rearrangement of the cell during nitrogen stress. In order to address the metabolic changes governed by nitrogen stress, several metabolites were listed and its role was discussed in Table. 2.1. The metabolic changes are mainly associated with the liberation of low molecular weight bio molecules and their levels during abiotic stress condition. The integrated and targeted metabolic analysis was

characterized by LC-MS analysis (Table. 2.2). The heat map results showed stress related non proteinogenic amino acids and energy equivalents elevated during nitrogen starvation (Fig. 2.14). The non proteinogenic amino acids like Gamma Amino Butyric Acid (GABA), glutamate and arginine were observed in maximum peak area at 72, 24 and 0 hr of nitrogen stress induction respectively. Also the energy equivalents such as NADH and ATP are highly reactive during 72, 0 h of nitrogen stress induction (Fig. 2.14).

Targeted metabolites	Role
GABA	Regulation of energy metabolism Bypasses two steps in TCA cycle
Glutamate	Precursor of chlorophyll
Arginine	Regulation of energy metabolism
Sucrose	Promotes cell expansion and storage
Citrate	Intermediate of TCA cycle.
Succinate	Intermediate between the glyoxylate cycle and TCA cycle.
GTP	Regulation of energy metabolism
ATP	Regulation of energy metabolism
Glucose-6-Phosphate	Intermediate of glycolysis
NAD	Regulation of energy metabolism
NADH	Regulation of energy metabolism
NADP	Regulation of energy metabolism
NADPH	Regulation of energy metabolism

Table. 2.1: Role of different metabolites induced by nitrogen stress in eukaryotes.

Metabolite	Control	0h	24h	48h	72h
GABA	703968.5	1004063	776965.5	873432	1180145
glu	443661	574720	648526.5	551677.5	644556
arg	1184005	1896099	1145729	733938.5	714445.5
CIT	6532084	10085954	3498695	2790677	2571782
SUC	844696.5	872646.5	1164225	1208297	1210913
GTP	4624835	2570644	2026399	1414486	1722994
ATP	6898568	13299689	11275060	7838441	10230891
SUC	2403608	1486642	1393702	1333580	2963405
G6P	3189667	2872579	3338921	3469893	3433004
NAD	1705166	2241628	1538069	1001045	2071430
NADH	2729403	1462470	2355313	1735672	5437777
NADP	550765.5	731297	614214.5	10300	12578

Table. 2.2: The liberation of stress metabolites during nitrogen starvation in *Scenedesmus quadricauda*. The peak intensities were extracted from LC-MS chromatogram and analyzed from average values of three independent experiments (n = 3).
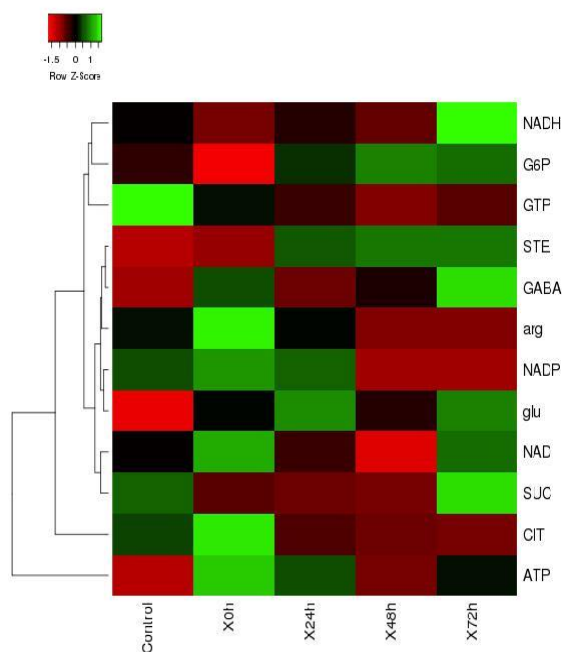
Fig. 2.14: The heat map of nitrogen stress induced *S. quadricauda* at 0, 24, 48 and 72 hour and the control *S. quadricauda* at 15th day represented in X axis. The targeted metabolites were represented in Y axis and the map was generated by heat mapper.

2.4. Discussion

Stress mediated morphological changes in *Scenedesmus* species were described by other research groups. According to Pancha et al. (2014), the cell size of *Scenedesmus* species was enlarged in nitrate starved condition. Similarly the cell length was doubled in *Acutodesmus dimorphus* under nitrogen starved conditions (Chokshi et al., 2017). *Symbiodinium*, when cultured under nitrogen stress, the average cell size was observed as 7.35 and 6.96 μm at day 5 and 7 when compared to control (6.54 μm). Moreover, significant changes in the size and lipid droplets induced the morphological changes in *Scenedesmus obtusiusculus* and *Symbiodinium* during nitrogen starvation (Jiang et al., 2014). In order to visualize the lipid droplet accumulation in each cell the nile red staining was performed in *Dunaliella salina* after being subjected to nitrogen stress (Yilancioglu et al., 2014). Major Lipid Droplet Protein (MLDP) was found to be the abundant protein in *C. reinhardtii* lipid droplet proteome analysis (Moellering and Benning, 2010, Nguyen et al., 2011). Tsai et al., (2014) reported MLDP abundance positively correlated with the TAG accumulation, indicating the co-regulation of lipid droplet and TAG. On the other hand, the lipid MLDP-RNAi silenced lines show about 40% increase in lipid droplet size in *C. reinhardtii* under nitrogen starved condition (Moellering and Benning, 2010). The present study also reveals that the increased lipid droplets during nitrogen starvation are the reason for the morphological variation.

Mitochondrion plays a major role in cellular adaptation to abiotic stresses and is known to induce oxidative stress (Pastore et al., 2007). Mitochondrial membrane potential ($\Delta\psi_m$) is the driving force for ATP synthesis in mitochondria and it is generated by the proton pumping in the electron transport chain. It has been reported that a correlation between membrane potential and ROS, as it generates more ROS at high membrane potential (Suski et al., 2012). Similarly mitochondrial membrane potential and ROS generation was elevated in *S. quadricauda* during nitrogen starvation. Rhodamine 123 is a cationic, lipophilic fluorescent probe used to assay mitochondrial membrane potential in populations of apoptotic cells and it was measured according to the rate of fluorescent decay which is proportional to the mitochondrial membrane potential (Baracca et al., 2003). The high membrane potential leads to increased ROS generation in *S. quadricauda* under nitrogen starvation.

Even though ROS are highly reactive and potent toxic to the cells, they are having beneficial roles in abiotic stress. These include (i) diversion of electrons from the photosynthetic machinery in chloroplast to prevent the overload of the antenna and subsequent damage (Choudhury et al., 2017); (ii) regulation of metabolic fluxes during abiotic stress; and vital role as (iii) signal transduction reactions mediating the activation of acclimation pathways during stress (Foyer and Noctor, 2013; Vaahtera et al., 2014; Considine et al., 2015; Dietz, 2015; Mignolet-Spruyt et al., 2016; Mittler, 2017). The predominant ROS species such as H_2O_2, $O_2^{\cdot-}$ and OH^- were determined in nitrogen starved *S. quadricauda*. Chokshi et al., 2017 reported that 3 days nitrogen starved *Acutodesmus dimorphus* showed 2 fold elevated levels of H_2O_2 than the control and simultaneously 4 fold reduction in $O_2^{\cdot-}$ in nitrogen starved cells. H_2O_2 and $O_2^{\cdot-}$ are showing inverse relationship, as highly reactive $O_2^{\cdot-}$ is converted into H_2O_2 by the enzyme superoxide dismutase (SOD). According to them the OH^- and MDA did not vary significantly in nitrogen stressed *A. dimorphus*. But in *Chlorella sorokiniana* C3 showed a significant increase in the MDA level during nitrogen starvation induced oxidative stress (Zhang et al., 2013). The over production of toxic ROS was neutralized by the antioxidant scavenging enzymes such as SOD, catalase and ascorbate peroxidase during nutrient starvation (Bhaduri and Fulekar, 2012; Ali et al., 2005; Yilancioglu et al., 2014; Zhang et al., 2013; Fan et al., 2014; Ruiz-Dominuez et al., 2015; Salbitani et al., 2015). Also the Yilancioglu et al., 2014 in *Dunaliella salina* observed an elevated level of catalase and peroxidase activity under nitrogen deficient conditions. Their experimental evidences suggested that the lipid accumulation might be partially induced by ROS mediated oxidative stress under nitrogen starvation. In order to prove that, they induced oxidative stress by H_2O_2 and the results showed that increased lipid accumulation during induced oxidative stress with full strength nitrogen source in *D. salina*. In addition to that they have claimed that oxidative stress itself can trigger lipid accumulation and suggested that the lipid accumulation was mediated by oxidative stress during nitrogen starvation.

The metabolic changes during nitrogen starvation showed low molecular weight secondary metabolite accumulation and metabolic rearrangement to cope up the stress (Salama et al., 2019). In order to adjust the metabolic changes, microalgal species modulates their metabolite synthesis (Paliwal et al., 2017). An elevated level of sugars (glucose, sucrose and fructose) was observed in salinity and they have a role

in osmotic homeostasis, carbon storage as well as scavenging of free radicals (Rosa et al., 2009). Several researchers proposed that the fatty acid synthesis was promoted by the hyper activity of Tri carboxylic acid (TCA) cycle (Lee et al., 2012; Sweetlove et al., 2010; Hockin et al., 2012). According to Guerra et al., 2013 the hyper activity of TCA cycle occurs because the lipid synthesis needs more ATP together with the reduction power of NADPH during nitrogen starvation. The lipid synthesis after nitrogen starvation creates a C/N imbalance and it can be adjusted by the protein degradation to take out the amino acids. The amino acids such as leucine, isoleucine and valine take part in the synthesis of Acetyl CoA (Allen et al., 2011; Ge et al., 2014) which is the precursor of fatty acid synthesis. Also the glutamate forms the precursor for chlorophyll synthesis. GABA is a non- protein amino acid whose levels are found to be increased during response to nitrogen stress (Xupeng et al., 2017). The present study also indicates that the energy equivalents and non proteinogenic amino acid like GABA were found elevated during nitrogen starvation in *S. quadricauda*. During abiotic stress metabolites of glycolysis and TCA cycle along with these amino acids showed an initial increase in levels followed by decrease (Zhang et al, 2016).

2.5. Conclusion

The morphological changes as cell size enlargement in *S. quadricauda* population were observed under nitrogen starvation. The nitrogen stress induces ROS which leads to lipid accumulation and lipid droplet maturation; here the major protein involved in maturation is Major Lipid Droplet Protein (MLDP). It was visualized using MLDP specific antibody through immuno staining. The nitrogen stress-induced biochemical changes rely on the mitochondrion, a vital organelle which is primarily affected due to the oxidative stress-induced Reactive Oxygen Species (ROS) generation at high membrane potential ($\Delta\psi_m$). The predominant ROS generated were H_2O_2, OH^-, $O_2^{\cdot-}$ and in order to suppress the ROS, antioxidant scavenging enzymes like peroxidase and catalase were quantified. The results showed an inverse correlation between $O_2^{\cdot-}$ and H_2O_2, also the OH^- and lipid peroxidation in terms of Malondialdehyde. The Metabolic changes are mainly associated with the liberation of low molecular weight bio molecules and their levels during abiotic stress condition. The integrated targeted metabolic analysis was characterized by LC-MS analysis and the results showed stress related non proteinogenic amino acids and energy equivalents elevated during nitrogen starvation.

CHAPTER

3

Mapping of nitrogen stress
associated proteins –a) Ribosomal
protein L23

3.1. Introduction

In general when *Scenedesmus quadricauda* subjected to nitrogen starvation it accumulate 2.27 fold more lipid as TAG (Anand and Arumugam, 2015). The reason for such lipid accumulation in microalgae was not well addressed and it is of current interest among researchers. The present investigations aim to understand the Stress Associated Proteins (SAPs) during nitrogen starvation in *S. quadricauda* along with morphological, biochemical and metabolic changes. There are several hypothesis that explains stress mediated lipid accumulation in microalgae such as (i) decrease in protein content per cell and rearrangement of chloroplast membrane lipids (ii) for maintaining cellular redox homeostasis due to excess amounts of reducing power (iii) storing energy in the form of lipid for the consumption in next favourable condition and (iv) the cell accumulate lipid during the cell cycle prior to cell division and when stress is recognized by the cell they block cycle progression that eventually leads to increased lipid content.

Guarnieri et al., 2011 and Gao et al., 2013, demonstrated the major triggering factor for the neutral lipid accumulation under nitrogen starvation. Most of the evidences mainly come across the genes in fatty acid biosynthetic pathways, photosynthetic system and carbon metabolic pathways. However the exact mechanism for activating these lipid synthetic genes was not addressed. The stress response genes may be activating the genes of lipidomic, carbon and other metabolic pathways leading to neutral lipid accumulation but the knowledge gap is still under study. Possibly the stress signalling molecules may be activating the signalling pathways during nitrogen starvation. According to that the nuclear and other organellar genome rearranges the up and down regulation of stress associated proteins at mRNA and protein level. Further the stress associated proteins may be channelling the carbon reallocation into TAG accumulation under nitrogen starvation.

In order to cope up the nitrogen stress, function of some proteins may be inhibited but the other proteins get induced or enhanced. Mapping of these SAPs clues mechanism of stress mediated lipid accumulation. Global Insilico, transcriptomic and proteomic analysis reveals many differentially expressed proteins but there is not much information is available for specific proteins. Thus the following two chapters describe about the mapping of SAPs during nitrogen starvation in *S. quadricauda*.

3.2. Materials and methods

3.2.1. Extraction of total protein from *S. quadricauda* in nitrogen starved (N⁻) and control (N⁺) conditions

For the proteomic studies, 400 ml of mid exponential phase control (N⁺) nitrogen rich and nitrogen starved (N⁻ at 24 h) *S. quadricauda* cells were centrifuged at 10000 rpm for 10 minutes at 4°C. Pellets were washed twice with double distilled autoclaved water and quickly frozen at -20°C.

For each condition, total protein was extracted from frozen cell pellets. Briefly, 1ml of lysis buffer was added to cell pellets and homogenized using liquid nitrogen in a sterile mortar and pestle. The cells were lysed by sonication in the presence of a protease inhibitor. Then the cell lysate was centrifuged at 12000 rpm for 20 minutes at 4 °C. The supernatant having soluble proteins were carefully transferred to clean autoclaved centrifuge tubes. The soluble proteins were precipitated by 10% trichloroacetic acid (TCA) and 0.07% β-mercaptoethanol, in ice cold acetone and kept overnight at -20°C. The pellets were collected by centrifugation at 12000 rpm for 20 minutes. The pellets were then washed thrice in ice cold acetone having 0.07% β-mercaptoethanol and the pellets were stored at -20°C. The total proteins were quantified by Bradford method (1976). The proteins were resolved in 12% SDS PAGE and visualized by Coomassie staining.

3.2.2. Two dimensional Poly Acrylamide Gel Electrophoresis (2D- PAGE) and mapping of SAPs

A total of 150 µl of solubilisation buffer containing the protein sample was incubated with the IPG gel strips (pH 3-10, 11cm, Bio-Rad) at 20°C for 15h. Isoelectric focusing (IEF) was initiated at 250V for 15 min, and gradually ramped to 10,000V over 5h, and remained at 10,000V for an additional 1h. After the IEF run, the strips were stored at -20°C. Before second dimension, the IPG strips were first incubated for 10 min in equilibration buffer I, and then incubated for an additional 10 min in equilibration buffer II. The second dimensional SDS- PAGE was carried out and run at 120V for 2h, followed by at 180V for 4h. The resolved proteins were stained with silver staining. Gels were scanned with a Chemi Doc ᵀᴹ MP Imaging

system (Bio-Rad). The densitometry analysis was carried out by Gel Quant software, in order to quantify the differentially expressed protein spots.

3.2.3. In-gel digestion and Peptide Mass Fingerprinting

The proteins were then subjected to in-gel digestion and peptide extraction. For that the SAP spots were excised from stained gels and transferred to micro centrifuge tubes under protease free conditions. The protein spots were destained using 200mM NH_4HCO_3 and 40% acetonitrile at 37^oC for 10 minutes. Subsequently, in-gel trypsin digestion was performed by adding 20µg/ml trypsin in 40mM NH_4HCO_3, 9% acetonitrile and 1mM HCl and incubated at 37^oC. After this step the supernatant having protein were collected for further identification by Matrix-Assisted Laser Desorption/Ionization-Time-Of Flight (MALDI-TOF).

3.2.4. Identification of SAPs by MALDI-TOF

After the in-gel digestion and peptide extraction, 1:1 ratio with 10-20 mg/ml peptide solution was spotted onto the plate for MALDI-TOF. Then the analysis was carried out using ultraflextreme MALDI-TOF/ TOF from Bruker Daltronik. Combined peptide mass fingerprinting (PMF) and MS/MS queries were performed by the MASCOT search engine against the NCBI database.

3.2.5. Gene level confirmation of SAPs in *S. quadricauda*

The identified protein sequence (protein and nucleotide) were retrieved from NCBI database. Primer sequence was designed for the particular proteins depending on the CDS sequence. The genomic DNA was isolated from *S. quadricauda* (Plant genomic DNA isolation kit, Sigma) and quantified using Nano Drop (ND 1000 spectrophotometer). The isolated DNA of *S. quadricauda* was visualized by 1% agarose gel electrophoresis. Further primer sequence was designed for the SAP2 (Stress Associated proteins 2 - Ribosomal protein L23) from the sequence of *S. obliquus* since the genome information of *S. quadricauda* was unknown. A set of primers as ORF (Open Reading Frame) specific primer and Real time primer were synthesized using clone manager software. The Ribosomal protein L23 (RPL 23) was amplified using orf specific primer (RPL23-F and RPL23-R) and real time primer (RPL23-RT-F and RPL23-RT-R) (Table. 3.1) by Polymerase Chain Reaction (PCR). PCR conditions (orf specific and real time primer) followed for amplifying RPL 23

was initial denaturation: 95°C for 5 minutes; denaturation: 95°C for 1 minute; annealing temperature: 48°C for 1 minute; extension: 65°C for 2 minutes and final extension: 65°C for 10 minutes. The amplicon was further purified and sequencing was carried out.

3.2.6. PCR product purification by Poly Ethylene Glycol (PEG)

About 50 µl of PCR amplicon was taken and to that added equal volume of PEG-8000 and mixed thoroughly by vortexing. Then the PCR and PEG mixture were incubated in a water bath at 37 °C for 15 minutes. The mixture then centrifuged at 5200 rpm for 15 minutes at room temperature. Removed the supernatant and pellet was washed with 125 µl of ice cold 80 % ethanol added to each PCR tube. Centrifuged for 2 minutes at 20 °C temperature at 3900 rpm and removed the supernatant. Dry off the pellet to remove any traces of ethanol. The pellet was dissolved in equal amount of 50 µl of nuclease free water and the concentration was quantified using Nano Drop.

3.2.7. Isolation of total RNA from control (N^+) and nitrogen starved (N^-) *S. quadricauda*

The *S. quadricauda* was grown in N^+ and N^- medium in biological triplicates. Both the samples biomass was harvested at 3, 6, 8, 24, 48 and 72 hours. The RNA was isolated using Pure Link mini kit Ambion, Life Technologies. The steps includes: collection of fresh biomass by centrifugation at 10000 rpm for 10 minutes. The working place, mortar and pestle (chilled) were wiped well with 70 % ethanol and after with RNase ZAP solution. Then the centrifuged pellets were reconstituted with the lysis buffer and immediately grind the cell using liquid nitrogen in mortar and pestle. Further the steps were followed as per the protocol. The eluted RNA was quantified spectrophotometrically. The finally eluted RNA sample was visualized in formaldehyde agarose gel electrophoresis.

3.2.8. cDNA synthesis

Resuspended 10 µg of RNA in 1x DNaseI reaction buffer to a final volume of 100 µl and add 2 units of DNase I (New England Biolabs), mixed thoroughly and incubated at 37 ºC for 10 minutes. 1 µl of 0.5 M EDTA was added prior to the heat inactivation at 75 ºC for 10 minutes. Then the DNase treated RNA was quantified

spectrophotometrically and the concentration were equalized in each sample. Further the cDNA was synthesized from the total RNA isolated from *S. quadricauda* using first strand cDNA synthesis kit (New England Biolabs).

3.2.9. Quantification of SAP2 (RPL 23) expression –Real Time PCR (RT- PCR)

The differential expression of Ribosomal Protein L23 (SAP2) was quantified using SYBR Green Real-time quantitative PCR (CFX 96^{TM} Real-Time System BIO-RAD). The reaction mix was prepared according to the protocol of DyNAmo HS SYBR Green qPCR Kit (Thermo scientific). The RPL 23 was located in chloroplast, thus organelle specific consecutive gene such as rbcl (Ribulose bisphosphate carboxylase) were used as internal control to normalize difference between the target genes. The reaction conditions were set as follows; 40 cycles of 95°C for 10 s, appropriate annealing temperature as 55°C for 1 minute, with an additional initial 5 minute denaturation at 95°C in Mini opticon Real Time – PCR system (BIO-RAD). The melt curve of temperature difference is 65- 95°C with a 0.5°C increment. The relative expression after the reaction was analysed and normalized graph were plotted using the software BIO-RAD CFX Manager.

Name of primer	Sequence	Used for
RPL23 F	5'ATGGCTGATTTTATTAAATACCCAGTAACAACTG3'	ORF specific primer
RPL23R	5'AAATTGAATAGATTGACCTTCTTTTAATGTTAAAATTAC3'	
RPL 23-RT-F	5'CATTTGATGTTGATTTACGATTAACAAAACCTC3'	Real time PCR
RPL 23-RT-R	5'CCAGCACGTACTTTTTTTCGTGGTGG3'	
RBCL-RT-F	5' GCTCAGTCTGAAACTGGTGAAATTAAAGGTCACTACTTAAACGC3'	Internal control for RT PCR
RBCL-RT-R	5' CCTGAGTGTAAGTGGTCACCACCTGACAGACGAAG3'	

Table. 3.1: List of primers used for amplification of Ribosomal protein L23

3.3. Results

3.3.1. Identification of SAPs during nitrogen starvation

The total proteins of nitrogen starved (N⁻) *S. quadricauda* were resolved using 12% SDS PAGE to view the change in protein profile of the respective conditions. The pattern of protein separation showed a marked difference in the gel (Fig. 3.1). Although there is a marked difference in SDS- PAGE protein bands cannot be identified. Thus 2D- PAGE was performed and it revealed the up regulated and down regulated protein spots in the control (N⁺) and nitrogen starved (N⁻) conditions. The differentially expressed protein spot on the 2D gel was named as nitrogen Stress Associated Proteins (SAP) and densitometry analysis was done by Gel Quant software (as described in materials and methods 3.2.2). There are about 10 protein spots marked as SAP (Fig. 3.2) in both N⁺ and N⁻ conditions. In that, SAP 1, 2 and 7 were present only in nitrogen starved condition. SAP 3 was about 11 fold up regulated in nitrogen starved *S. quadricauda*. The down regulated protein SAP 10 was 10.27 fold down regulated in nitrogen stressed condition. The other proteins SAP 4, 5, 6, 8 and 9 were down regulated as 1, 1.85, 1, 2.7 and 2.3 fold respectively (Table. 3.2 &Fig. 3.3). Thus the 2D profile of nitrogen starved sample indicates that there is a marked difference in the protein expression when compared to nitrogen rich condition.

SAP 1-5 protein spots were excised from the 2D gel and analysed by MALDI-TOF (Scheme. 3.1). The MASCOT analysis revealed possible matches of protein mass ratio of SAP 1 as mitochondrial ORF 151 protein, SAP 2 as ribosomal protein L23 (RPL 23) and SAP 3 as envelope membrane protein in *Acutodesmus obliquus*. The SAP 4 shows matches with ATP synthase β subunit of *Scenedesmus quadricaudus* (Table. 3.3). Further studies were carried out with SAP 1 and SAP 2.
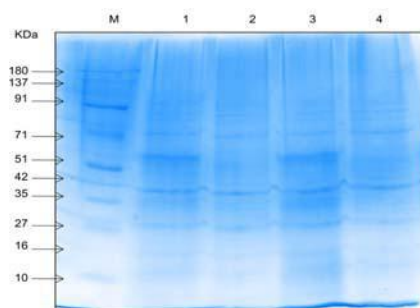
Fig. 3.1: Total protein profile of control (N⁺) and nitrogen starved (N⁻) *S. quadricauda*. M; Marker, Lane 1 and 3: control protein samples in 50 and 100 μg; Lane 2 and 4: nitrogen starved protein samples in 50 and 100 μg.
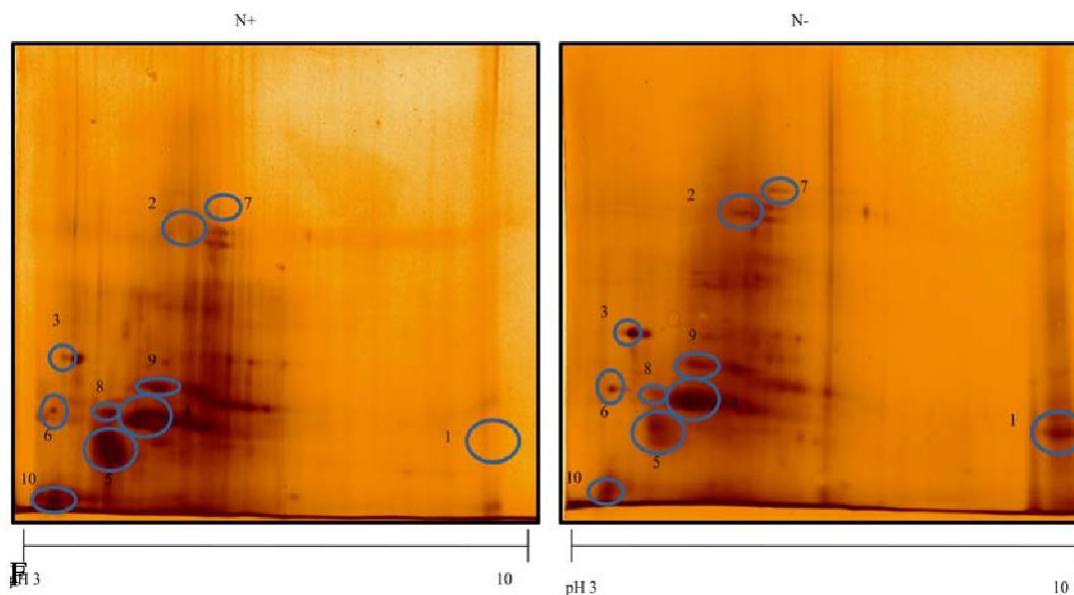
Fig. 3.2: Protein profiling of control (N^+) and nitrogen starved (N^-) *S. quadricauda* by 2D- PAGE. The total protein samples were precipitated by TCA- Acetone method and the pelleted protein were redissolved in rehydration buffer. The normalized protein sample were subjected to Isoelectric focusing in pH 3-10, 11 cm IPG strips and further visualized by SDS - PAGE.

Stress Associated Proteins	N+	N-
SAP-1	-	+
SAP-2	-	+
SAP-3	1	11.06
SAP-4	1	-1.09
SAP-5	1	-1.85
SAP-6	1	-1.14
SAP-7	-	+
SAP-8	1	-2.7
SAP-9	1	-2.26
SAP-10	1	-10.27

Table. 3.2: Densitometry quantification of Nitrogen Stress Associated Proteins expression during nitrogen stress (SAP 1-10). SAP 1, 2 and 7 are only expressed in the N^- condition. Though the differential expression of these proteins cannot be calculated by densitometrically.
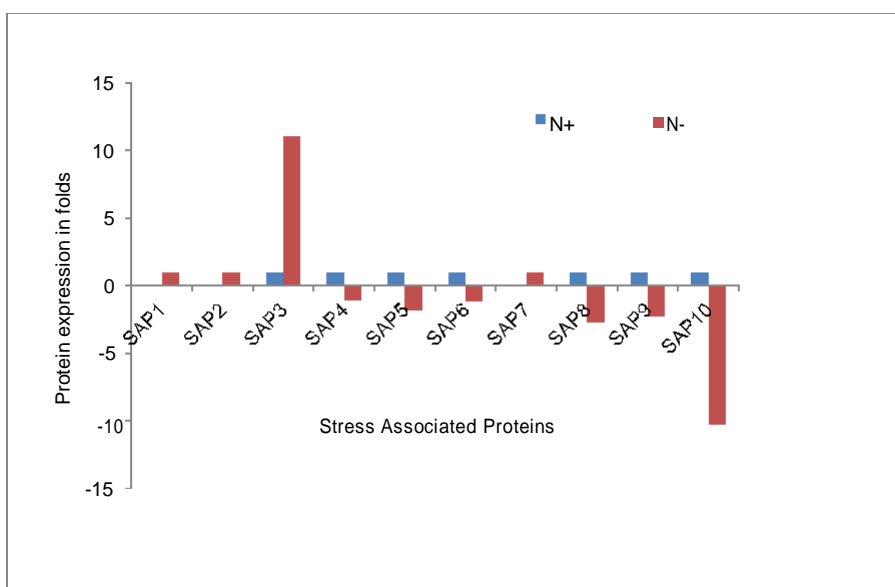
 Fig. 3.3: Densitometry quantification of Nitrogen Stress Associated proteins (SAP 1-10). The X axis represents the stress associated proteins and Y axis represents the protein expression in folds.
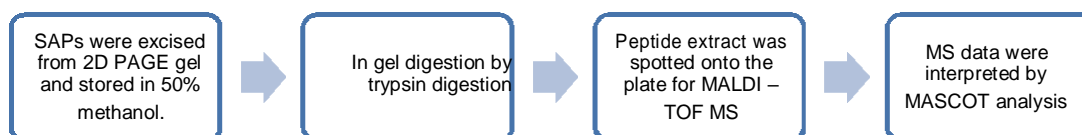
Scheme. 3.1: Flow chart describing the mapping of stress associated proteins in nitrogen deficient *S. quadricauda.*

Spot ID	GI Number /Name	Mass
SAP1	gi|7711048 ORF151 (mitochondrion) [*Acutodesmus obliquus*]	17943
SAP 2	gi|124021007 Ribosomal Protein L23(Chloroplast) [*Acutodesmus obliquus*]	10496
SAP 3	gi|108773073 Envelope membrane protein (chloroplast) [*Acutodesmus obliquus*]	50073
SAP4	gi|23503589 ATP synthase beta-subunit, partial (chloroplast) [*Scenedesmus quadricaudus*]	40772

Table. 3.3: Mapping of nitrogen stress associated proteins in *S. quadricauda* by MALDI-TOF.

3.3.2. Gene level confirmation of RPL 23 in *S. quadricauda*

The MALDI- TOF analysis of stress associated proteins revealed SAP 2 as ribosomal protein L23 (RPL 23) of *Scenedesmus obliquus*. Then the protein and nucleotide sequence of ribosomal protein L23 were retrieved from NCBI. In order to confirm these proteins at gene level the primers were designed based on the RPL 23 sequence of *S. obliquus* in *S. quadricauda*. The ribosomal protein L23 was amplified using ORF specific primer, RPL23-F& RPL23-R and real time primer (RPL23-RT-F & RPL23-RT-R) yielded amplicon size of about 270 bp and 121 bp respectively (Table. 3.1; Fig. 3.4 a & b). Further the 270 bp product was purified by Poly Ethylene Glycol PCR product precipitation method as the amplicon is having a single product. The purified DNA has 40 ng/µl with a 260/280 of 1.82. Then the purified PCR product of RPL 23 was subjected for sequencing (Fig. 3.4c). The trimmed sequence of RPL 23 was then aligned for sequence similarity by NCBI-nBLAST, CLUSTAL W2 pair wise alignment tool. The sequence similarity by nBLAST showed about 90 % identity to *Scenedesmus obliquus* (Fig. 3.5). The alignment results showed that 70.4% identity to the RPL 23 of *Acutodesmus obliquus* (Fig. 3.6).

C

Ribosomal Protein L23 (RPL23) Forward (211 bp)

5'TTATTTAAAATAAACAATACACATTTGATGTTG
ATTCAAGATTAACAAAACCTCAAATCAAAAAATT
ATTTGAAACATTATTTGGTGTAAATGTTATTGGA
ATTAACACGCATAGACCACCTCGAAAAAAAGTT
GTACTGGAACATCAACTGGTTATAAACCAGCAT
ATAAAAGAGTAATTTTAACATTAAAAGAAGGTCA
ATCTATTCA3'
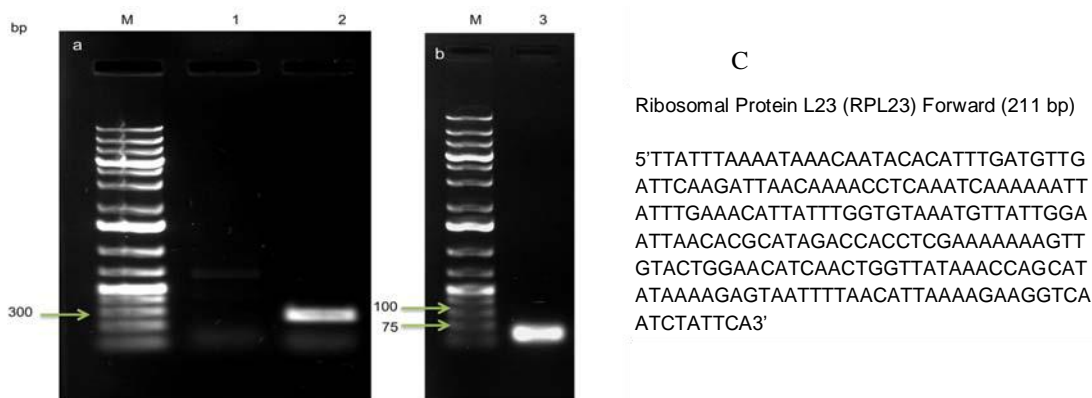
Fig. 3.4: Gene level confirmation of Ribosomal protein L23 in *S. quadricauda.* a) M: Marker; lane1: SAP1; lane 2: SAP2 (RPL 23) amplification with ORF specific primer; b) lane 3: RPL 23 amplification with real time primer and c) represents the trimmed sequence of RPL 23 in *S. quadricauda*.
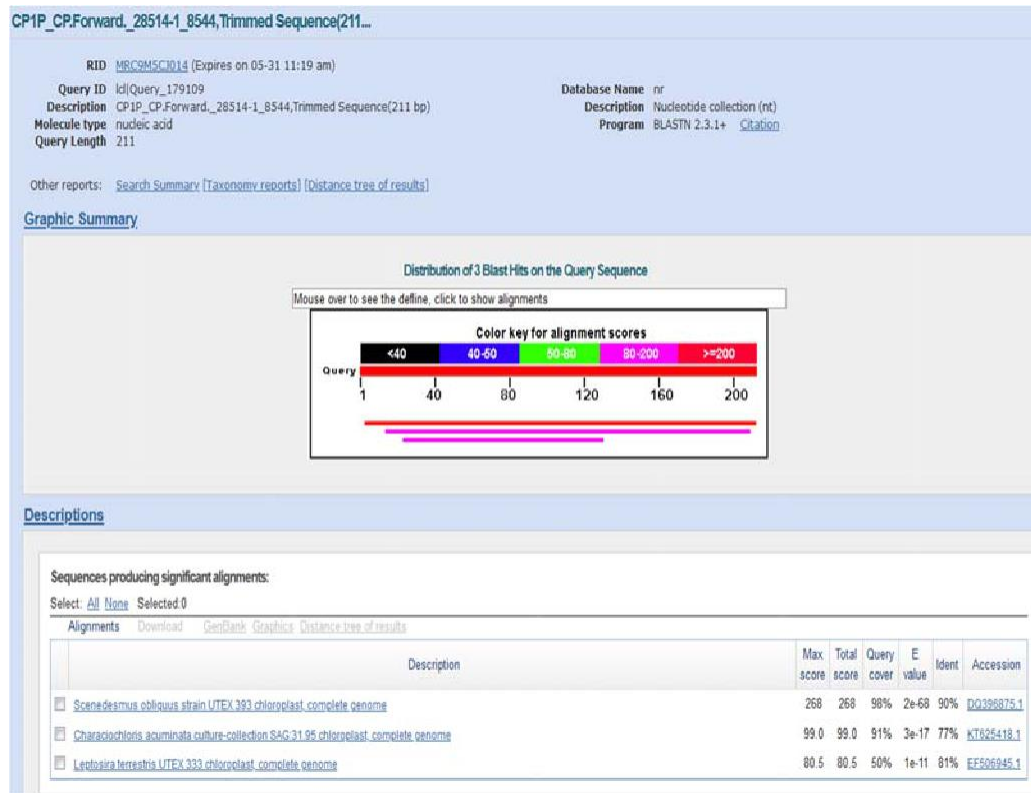
Fig. 3.5: Sequence similarity searches for sequence of RPL 23 by nBLAST.
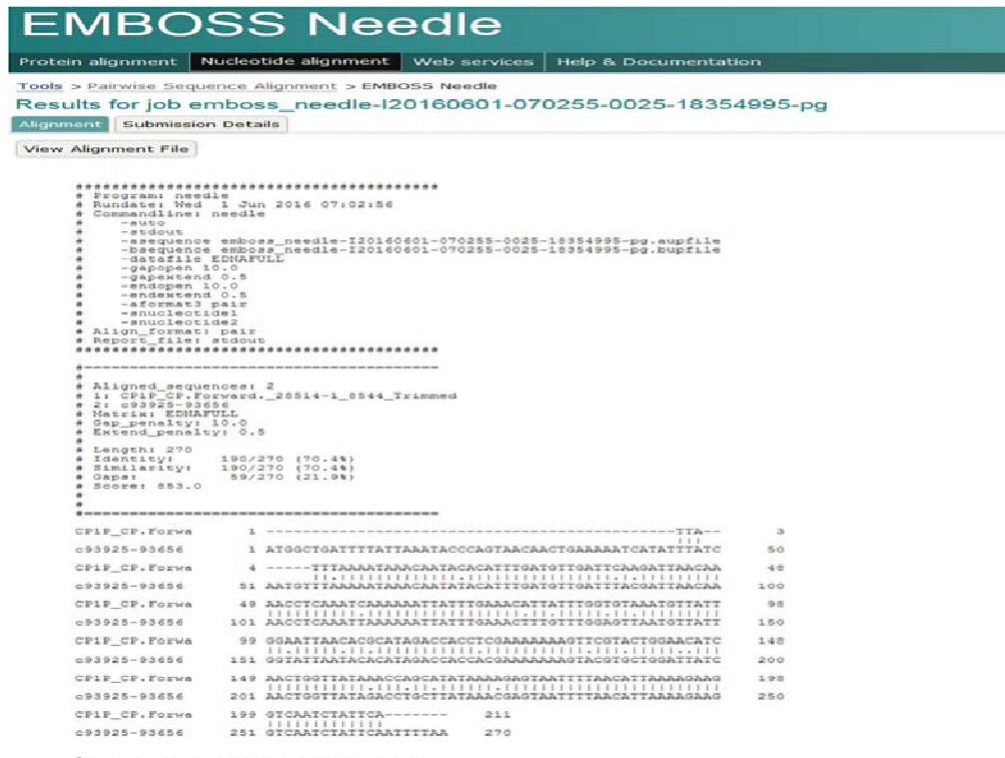
Fig. 3.6: Sequence alignment of RPL 23 by CLUSTAL W2.

L23 **3.3.3. RPL 23 and its characteristics**

Ribosomal proteins have conjunction with rRNA and make up the ribosomal subunits involved in the translation process. The RPL 23, its function and other characteristics were searched in Uniprot and PDB server. The molecular function of RPL 23 was described as rRNA binding, and it specifically binds to 23 S rRNA and is involved mainly in translation. It has a molecular weight of 10317 Da and it is a part of the 50 S ribosomal subunit (Fig. 3.7). The RPL 23 was located in chloroplast and mainly comes in the family of universal ribosomal protein uL23. The previous reports about RPL 23 in plants suggest that they have a role in abiotic stress. The individual protein was not yet studied and also its role during nitrogen starvation is an interesting area to elucidate.

SAP 2 [Ribosomal Protein L23 (RPL 23)]
Function   : Binds to 23srRNA
Molecular function : rRNA binding
Biological process   : Translation
Molecular size   : 10317Da
Subcellular location: Chloroplast
Interaction   : part of the 50s ribosomal subunit
Family &Domain   : universal ribosomal protein uL23 family.
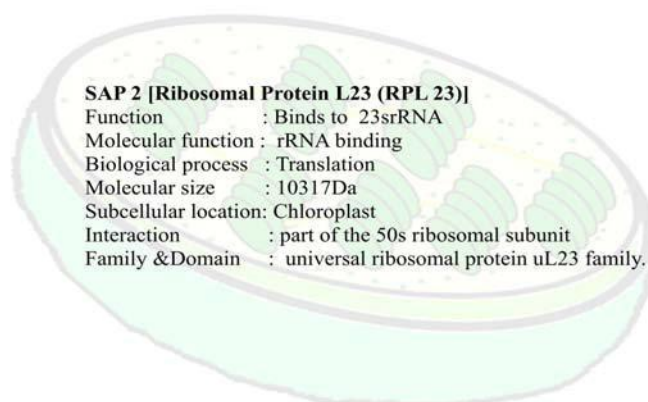
Fig. 3.7: Characteristics of SAP 2 [Ribosomal protein L23 (RPL 23)] and its basic information from Uniprot and PIR.

3.3.4. Quantification of differential expression of RPL 23

For quantifying the differential expression of RPL 23, RNA samples were extracted at 3, 6, 8, 24, 48 and 72 hours from nitrogen starved (N^-) and control (N^+) *S. quadricauda* (Fig. 3.8). The DNase treated RNA was used for synthesis of cDNA (Table. 3.3). The time course $\Delta\Delta$Ct curve analysis of Ribosomal protein L23 showed that the gene was up regulated to 2.6 fold at 6 hours in nitrogen stress induced samples compared to control. After that there is a sharp decline in the expression of RPL 23 (0.47) during 8 hour of nitrogen stress induction (Fig. 3.9). The rbcl gene of chloroplast was used as internal control for normalizing differential expression of ribosomal protein L23. The RBCL gene was amplified using primers of RBCL-RT-F and RBCL-RT-R (Table. 3.1).
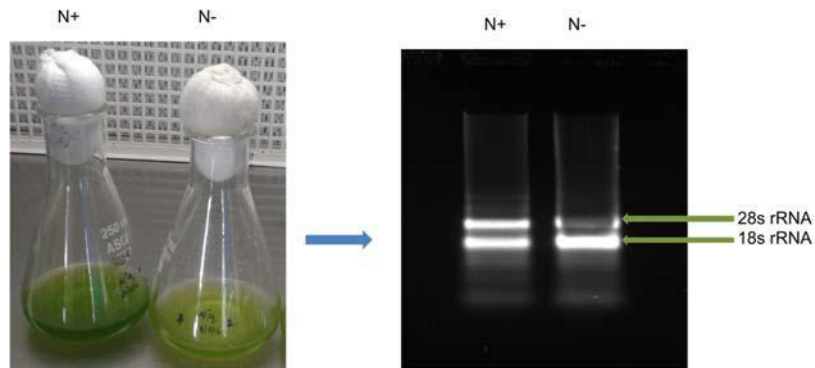
Fig. 3.8: Total RNA isolation from *S. quadricauda*. RNA was isolated from nitrogen sufficient (N+) and nitrogen deficient (N-) *S. quadricauda*, further visualized in formaldehyde agarose gel.

Sl.No.	Sample	Concentration (ng/µl)	260/280
1	N$^+$ 3hr	127.8	2.20
2	N$^-$3hr	182.2	2.22
3	N$^+$ 6hr	472.4	2.16
4	N$^-$6hr	292.8	2.20
5	N$^+$ 8hr	759.3	2.23
6	N$^-$8hr	504.6	2.16
7	N$^+$ 24hr	229.2	2.10
8	N$^-$24hr	87.8	2.06
9	N$^+$ 48hr	149.0	2.23
10	N$^-$48hr	167.9	2.09
11	N$^+$ 72hr	537.8	2.10
12	N$^-$72hr	133.5	2.09

Table. 3.4: Total RNA isolation from control (N+) and nitrogen starved (N-) *S. quadricauda*. Concentration of RNA and quality were assessed using spectrophotometer.
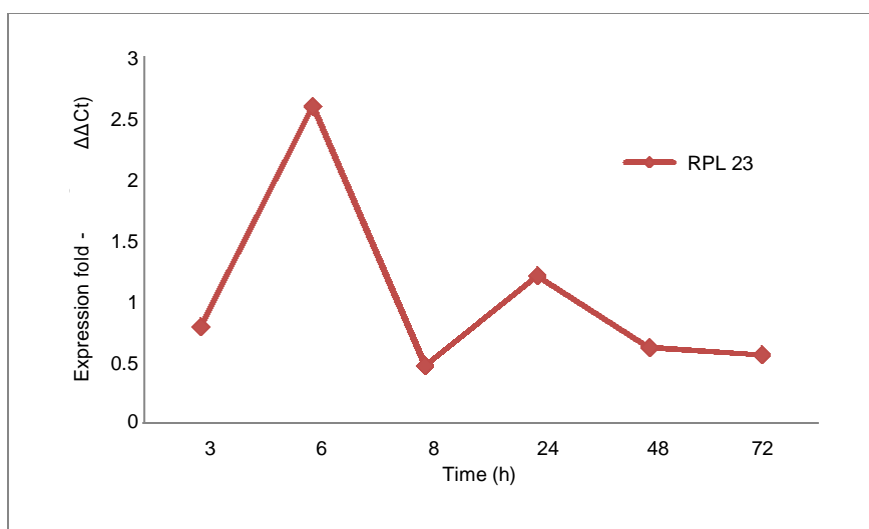
Fig. 3.9: Differential expression and quantification of RPL 23 by RT-PCR using control (N+) and nitrogen starved (N-) cDNA of *S. quadricauda*.

3.4. Discussion

Nitrogen stress causes halt in cell division followed by metabolic rearrangement in microalgae. In order to cope up the stress microalgae alters protein expression. It is governed through inhibition of functional protein by down regulation of genes, and other proteins get induced by up regulation of genes. Proteomics has been an effective omics study to study the changes in protein during induced and uninduced conditions (Zhao et al., 2016). In order to visualize the differential expression of proteins MALDI-TOF analysis along with large 2 Dimensional gel electrophoresis has become a powerful tool (Castielli et al., 2009).

De Lomana et al., 2015 proposed a mechanistic model of Transcriptional Regulatory Network (TRN) controlling the lipid accumulation during nitrogen stress. When *C. reinharditi* was subjected to nitrogen starvation, the early stress response was triggered within 12 minutes. The early nitrogen stress response activated key signaling pathways while simultaneously preparing the lipid accumulation for later stages and ubiquitin mediated protein degradation (De Lomana et al., 2015). Similarly, proteomics is also employed for studying the effects of nitrogen starvation in *C. reinharditi* (Wase et al., 2015), *Nannochloropsis oceanica* (Dong et al., 2013) and *Chlorella protothecoides* (Gao et al., 2014).

Further one of the nitrogen stress associated protein in *S. quadricauda* was identified as RPL 23 (Chloroplast). Generally ribosome biogenesis is a tightly organized multistep process, at that time ribosomal proteins are synthesized in the cytoplasm and immediately transported to the nucleolus where they are assembled into the pre-ribosome with the rRNA. According to Zhang and Lu, 2009; Zhou et al., 2012 and Zhou et al., 2015 when ribosomal stress or nucleolar stress occurs it resulted in accumulation of ribosome free form of ribosomal proteins. The ribosomal stress was induced by disturbances in any of the steps in ribosome biogenesis. The ribosomal stress causing stimuli are (i) chemical agents or radiation, (ii) lack of nutrients including serum or glucose starvation and (iii) gene deregulation.

The RPL 23 was not studied in microalgae particularly under nitrogen starvation. Thus the available information of RPL 23 during abiotic stress was reported in plants. Chloroplat ribosomal proteins have a major role in plant growth and development. But the functions of individual ribosomal proteins remain unknown. Zhang et al., 2016 reported that ribosomal protein S5 (RPS 5) in translation, other than that it is involved in photosynthesis and cold stress resistance in *Arabidopsis*.

3.5. Conclusion

Scenedesmus quadricauda when exposed to nitrogen stress leads to TAG accumulation with a drastic reduction in total protein. The total protein pattern of nitrogen sufficient and deficient showed a differential expression of proteins. Those nitrogen Stress Associated Proteins (SAPs) were identified as mitochondrial orf 151 (SAP 1), Ribosomal protein L23 (RPL 23) (SAP 2), envelope membrane protein (SAP 3) and ATP synthase β subunit partial (SAP 4) of *S. obliquus*. From these identified proteins, RPL 23 was confirmed at gene level in *S. quadricauda*. Further the differential expression quantification of RPL 23 revealed an up regulation of the mRNA at 6 hour of nitrogen stress induction i.e., in the early stage of nitrogen starvation in *S. quadricauda*. But the actual role of RPL 23 during nitrogen starvation is a curious study to elucidate the relation between stress biology and ribosomal proteins.

CHAPTER

4

Mapping of nitrogen stress
associated proteins

b) LAGLIDADG Homing

Endonuclease

4.1. Introduction

The lipid biosynthetic pathway may play a major role in the abiotic stress response, in addition to functioning as carbon and energy reserve under environmental stress conditions in algae (Hu et al., 2008). The metabolic rearrangement of carbon and lipid pathways may be activated by the stress response genes during environmental harsh condition. The major evidences for the query covers different omics approaches like transcriptomics, proteomics, lipidomics and metabolomics which explains the key regulators and proteins for TAG accumulation under nitrogen starvation (Guarnieri et al., 2011). The individual stress response proteins and its function during nitrogen starvation are poorly studied.

The Nitrogen Stress Associated Protein 1 (SAP1) was identified as mitochondrial ORF 151 of *S. obliquus*. SAP1 got more interest for further study as it is from mitochondrial origin. Mitochondria are the energy house of a cell and are principal regulators of cellular function and metabolism. They produce ATP and regulate energy homeostasis, Ca homeostasis, apoptosis and fatty acid oxidation. In addition to that, they also play a major role in signaling through the production of Reactive Oxygen Species that mediate redox signaling (Hill and Remmen, 2014). Mitochondria are thought to have originated from an alpha-proteobacterial ancestor that was engulfed by a primitive eukaryotic host. The mitochondrial genes were either transferred to nucleus or lost completely (Barbrook et al., 2010), thus exhibiting a limited number of genes in the genome. The structural alignment of mitochondrial genome varies among eukaryotic lineages; whereas the common structure is a contiguous circular DNA molecule (Gray et al., 2012). Two types of mitochondrial genomes have been reported in green algal lineages (Nedelcu et al., 2000). i) The *Chlamydomonas*- like type having a small genome size (16-25 kb), limited gene content and rRNA coding regions. ii) The *Prototheca* – like type having a larger genome size (45-55 kb), a more complex set of protein- coding, tRNA and rRNA genes (Nedelcu et al., 2000; Nedelcu 1998; Gray et al., 1998; Turmel et al., 1999).

LAGLIDADG Endonuclease was differentially expressed in *S. quadricauda* during nitrogen starvation as a stress associated protein. LAGLIDADG endonuclease comes under the Homing endonuclease (HE) family. Homing involves an intervening sequence that is being copied into a cognate allele that lacks it. LAGLIDADG

Homing Endonuclease (LHE) are highly specific DNA-cleaving enzymes that recognize long DNA sequences and generate double strand breaks. They are also known as mega nucleases, which are highly sequence-specific enzymes with recognition sequence ranging from 12-45 bp in length. HEs are grouped into several families, of which LAGLIDADG family is the most abundant. Members of the LAGLIDADG family are of two types. Enzymes that contain a single LAGLIDADG motif, such as I-Cre I and I-Ceu I act as homodimer and recognize consensus DNA target sites. Enzymes that have two LAGLIDADG motifs act as monomers. For example I-Cre I is active when a divalent cation (Ca^{2+}) is bound to its active site (D20). Further the LHE conformational change observed in two loop regions. Residues of 29-37 connects β1, β2 strand to participate in DNA binding and it donates side chains (Asn-30, Ser-32, and Tyr-33) to nucleotide contacts at the ends of the homing site in Cre-I and finally together with many conformational change they performs the DNA cleavage (Jurica et al., 1998).

Mitochondrial stress responsive genes include ion and water transporters, ROS scavengers, signaling and transcriptional regulation. Mitochondria and chloroplasts are the primary sites for the production of the ROS (Date et al., 2000; Van Breusegem et al., 2001). The cells under stress initiates stress adaptive mechanisms by stress response inducers like signaling molecules for survival. During that time the cell defense mechanism is mainly controlled by the expression of stress responsible genes and proteins. One such gene is SAP1, its expression and relevance in *S. quadricauda* during nitrogen starvation is reported in the present study. The over expression of protective genes might help to reduce the deleterious effects of the abiotic stress.

Like chloroplasts, mitochondria also generate retrograde signals that are crucial for stress responses. Mitochondrion produces ROS and many metabolites, some of which may serve as retrograde signals (Ng et al., 2014). For example, mitochondrial DEXH box RNA helicase or mitochondrial pentatricopeptide repeat protein dysfunction causes ROS accumulation and plant stress hormone abscisic acid (He et al., 2012). Mitochondrial Retrograde Signaling (MRS) communicates the dysfunctional mitochondrial status to the nucleus and triggers subsequent induction of genes encoding proteins involved in recovering mitochondrial functions. Plant MRS mainly targets nuclear transcripts involved in protein synthesis, photosynthetic light reactions and plant pathogen interactions (Schwarzlander et al., 2012). The signaling

sources of MRS include ROS, redox and calcium (Rhoads, 2011). Protein kinases such as CDKE1 (Ng et al., 2013) play important roles in MRS transduction via phosphorylation cascades that respond to the stress (Kovtun et al., 2000). Stress responsive transcription factors such as WRKY, bZIP and Dof families (Zhang et al., 1994; Chen et al., 2002) are potential candidate for MRS in regulating nuclear gene expression. With this accumulating knowledge, the actual sensors within the organelle and the secondary messengers of the signaling cascades involved in nitrogen stress mediated lipid accumulation are still largely unknown.

4.2. Materials and methods

4.2.1. Confirmation of SAP 1 in *S. quadricauda*

The identified protein sequence (protein and nucleotide) were retrieved from NCBI database. The genomic DNA was isolated as described in materials and methods of chapter 3.2.5. Further primer sequence was designed for the SAP1 (Stress Associated proteins 1- Mitochondrial ORF 151) from the sequence of *S. obliquus* since the whole genome of *S. quadricauda* was not yet sequenced. A set of primers as ORF (Open Reading Frame) specific primer and Real time primer (Mt151-F & Mt151-R; Mt151-IP-F & Mt151-IP-R) were synthesized using clone manager software (Table. 4.1). Along with these primer sets, housekeeping gene primers such as COX1-RT-F & COX1-RT-R were also synthesized (Cox1) as internal control for the expression analysis (Table. 4.1). The mitochondrial orf 151 was amplified using ORF specific primer by PCR. PCR conditions (ORF specific) followed for amplifying ORF 151 was subjected to initial denaturation: 95°C for 5 minutes; denaturation: 95°C for 1 minute; annealing temperature: 52°C for 1 minute; extension: 75°C for 1 minutes and final extension: 75°C for 10 minutes. The ORF specific primer should give a product of 500 bp instead it was obtained as a 700bp product. Similarly the other primers also tried to amplify ORF 151 in *S. quadricauda*. But the amplification of mitochondrial ORF 151 failed in *S. quadricauda*. Since sequence homology based primer of *S. obliquus* are different from *S. quadricauda*, thus we decided to go for mitochondrial genome sequencing of *S. quadricauda* CASA CC202 at Genotypic Technologies.

4.2.2. Mitochondrial Genome Sequencing of *S. quadricauda* CASA CC202

Illumina NextSeq500 Paired-end sequencing with 150*2 was used for the mitochondrial genome sequencing of green microalgae *Scenedesmus quadricauda*. The Illumina paired end raw reads were quality checked using Fast QC1. Illumina raw reads were processed by in-house Perl script for adapters and low quality bases trimming towards 3'-end.

Assembly of Illumina Next Seq data was carried out with SPAdes-3.5.02; the assembled contigs were scaffolded using SPAdes built in scaffolding program. Protein-coding genes were predicted using GeneMarkS 4.283/ ORFfinder7. Predicted proteins were annotated by the homology search against NCBI NR database using BLAST-2.5.04. rRNA prediction was performed using RNAmmer-1.25/ RNAweasel8 and one rRNAs was predicted. tRNA genes were predicted using tRNAscan-SE-1.216 (Scheme. 4.1).
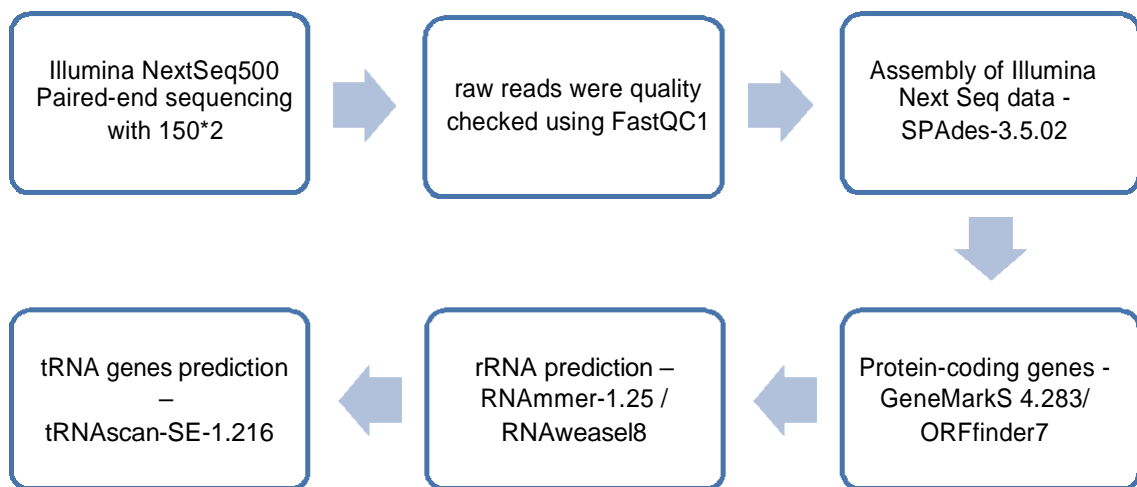
Scheme. 4.1: Protocols for whole mitochondrial genome sequencing of *S. quadricauda* CASA CC202.

4.2.3. Conservation of *S. quadricauda* mitochondrial genome

In order to construct phylogenetic tree Sequences were aligned with MUSCLE. After alignment, ambiguous regions (i.e. containing gaps and/or poorly aligned) were removed with Gblocks. Forty mitochondrial genome of different microalgae were collected from NCBI (Table. 4.4). The phylogenetic tree was reconstructed using the maximum likelihood method implemented in the PhyML program. The HKY85 substitution model was selected assuming an estimated

proportion of invariant sites (of 0.069) and 4 gamma-distributed rate categories to account for rate heterogeneity across sites. The gamma shape parameter was estimated directly from the data (gamma=0.835). Reliability for internal branch was assessed using the aLRT test (SH-Like). Graphical representation and edition of the phylogenetic tree were performed with TreeDyn.

4.2.4. LAGLIDADG Endonuclease motif search and structure prediction in *S. quadricauda*

The predicted protein sequences of *S. quadricauda* whole mitochondrial genome were searched for LAGLIDADG motif using NCBI Conserved Domain Search –NIH. Then the protein sequence of LAGLIDADG Endonuclease in microalgae was retrieved from NCBI and sequence aligned using CLUSTAL W2. The secondary structure of LAGLIDADG endonuclease was predicted by Swiss model and Phyre.2.0 software. The predicted secondary structure was validated by Ramachandran Plot. The LAGLIDADG Endonuclease structure was aligned using PYMOL software. As the LHE is an endonuclease it binds to the DNA, therefore DNA binding sites were determined by Protein Predict software. Molecular weight and amino acid composition of LHE were calculated by Protein Information Resource (PIR).

4.2.5. Gene level confirmation of LAGLIDADG Homing Endonuclease (LHE) in *S. quadricauda*

The LHE gene was amplified using the isolated *S. quadricauda* DNA (Materials and methods 3.2.5). The reaction condition was as follows, for ORF specific primer (LAL-ORF-F & LAL-ORF-R) initial denaturation of 95 °C for 5 minute, denaturation at 95 °C for 1 minute, annealing at 58 °C for 1 minute, extension at 72 °C for 1 minute and final extension as 72 °C for 10 minutes (Table. 4.1). Since the ORF specific primer not covering the full length sequence of LHE. Therefore the primers were designed 300 bps away from LHE in both upstream and downstream. Further the upstream downstream primers (LAL-UD1F & LAL-UD1R; LAL-UD2F & LAL-UD2R) were used in order to get full length of the sequence (Table. 4.1). The PCR reaction conditions as initial denaturation of 95 °C for 5 minute, denaturation at 95 °C for 1 minute and 15 seconds, annealing at 50 °C for 1 minute, extension at 72 °C for 1 minute and final extension as 72 °C for 10 minutes. Then the amplicons

sequence confirmed by Sanger's sequencing method. Then the LHE gene sequence was submitted in GenBank - NCBI, a public gene repository.

4.2.6. Expression analysis of LAGLIDADG endonuclease by RT- PCR

The RNA was isolated from control (N^+) and nitrogen starved (N^-) *S. quadricauda* and treated with DNase to remove the genomic DNA. The cDNA was synthesized as explained in materials and methods (Chapter. 3.2.8). The differential expression of LHE (SAP1) was quantified by SYBR Green Real-time quantitative PCR (CFX 96^{TM} Real-Time System BIO-RAD) using the real time primer sets such as LAL-RT1-F & LAL-RT1-R; LAL-RT2-F & LAL-RT2-R (Table. 4.1). COX1 (COX1-RT-F & COX1-RT-R) was used as internal control to normalize differences between the target genes as LHE is from mitochondrial origin (Table. 4.1). The reaction conditions were set as follows; 40 cycles of 94°C for 10 s, appropriate annealing temperatures for 30 s, and 72°C for 30 s, with an additional initial 15 minute denaturation at 95°C and a 5-minute final extension at 72°C. The relative expression was analysed and the normalized values were plotted as a graph using the software BIO-RAD CFX Manager.

4.2.7. Cloning of LAGLIDADG endonuclease of *S. quadricauda*

4.2.7.1. Restriction digestion of LHE and plasmid DNA

The LHE gene was amplified using primer (LAL-C-F & LAL-C-R) with restriction sites of BamHI and HindIII (Table. 4.1). The PCR conditions were set to be, initial denaturation of 95 °C for 5 minute, denaturation at 95 °C for 1 minute, annealing at 58 °C for 1 minute, extension at 72 °C for 1 minute and final extension as 72 °C for 10 minutes. The amplicon were visualized in agarose gel and purified by gel extraction kit (Qiagen). Simultaneously plasmid DNA of pET28a was isolated from *Escherichia coli* BL21DE3 cells using Plasmid DNA isolation kit (Mini prep isolation kit-Qiagen). The plasmid DNA and LHE gene concentration was quantified using Nano Drop (ND1000- Spectrophotometer). Plasmid DNA and LHE gene were then double digested with restriction enzymes as BamHI and HindIII. For 1 µg of DNA 1µl of enzymes were added and incubated at 37 °C for 1 h. After that the double digested plasmid DNA and LHE were gel extracted and purified. The purified

LHE and plasmid DNA of pET-28a were ligated using Quick T4 DNA ligase (New England Biolabs) for 5 minutes at 25 ℃.

4.2.7.2. Transformation and antibiotic selection of transformants

E. coli BL21DE3 competent cells were transformed with 10 µl of ligated product and by heat shock at 42 ℃ for 60 seconds. The tubes were kept back in ice after the heat shock for 3 minutes. The transformants were revived by adding 900 µl of Luria Bertani (LB) broth and incubated at 37 ℃ for 2h, 200 rpm. After incubation the tubes were centrifuged at 8000 rpm for 2 minutes and the pellet were dropped on to an LB plate with Kanamycin selection (100µg/ml). The positive transformants were analysed by colony PCR. Further the plasmid DNA was isolated from positive clones and PCR was carried out using vector and LHE primer sets LAL-C-F & LAL-C-R (Table. 4.1). Then the plasmid DNA was double digested with BamHI and HindIII, to observe the insert release and gene orientation analysis. Also it was confirmed by sequencing. The sequencing results of clone plasmid DNA with LHE gene was then aligned using CLUSTAL W2 pair wise alignment method.

4.2.8. Clone over expression in *Escherichia coli*

A culture of each clone carrying a LHE gene was grown in LB broth (50 ml) at 37 ℃, 200 rpm. At mid-exponential phase (0.6 OD at 600 nm) gene expression was induced by adding IPTG to a final concentration of 1mM. Cells were further incubated for 3 hour and collected by centrifugation at 8000 rpm for 5 minutes. Then the pellet of uninduced and induced cultures were resuspended in 1.5 ml of ice cold buffer containing 50 mM Sodium phosphate buffer pH-8.0, 0.5 mM NaCl and 1 mM PMSF. The resuspended cells were disrupted in an ultra sonicator with the following conditions pulser 1s on off cycle, 30 % amplitude at 4 ℃ until the cell turbidity becomes clear. Then the tubes were centrifuged at 12000 rpm for 30 minutes at 4 ℃. Carefully collect the supernatant and pellet separately and keep the samples at 4 ℃. The protein concentration of the cell lysate was quantified by Bradford method (1976). Then the normalized protein samples were visualized in a 12 % SDS- PAGE followed by Coomassie staining.

Name of primer	Sequence	Used for
Mt151-F	5'ATGCTGCCACCTTTTCTTTTTGAAG3'	Orf 151 of *S. obliquus* amplification in *S. quadricauda*
Mt151-R	5'TGAGCTCTTCAACTATTTGAATATTTTCTTTTTG3'	
Mt151-IP-F	5'GATTGGGAGATAGGAGTTAGTATACCACTAAAA CAAAAGGCTC3'	Orf 151 of *S. obliquus* amplification in *S. quadricauda* for real time PCR
Mt151-IP-R	5'GAGTAAATCCCATTGTTCTCTAAATAATTTCGTTA TTTTCTGC3'	
SQORF42-F	5'ATGAAGGTGTCTCCGATCGACTCTAGTG3'	Amplification of ORF 42 in *S. quadricauda*
SQORF42-R	5' TTAATTCTTGTTATTCAGACTATCCAGATGCTCCC3'	
LAL-UD1F	5'CTTTCCTTTGGCAGCAAAGC3'	Full length amplification of LHE by upstream downstream primer
LAL-UD1R	5'ACTAGTAAACGGCAACTAGC3'	
LAL-UD2F	5'GTAGTTACTTGGCGGGATTG3'	Full length amplification of LHE by upstream downstream primer
LAL-UD2R	5'GCACCAATCATTACGGGAAC3'	
LAL-RT1-F	5'CGAGTACAAACCACATATCG3'	LHE amplification for RT- PCR
LAL-RT1-R	5'AGGAAGTGTAAGATTTACCC3'	
LAL-RT2-F	5'CGAGTACAAACCACATATCG3'	LHE amplification for RT- PCR
LAL-RT2-R	5'ACAGGAAGTGTAAGATTTACC3'	
COX1-RT-F	5'CCTCTCTTTGTATGGGCATTGTGCTTTGTAAG3'	Consecutive primer for RT PCR
COX1-RT-R	5'GGTGAGCCCACACCTAGAACCCCTACACG3'	
MTCOX2-RT-F	5'GGAGGGGATCTCTGATTTGAATGCAGAC 3'	Consecutive primer for RT PCR
MTCOX2-RT-R	5'GACGACCAATAACTTTAACAGTTAGCATGGGC3'	
LAL - C-F	5'GGATCCATGAAGGTGTCTCCGATCGACTCTA GTG3'	LHE amplification with the Restriction sites of Bam HI and HindIII for cloning in pET28a vector
LAL-C-R	5'AAGCTTTTAATTCTTGTTATTCAGACTATCCAGA TGCTCCC3 '	

Table. 4.1: List of primers used for amplification of LHE.

4.3. Results

4.3.1. Gene level confirmation of SAP 1 in *S. quadricauda*

The MALDI- TOF analysis of stress associated proteins revealed that SAP 1 as mitochondrial ORF 151 of *Scenedesmus obliquus*. Then the protein and nucleotide sequence of ORF 151 was retrieved from NCBI. In order to understand the biological function of ORF 151 the primers were designed (Mt151-F & Mt151-R) based on the ORF 151 sequence of *S. obliquus* in *S. quadricauda* (Table. 4.1). The ORF 151 PCR amplification was failed even with a different primer set, which is specific to the middle region (Mt151-IP-F & Mt151-IP-R) (Table. 4.1, Fig. 4.1). Although *S. obliquus* and *S. quadricauda* belongs to same genera, the PCR didn't yield any product (Fig. 4.1a & b) or nonspecific bands (Fig. 4.1c) even with different set of primers. Perhaps due to the sequence variation between these microalgae the expected size of PCR product was not obtained. Therefore in order to obtain the exact SAP1 gene whole mitochondrial genome sequencing of *S. quadricauda* was performed.
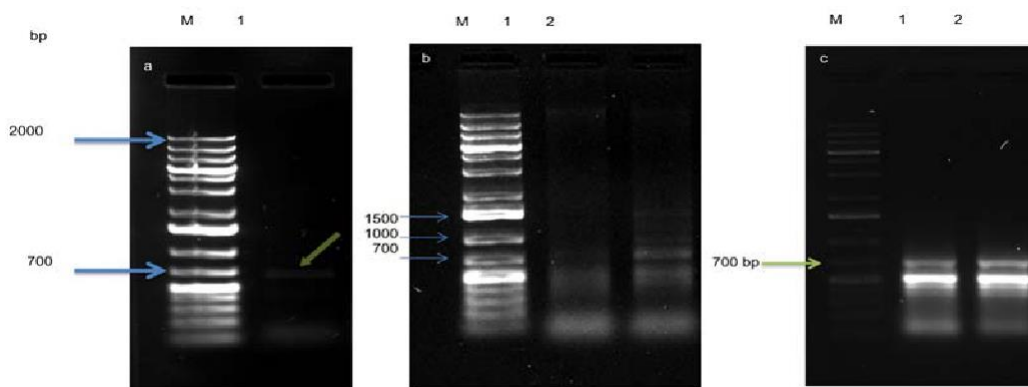
Fig. 4.1: SAP 1 amplification using designed primers of *S. obliquus* sequence; a represents SAP 1 amplification using orf specific primer (500bp); b: SAP 1 amplification using upstream downstream primer (860bp); c: SAP 1 amplification using upstream downstream primer with gel eluted product as template DNA (860bp).

4.3.2. Whole Mitochondrial Genome sequencing of *S. quadricauda* CASA CC202

Pure genomic DNA of mid- exponential phase of *S. quadricauda* was subjected for Illumina NextSeq500 Paired-end sequencing with 150*2. The complete mitochondrial genome showed 30301 bp sequences. The mitochondrial genome annotated for prediction of proteins, rRNA and tRNA (Table. 4.2 & Fig. 4.2).

The protein coding genes were predicted using GeneMarkS 4.283/ ORFfinder7. Predicted proteins were annotated by the homology search against NCBI non redundant database using BLAST-2.5.04. The list of predicted proteins of *S. quadricauda* mitochondrial genome was listed in Table. 4.3. Most of the proteins are related with the electron transport chain as NAD, Cox, Cob and ATP. In addition to that a hypothetical protein of unknown function was also predicted (Table. 4.3).

Summary	Sample
Scaffolds Generated	1
Total Scaffolds Length	30301
Total Number of Non-ATGC Characters	0
Percentage of Non-ATGC Characters	0
Scaffolds>= 1 Kb	1
Scaffolds >= 10 Kb	1
N50 Value	30301

Table. 4.2: Mitochondrial Genome Assembly Statistics of *S. quadricauda* CASA CC202.
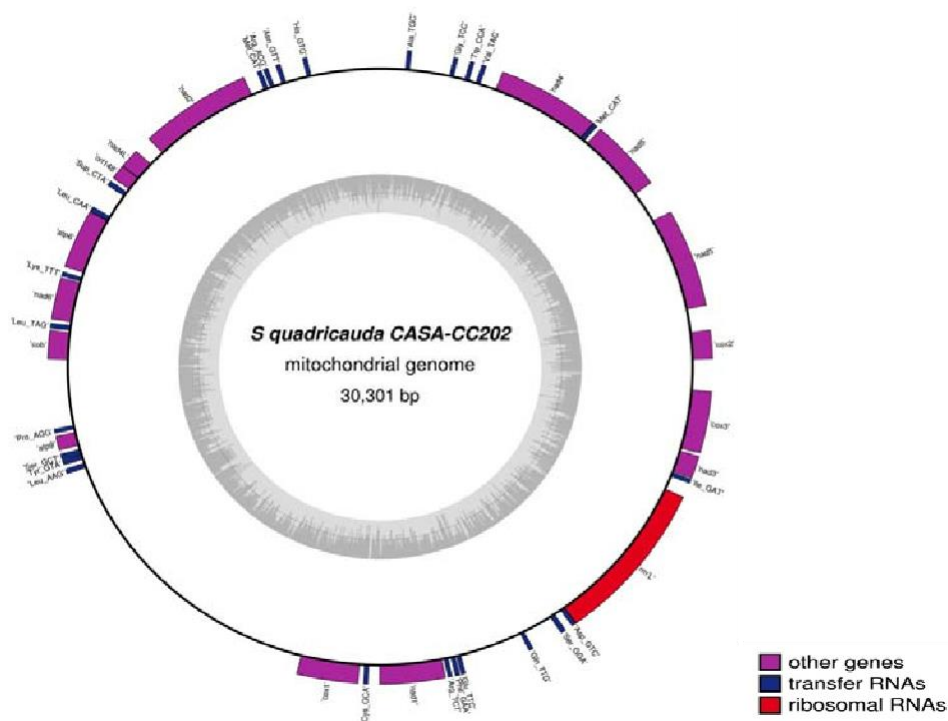
Fig. 4.2: Circular map of mitochondrial genome of *S.quadricauda* CASA CC202.

Sl. No.	Predicted protein	Name of gene	Identity (%)	Similarity (%)
1	ORF 1	Nad 5	39.3	45.1
2	ORF 17	Cox1	49.8	52.4
3	ORF 18	Nad 1	69.1	74.7
4	ORF 25	Nad3	84.6	92.3
5	ORF 26	Cox 2	67.3	77.3
6	ORF 29	Nad 4	4.9	6.7
7	ORF 33	Nad 6	72.1	77.5
8	ORF 34	Cob	33.3	34.8
9	ORF 36	Atp 9	91.8	91.8
10	ORF 42	Hypothetical protein	-	-
11	ORF 55	Cox 3	60.2	74
12	ORF 56	Nad 5	32.8	40.9
13	ORF 64	Nad 2	59.8	69.1
14	ORF 65	Nad 4L	87	91
15	ORF 66 (ORF 148)	-	27	31.8
16	ORF 67	Atp 6	63.6	69.8
17	ORF 71	Cob	49.5	53.8
18	ORF 75	Cox 1	14.8	16.1
19	ORF 79	Cox 1	25	26.4

Table.4.3: Predicted proteins of *S.quadricauda* mitochondrial genome. Protein-coding genes were predicted by GeneMarkS 4.283/ ORFfinder7.

4.3.2.1. Conservation of *S. quadricauda* CASA CC202 mitochondrial genome

For constructing phylogenetic tree of *S. quadricauda* to compare the evolutionary relationship with different micro algal mitochondrial genome, 40 mitochondrial genome sequences were collected from NCBI (Table. 4.4). Sequences were aligned with MUltiple Sequence Comparison by Log Expectation (MUSCLE). The phylogenetic tree shows that *Scenedesmus quadricauda*, *Hariotina*, *Scenedesmus obliquus* and *Tetradesmus obliquus* mitochondrial sequences form a strongly supported clade. Even though *Scenedesmus obliquus* and *Tetradesmus obliquus* fall in the same clade, there is divergence of sequence. *S. quadricauda* CASA CC202 sequence information is not known (Fig. 4.3).

Sl. No.	Mitochondrial genome	Accession no.	Class
1	*Chlamydomonas moewusii*	NC001872	Chlorophyceae
2	*Dunaliella salina*	NC012930	Chlorophyceae
3	*Chlamydomonas reinhardtii*	X66484	Chlorophyceae
4	*Volvox carteri f. nagariensis*	GU048821	Chlorophyceae
5	*Hariotina* sp. F30	KU145405	Chlorophyceae
6	*Polytomella magna*	NC023091	Chlorophyceae
7	*Scenedesmus obliquus*	AF204057	Chlorophyceae
9	*Chlorotetraedron incus*	NC024757	Chlorophyceae
10	*Neochloris aquatica*	NC024761	Chlorophyceae
11	*Ourococcus multisporus*	NC024762	Chlorophyceae
12	*Monoraphidium neglectum*	NW014013625	Chlorophyceae
13	*Chromochloris zofingiensis*	NC024758	Chlorophyceae
14	*Pseudomuriella schumacherensis*	NC024763	Chlorophyceae
15	*Bracteacoccus aerius*	NC024755	Chlorophyceae
16	*Bracteacoccus minor*	NC024756	Chlorophyceae
17	*Mychonastes homosphaera*	NC024760	Chlorophyceae
18	*Nannochloropsis oceanica*	IMET1	Eustigmatophyceae
19	*Nannochloropsis oceanica*	CCMP531	Eustigmatophyceae
20	*N. salina*	CCMP537	Eustigmatophyceae
21	*N. gaditana*	CCMP527	Eustigmatophyceae
22	*N. oculata*	CCMP525	Eustigmatophyceae
23	*N. limnetica*	CCMP505	Eustigmatophyceae
24	*N. granulata*	CCMP529	Eustigmatophyceae
25	*Chlorogonium elongatum*	Y07814	Chlorophyceae
26	*Sphaeropleales sp.*	KT259054	Chlorophyceae
27	*Pediastrum duplex*	KR026340	Chlorophyceae
28	*Chlamydomonas leiostraca*	NC026573	Chlorophyceae
29	*Polytoma uvella*	NC026572	Chlorophyceae
30	*Dunaliella viridis*	NC026571	Chlorophyceae
31	*Lobosphaera incisa*	NC027060	Trebouxiophyceae
32	*Gonium pectorale*	AP012493	Chlorophyceae
33	*Chlorella sorokiniana*	KM241869	Trebouxiophyceae
34	*Chlorella variabilis*	NC025413	Trebouxiophyceae
35	*Phaeodactylum tricornutum*	HQ840789	Bacillariophytaincertaesedis
36	*Coccomyxa sp.*	NC015316	Chlorophyceae
37	*Tetradesmus obliquus*	NC002254	Chlorophyceae
38	*Pleodorina starrii*	NC021108	Chlorophyceae
39	*Polytomella parva*	NC016916	Chlorophyceae
40	*Polytomella sp.*	NC013472	Chlorophyceae

Table.4.4: List of mitochondrial genome of different microalgae were collected from NCBI and analyzed for phylogeny.
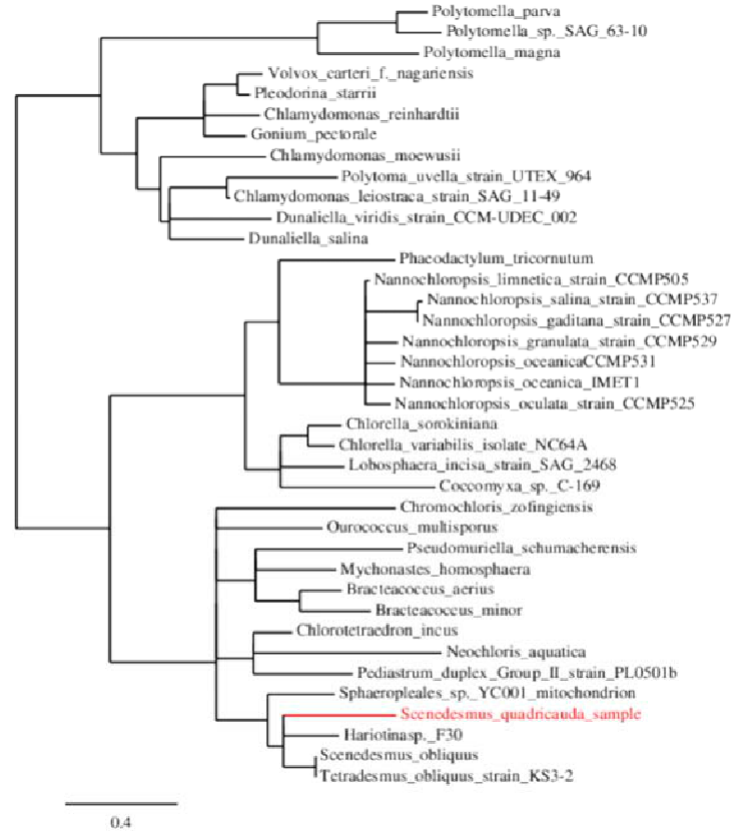
Fig. 4.3: Evolutionary conservation of *S.quadricauda* mitochondrial genome. The sequences were aligned with MUSCLE. The phylogenetic tree was constructed using the maximum likelihood method.

4.3.3. Identification of SAP1 of *S. quadricauda* mitochondrial genome

The MALDI-TOF predicted SAP1 of *S. obliquus* shows a molecular function as an endonuclease activity and a conserved motif of LAGLIDADG_2 super family. They were having two LAGLIDADG motifs in its sequence (Fig. 4.4b). The basic information of ORF 151 of *S. obliquus* from Uniprot KB is presented in Fig. 4.4a and LAGLIDADG motif in Fig.4.4b. Using this information the conserved LAGLIDADG domain containing proteins were searched from mitochondrial genome of *S. quadricauda*. Based on these conserved domain search, ORF 42 revealed that it has a LAGLIDADG motif which is comparable to that of SAP1 of *S. obliquus* (Fig. 4.5). Here after ORF 42 was named as LAGLIDADG Homing Endonuclease (LHE). The LAGLIDADG endonuclease sequence of different microalgae was retrieved from NCBI and the sequence was aligned using CLUSTAL OMEGA. The sequence

71

alignment showed the conserved LAGLIDADG motif and the sequence similarity

between other microalgae (Fig. 4.6)

a

b
MLPPFLFEV **AIGNRLGDR** SLYTTKTKGSKI
KLEQGRVNKDYLYHLFELYKGWTNYEKPYRYI
PKVTKGTYTRGVIKSYSFRTITHPAFDKIYNFFIC
NGKKTYKEGLITNHLTSVG **LSYWVRDDG**
SLQKITKLFREQWDLLKKKIFKLLKS

SAP 1 (Orf 151)

Molecular function	:	Endonuclease activity
Molecular size	:	17896 Da
Subcellular location	:	mitochondrion
Domain	:	LAGLIDADG_2
Function	:	Unknown

Fig.4.4: a; Characteristics of SAP1 (ORF 151) of *S. obliquus* from the available
protein database. b; ORF 151 having two LAGLIDADG motifs.

Conserved domains on [lcl|seqsig_MKVSP_f37655c9e8d9e13c2ef9a9040dfc53bc]
View Concise Results
orf 42

Protein Classification

similar to intron-encoded endonuclease aI3 (domain architecture ID 10469810)
protein similar to intron-encoded endonuclease aI3

Graphical summary ☐ Zoom to residue level   show extra options »

Query seq.		
Specific hits		LAGLIDADG_1
Superfamilies		LAGLIDADG_1 superfamily

Search for similar domain architectures   Refine search

List of domain hits

Name	Accession	Description	Interval	E-value
LAGLIDADG_1	pfam00961	LAGLIDADG endonuclease;	17-138	1.60e-12

LAGLIDADG endonuclease;

>lcl|ORF42_Mitochondria:19739:20275 hypothetical protein

MKVSPIDSSDFSTNAW LTGFSEADS NFSIRITVRNK KTGNI RVQ TTYRLEI STKIN FKLNS
FDNNVYHTKEFLT KICNFFGRAFYIRERFN KDWGKSYTSCIVIR FNQRSV QK VYDYFHKY
PF KGSKYLNFMDWAKVVEMPKPLSESRKKQCVSIRENYNSTRTVFSWEHLDSLNNKN

Fig. 4.5: Motif search in ORF 42 of *S.quadricauda* by NCBI Conserved domain
search. LAGLIDADG motif in ORF 42.

```
S.quadricauda    -----MKVSPIDSSDFSTNAWLTGFSEADSNFSIRITVRNKKTGNIRVQTTYRLEISTKI
Haematococcus    --------------MQLTDKWVGFVDGDGCFKIINA---------KTGKRYCFVVSQDK
Monomastix       -------MTTKNTLQPTEAAYIAGFLDGDGSIYAKLIPRPDYK-DIKYQVSLAISFIQRK
Chlorella        -------AQPTNFHDQLKFAWLAGFVDADGCINAQIVSREDYL--LKYQVRVSLTVFQST
T.obliquus       MTNNNMQNKGMKIIDKDELIYLAGFIDGDGSLIAQMVRRHDYK--FKYQIKCTVQITQLK
C.reinhardtii    ---------MNTKYNKEFLLYLAGFVDGDGSIIAQIKPNQSHK--FKHQLSLTFQVTEKT
                                    ::.**  :.*. :                     :       . .

S.quadricauda    NFKLNSFDNNVYHTKEFLTKICNFFGRAFYIRERFNKDWGKSYTSCIVIRFN--QRSVQK
Haematococcus    -----------RSVNYLYALKKKFGC------GSVNKVGKNMREYRVSSKKDLI---EI
Monomastix       -----------DKFPYLQDIYDQLGK----RGNLRKDRGDGIADYTIIGSTHLSIILPD
Chlorella        -----------TQHFLLDIQKILG------GTVRKRNDGMSEFCVVGGTSLQTTLEK
T.obliquus       -----------KRRHILEKIQESIGV------GIIRDRG-TISDYVLVEPKCVYWLLKQ
C.reinhardtii    -----------QRRWILDKLVDEIGV------GYVRDRG-SVSDYILSEIKPLHNFLTQ
                            *   :  .   :.:*

S.quadricauda    VYDYFHKYPFKGSKYLNFMDWAKVVEMPK---------------PLSESRKKQCVSIRENY
Haematococcus    ILPFFEKNPLQTEKLKDFQILYEDLTDKKLLLPGKTICRDWLTGFIDAEANFHVSMVKNY
Monomastix       LVPYLRIKKKQANRILH--------------------------------IINLY
Chlorella        LLPYLNLKRAQAKLVLQ--------------------------------IIKKL
T.obliquus       LSPFLRLKKKQADLIIR--------------------------------IIEQL
C.reinhardtii    LQPFLKLKQKQANLVLK--------------------------------IIEQL
                  :   ::.      :  .                                  : :

S.quadricauda    NSTRTVFS-----WEHLDSLNNKN---------------------------------
Haematococcus    PRPQFVIGLHLKEKEILESIQNWMRSFTNSNYSGGTVYEKKKKNGSNYLVYQISSLTGFL
Monomastix       PQAQKNPSKFLDLVKIVDDVQNLNKRADE-------------LKSTNYD---------
Chlorella        PNTKDPS-VLMEAALLADKVGLLTDGKKR-------------TILAE----------
T.obliquus       TSSKNSAVLFVQLCRLTDQVALLNDSKSR-------------TITAE----------
C.reinhardtii    PSAKESPDKFLEVCTWVDQIAALNDSKTR-------------KTTSE----------
                  :                :.:

S.quadricauda    ----------------------------------------------------------
Haematococcus    EIIKVCTTNTNRCLLKTSKRIDFLKFKQIIRIIQQKRHLTDNGILIIKKIQQKLVV
Monomastix       ---------RLLEEFLKAG---------KIESSP-----------------------
Chlorella        ---------NVRECLKKLG---------HVVSAALEHHHHHH----------------
T.obliquus       ---------VVETTLRELG---------LI---------------------------
C.reinhardtii    ---------TVRAVLDSLS---------EKKKSSP----------------------
```

Fig.4.6: Functional conservation of catalytic residues in LAGLIDADG Homing Endonuclease among microalgae. The conserved LAGLIDADG motif, lysine and glycine amino acids (basic pocket) were also highlighted. The multiple sequence alignment was done by CLUSTAL Omega.

4.3.4. Gene level confirmation of LAGLIDADG endonuclease in *S. quadricauda*

Based on the sequence of LAGLIDADG endonuclease designed three sets of primers as ORF specific primer, real time primer and upstream downstream primer were designed (Table. 4.1 & Fig. 4.7a). Then the genomic DNA of *S. quadricauda* was used as template for the PCR reaction. When ORF specific primer was used the expected size product of 530bp size was obtained (Fig. 4.7b). The real time primer gives an expected size of 178bp product; upstream downstream primer gives about 833 bp and 1426 bp product (Fig. 4.8). Further the amplicons were sequenced and aligned with the LHE of *S. quadricauda* and confirms 100 % similarity (Fig. 4.9). After confirmation of LHE gene sequences of *S. quadricauda* were submitted to the NCBI- Gen Bank with the accession number as MN648648.

>LHE FRUN13-20172011-08-25-03-16-1303-16-13(2).ab1

5'ACAGGTTTTAGTGAAGCGGATAGTAATTTTTCTATTAGAATTA
CAGTTCGTAATAAAAAAACTGGTAATATTCGAGTACAAACCAC
ATATCGATTGGAAATTTCTACAAAAATAAACTTCAAACTAAATA
GTTTTGATAATAATGTGTATCATACAAAAGAATTTCTTACTAAA
ATTTGTAATTTTTTTGGTAGAGCTTTTTATATTCGAGAACGTTTT
AATAAGGATTGGGGTAAATCTTACACTTCCTGTATTGTAATAAG
GTTTAATCAAAGATCTGTACAAAAAGTTTATGATTACTTTCACA
AATATCCATTTAAAGGCAGTAAATATTTGAATTTTATGGATTGG
GCAAAAGTGGTAGAAATGCCAAAGCCTTTGAGTGAAAGTAGG
AAAAAACAGTGCGTTTCTATTCGTGAAAACTATAATAGCACAC
GTACTGTTTTTAGTTGGGAGCATCTGGATAGTCTGA3'

Fig.4.7: Gene level confirmation of LHE in *S. quadricauda*. a: represents primers used for LHE amplification; b: LHE amplification using ORF specific primer; c: Sequencing result of LHE.
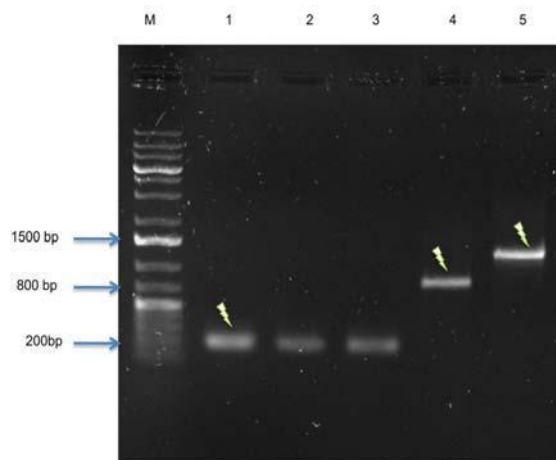
Fig.4.8: LHE amplification in *S. quadricauda* with upstream downstream and real time primers. Lane 1-3: Real time primer, Lane 4 and 5: upstream downstream primer.

>SUDI-UDIPFRUN13-20182011-09-22-00-37-4800-37-48.ab1

5'AATACTTATGTTGTTCTTAAATTTCAATCCATTAGTAGTGTATATTTGGTTTGTCGTATAATTAATGGTTATTAGCGTAC
ACCAAAGCATAAAAAGTTTGAAAGTTTGGTACAGTTTGGAAATAAAAATCTATGTTATCGTATGAAGGTGTCTCCGATC
GACTCTAGTGATTTTAGCACAAATGCTTGGCTAACAGGTTTTAGTGAAGCGGATAGTAATTTTTCTATTAGAATTACAGT
TCGTAATAAAAAAACTGGTAATATTCGAGTACAAACCACATATCGATTGGAAATTTCTACAAAAATAAACTTCAAACTA
AATAGTTTTGATAATAATGTGTATCATACAAAARAATTTCTTACTAAAATTTGTAATTTTTTTGGTAGAGCTTTTTATATT
CGAGAACGTTTTAATAAGGATTGGGGTAAATCTTACACTTCCKGWATTGTAATAAGGTTTAATCAAAGATCTGTACAAA
AAGTTTATGATTACTTTCACAAATATCCATTTAAAGGCAGTAAATATTTGAATTTTATGGATTGGGCAAAAGTGGTAGAA
ATGCCAAAGCCTTTGAGTGAAAGTAGGAAAAAACAGTGCGTTTCTATTCGTGAAAACTATAATAGCACACGTACKGTTT
TTAGTTGGGAGCATCTGGATAGTCTGAATAACAAGAATTAACATCAAAGCTTCGTTACAAGCGTATAATTGAAAATTAG
TTTAATTTACTATTATTTAGTAATAGTAAAATAAAGCTAGTT 3'

>SUD2-UD2PFRUN13-20182011-09-22-00-37-4800-37-48.ab1

5' ACCTTATTACTATAAAACAGTTCGTAAAGCTGGAAAAGCGGTAACTAAAAAGCAAAAAAATTATCCAATAATCAAAA
TTTGTTTTCCAAAAGAAGACTTTCCTTTGGCAGCAAAGCTACAATCTATTTTTGGTGGAGTTTTCGAGCATAGTAAAAAA
AATACTTATGTTGTTCTTAAATTTCAATCCATTAGTAGTGTATATTTGGTTTGTCGTATAATTAAKGGTTATTAGCGTACA
CCAAAGCATAAAAAGTTTGAAAGTTTGGTACAGTTTGGAAATAAAAATCTATGTTATCGTATGAAGGTGTCTCCGATCG
ACTCTAGTGATTTTAGCACAAATGCTTGGCTAACAGGTTTTAGTGAAGCGGATAGTAATTTTTCTATTAGAATTACAGTT
CGTAATAAAAAAACTGGTAATATTCGAGTACAAACCACATATCGATTGGAAATTTCTACAAAAATAAACTTCAAACTAA
ATAGTTTTGATAATAAKGTGTATCATACAAAAGAATTTCTTACTAAAATTTGTAATTTTTTTGGTAGAGCTTTTTATATTC
GAGAACGTTTTAATAAGGATTGGGGTAAATCTTACACTTCCKGTATTGTAATAAGGTTTAATCAAAGATCTGTACAAAA
AGTTTATGATTACTTTCACAAATATCCATTTAAAGGCAGTAAATATTTGAATTTTATGGATTGGGCAAAAGTGGTAGAAA
TGCCAAAGCCTTTGAGTGAAAGTAGGAAAAAACAGTGCGTTTCTATTCGTGAAAACTATAATAGCACACGTACTGTTTTT
AGTTGGGAGCATCTGGATAGTCTGAATAACAAGAATTAACATCAAAGCTTCGTTACAAGCGTATAATTGAAAATTAGTTT
AATTTACTA 3'

Fig. 4.9: Sequencing results of LHE using upstream downstream primers.

4.3.5. Quantification of LHE expression in *S. quadricauda* under nitrogen starvation

For quantifying the LHE gene expression RNA samples were extracted at 3, 6, 8, 24, 48 and 72 hours from nitrogen starved (N⁻) and control (N⁺) *S. quadricauda* as described in materials and methods (3.2.8). The DNase treated RNA was used for the synthesis of cDNA. The time course ΔΔCt curve analysis of revealed that LHE was 4.2 fold elevated during 48 hours of nitrogen stress induced samples than control samples (Fig.4.10). The LHE gene expression was normalized using mitochondrial COX 1 as an internal control.
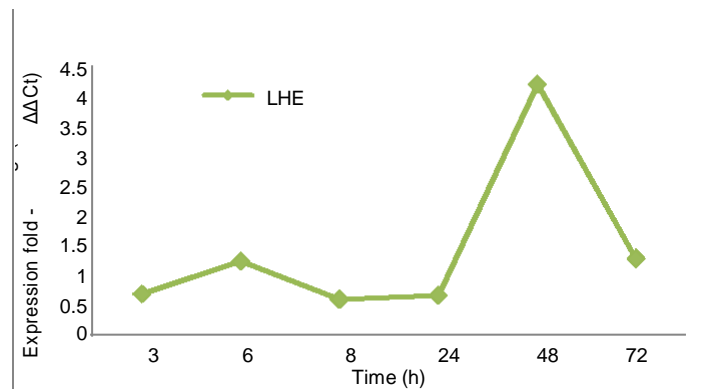
Fig.4.10: Quantification of LHE gene expression by RT-PCR using control (N⁺) and nitrogen starved (N⁻) cDNA of *S. quadricauda*.

4.3.6. In silico analysis of LALLIDADG endonuclease of *S. quadricauda*

4.3.6.1. Homology modelling of LAGLIDADG Endonuclease (LHE)

The tertiary structure of LHE was predicted by Swiss model and Phyre.2.0 software. LHE of *S. quadricauda* three dimensional structure implies it is a homodimer and showed a core α-ββ-α-ββ-α domain fold in a single peptide chain (Fig. 4.11a). Since the whole genome sequence of *S. quadricauda* was not available and thus LHE gene sequence as well. Therefore the homology modelling of LHE was build using the crystal structure solved *Chlamydomonas reinhardtii* I-CreI (PDB ID 2O7M) as template. Further the predicted homology structure was validated using Ramachandran plot using the RAMPAGE software as described in materials and methods (4.2.4). According to the plot number of residues in the favoured region was 86.5% amino acids and number of residues in allowed region was 9.7%. Also the number of residues in outlier region was about 3.9%. The predicted homology model was valid because more number of amino acids lies in the favoured region (Fig. 4.11b).
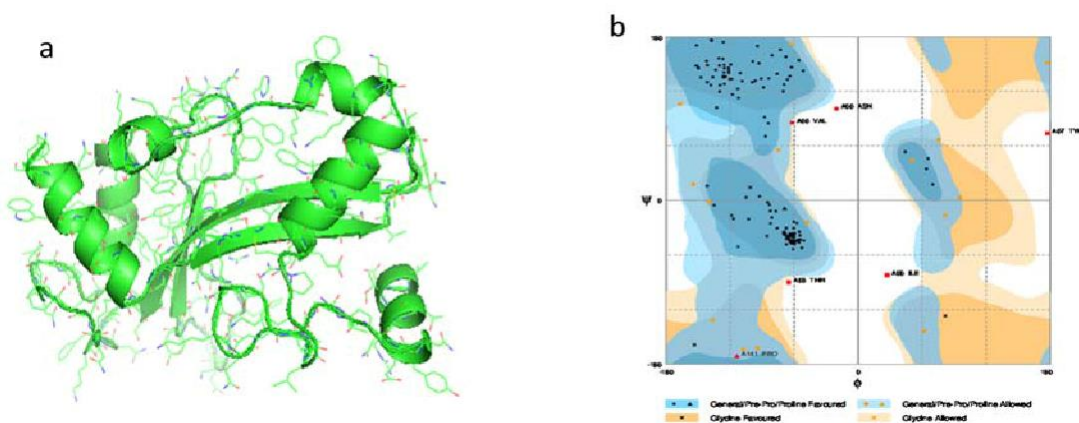
Fig. 4.11: Protein modeling and validation of LHE by Swiss model and Ramachandran plot (RAM PAGE), a: represents LHE modeled structure in *S. quadricauda*; and b: represents Ramachandran plot.

4.3.6.2. Structural alignment and molecular weight determination of LHE

The tertiary structure of LHE was aligned with Cre-I (template) and the green ribbon represents Cre-I and cyan as LHE of *S. quadricauda*. The active site, aspartic acid (D) was highlighted in red and yellow spheres (Fig. 4.6 & 4.12). The conserved motif of LHE in *S. quadricauda* was identified as LTGFSEADS and the basic pocket as K (lysine) at 69th position (Table. 4.5). The conserved motif, LAGLIDADG of different microalgae presented in Table. 4.5. The LHE of *S.quadricauda* was also created as a homodimer. As the LHE is an endonuclease it binds to the DNA, therefore DNA binding sites were predicted by Protein Predict software using I-CreI as reference. The DNA binding amino acid position was labelled as red sticks (Fig. 4.13). Molecular weight and amino acid composition of LHE was calculated by Protein Information Resource (PIR). The molecular weight of LHE of *S. quadricauda* was calculated as 21.2 KDa and the number of residues was 178 (Fig. 4.14).
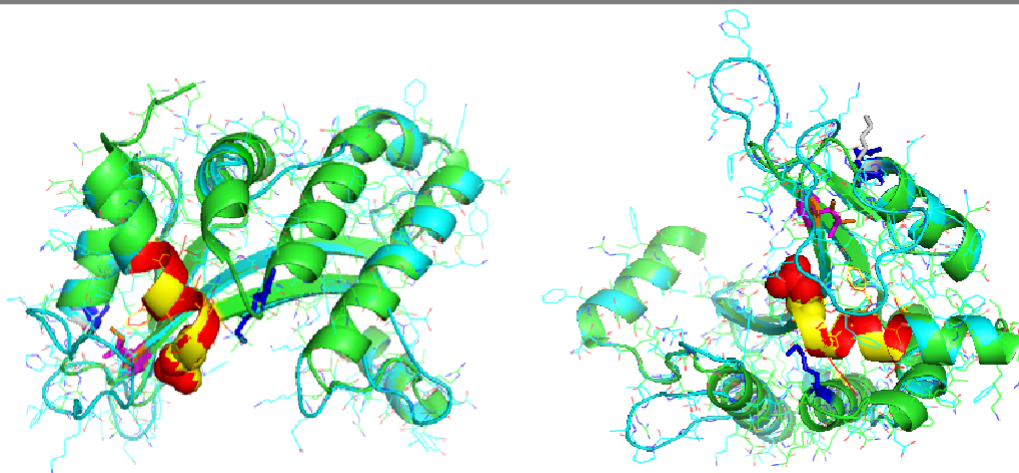
Fig.4.12: Homology modeling of LHE and template Cre-I. Secondary structure alignment of LAGLIDADG endonuclease and Cre-I by Pymol software. The red and yellow sphere represents the LAGLIDADG motif. Green and cyan colour represents Cre I and LAGLIDADG endonuclease respectively.

Enzyme	LAGLIDADnG	Metal binding		Basic Pocket	
I-CreI	LAGFVDGDG	D20	Q47	K98	R51
I-MsoI	IAGFLDGDG	D21	Q49	K104	K54
I-DmoI	LIGLIIGDG	D21	Q42	K120	K43
	IKGLYVAEG	E117	N129	-	K130
I-AniI	LVGLEFGDG	D15	L36	K94	D40
	LVGFIEAEG	E148	Q171	K227	G174
I-Sce I	GIGLILGDA	D44	E61	K122	-
	LAYWFMDDG	D145	N192	K223	-
PI-Sce I	LIGLWIGDG	D218	D229	K301	R231
	LAGLIDSDG	D326	T341	K403	H343
PI-PfuI	LAGFIAGDG	D149	D173	L220	-
	IAGLFDAEG	E250	M263	K322	-
I-SquI	LTGFSEADS	D24	S51	-	K69

Table.4.5: LAGLIDADG motif in different LHEs and structural features. I-SquI represents LAGLIDADG Endonuclease of *S. quadricauda*.
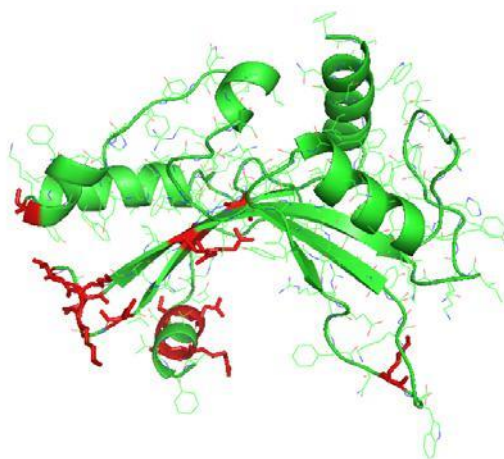
Fig. 4.13: DNA binding residues of LHE in *S. quadricauda* was predicted by Protein Predict software. The red colour indicates the DNA binding amino acids.

```
         ---------+---------+---------+---------+---------+---------+---------+---------+
   1     MKVSPIDSSDFSTNAWLTGFSEADSNFSIRITVRNKKTGNIRVQTTYRLEISTKINFKLNSFDNNVYHTKEFLTKICNFF
  81     GRAFYIRERFNKDWGKSYTSCIVIRFNQRSVQKVYDYFHKYPFKGSKYLNFMDWAKVVEMPKPLSESRKKQCVSIRENYN
 161     STRTVFSWEHLDSLNNKN
```

COMPOSITION:

code	A	B	C	D	E	F	G	H	I	K	L	M	N	P	Q	R	S	T	V	W	Y	Z
count	4	3	8	8	15	5	3	11	18	8	3	17	4	4	12	19	12	11	4	9		

Number of residues = 178   Molecular weight = 21206.95
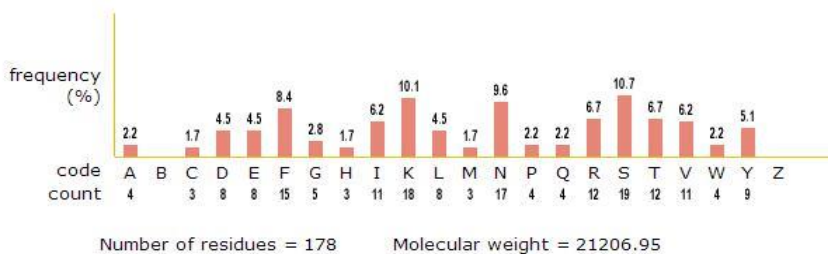
CALCULATION NOTES:

1. Molecular weight = sum of individual residues weights - water molecular weight ` (number of residues - 1)

where, water molecular weight = 18.015;

2. For each residue, the table gives the molecular weight:

A	Ala	89.09	G	Gly	75.07	N	Asn	132.12	V	Val	117.15
B	Asx	132.61	H	His	155.16	P	Pro	115.13	W	Trp	204.23
C	Cys	121.15	I	Ile	131.17	Q	Gln	146.15	Y	Tyr	181.19
D	Asp	133.10	K	Lys	146.19	R	Arg	174.20	Z	Glx	146.64
E	Glu	147.13	L	Leu	131.17	S	Ser	105.09			
F	Phe	165.19	M	Met	149.21	T	Thr	119.12	X	else	128.16

Fig.4.14: Molecular weight and amino acid composition of LHE. Molecular weight determination of LHE was carried out by PIR.

4.3.7. Cloning and over expression of LAGLIDADG endonuclease of *S. quadricauda*

The LAGLIDADG endonuclease of *S. quadricauda* gene specific primer (LAL-C-F & LAL-C-R) got amplified with an amplicon size of about 530 bp (Table. 4.1). Restriction digestion, ligation and transformation were performed as described in materials and methods (4.2.7). The colony PCR was performed using primer specific to T7 promoter of pET-28a revealed that the four positive clones are having the expected LHE gene (Fig. 4.15). The control (plasmid DNA without LHE) also showed a product size of about 315 bp using the T7 promoter primer. Subsequently plasmid DNA was isolated from the positive clones in order to check gene orientation using different combination of primers. The primers such as LHE gene primer, gene forward- T7 reverse and T7 forward- gene reverse were used to amplify the clone plasmid DNA. The PCR products were obtained as 530 bp, 640 bp and 740 bp respectively (Fig. 4.16) confirm the right orientation of LHE gene in pET-28a vector.

Further sequencing results of the positive clone plasmid DNA was aligned with the LHE gene sequence using CLUSTAL W2 (Fig. 4.17). The sequence alignment shows 100 % similarity to the LHE ie., gene of interest (Fig. 4.18). Also the plasmid DNA with LHE gene was double digested and the insert release was observed in the agarose gel (Fig. 15c). The over expression of LHE gene was induced by IPTG and it should get a protein size of about 21 KDa with the His-Tag. But the over expression was not consistent to purify the protein to show its activity (Fig. 4.19). The repeated attempts towards expression of LHE gene in *E. coli* were unsuccessful. Perhaps the possible reason could be LHE belongs to eukaryotic origin may not be over expressed in *E. coli* due to different codon usage.
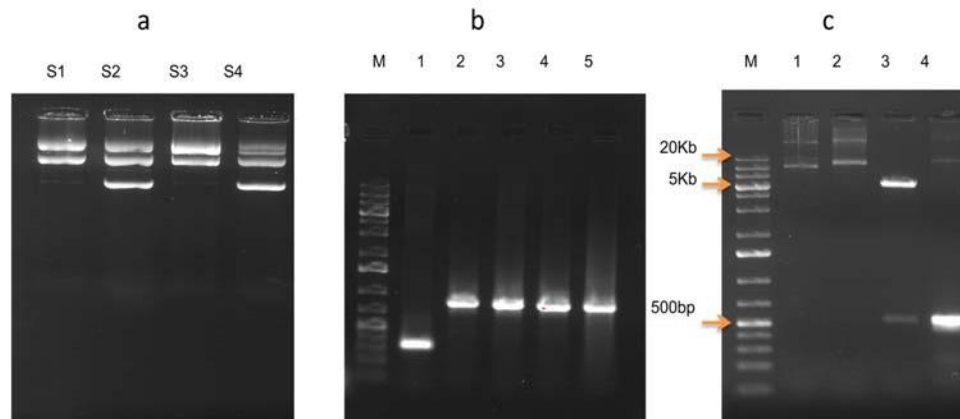
Fig. 4.15: Clone plasmid DNA isolation and amplification of LHE using T7 primer a : plasmid DNA of clones (s1-4 indicates 4 clones) b: Amplification of LHE using T7 primer from clone DNA, here lane1: Amplification of T7 promoter of pET 28a, lane 2: Amplification of T7 promoter with the insert of S1plasmid DNA, lane 3: Amplification of T7 promoter with the insert of S2plasmid DNA, lane 4: Amplification of T7 promoter with the insert of S3 plasmid DNA and lane 5: Amplification of T7 promoter with the insert of S4plasmid DNA .c: LHE release from clone plasmid DNA, here lane 1: Plasmid DNA of pET-28-a, lane 2: Plasmid DNA of transformed colony1 (S1), lane 3: Restriction digested S1 plasmid DNA and insert release and lane 4: LHE amplification from S1 plasmid DNA.
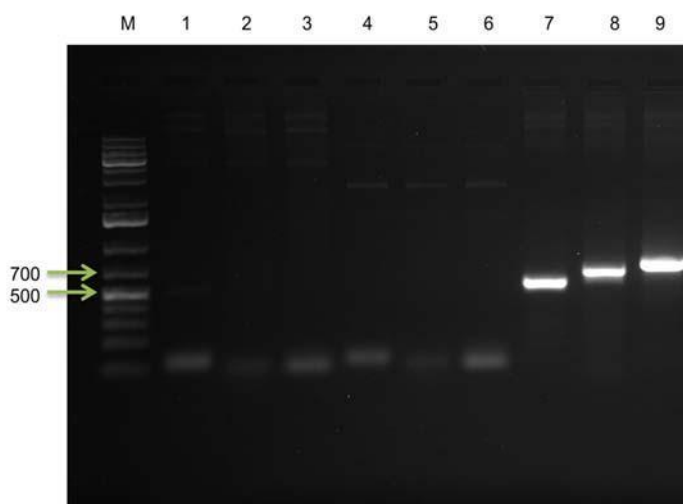
Fig.4.16: Amplification of LHE from transformed colonies. Here lane 1-3: LHE amplification from colony 1 using gene specific primer(1), Gene primer forward and T7 reverse (2) and T7 forward and gene primer reverse (3), lane 4-6: LHE amplification from colony 2 using gene specific primer(1), Gene primer forward and T7 reverse (2) and T7 forward and gene primer reverse (3) and lane 7-9: LHE amplification from colony 3 using gene specific primer(1), Gene primer forward and T7 reverse (2) and T7 forward and gene primer reverse (3).

>S1_T7.Forward_17357-1_P2487, Trimmed Sequence (962 bp)

5'ATTTTGTTTAACTTTAAGAAGGAGATATACCATGGGCAGCAGCCATCATCATCATCATCACAGCAGCGGCCTGGT
GCCGCGCGGCAGCCATATGGCTAGCATGACTGGTGGACAGCAAATGGGTCGCGGATCCATGAAGGTGTCTCCGA
TCGACTCTAGTGATTTTAGCACAAATGCTTGGCTAACAGGTTTTAGTGAAGCGGATAGTAATTTTTCTATTAGAATTA
CAGTTCGTAATAAAAAAACTGGTAATATTCGAGTACAAACCACATATCGATTGGAAATTTCTACAAAAATAAACTTCA
AACTAAATAGTTTTGATAATAATGTGTATCATACAAAAGAATTTCTTACTAAAATTTGTAATTTTTTTGGTAGAGCTTTT
TATATTCGAGAACGTTTTAATAAGGATTGGGGTAAATCTTACACTTCCTGTATTGTAATAAGGTTTAATCAAAGATCT
GTACAAAAAGTTTATGATTACTTTCACAAATATCCATTTAAAGGCAGTAAATATTTGAATTTTATGGATTGGGCAAAA
GTGGTAGAAATGCCAAAGCCTTTGAGTGAAAGTAGGAAAAAACAGTGCGTTTCTATTCGTGAAAACTATAATAGCAC
ACGTACTGTTTTTAGTTGGGAGCATCTGGATAGTCTGAATAACAAGAATTAAAAGCTTGCGGCCGCACTCGAGCAC
CACCACCACCACCACTGAGATCCGGCTGCTAACAAAGCCCGAAAGGAAGCTGAGTTGGCTGCTGCCACCGCTGA
GCAATAACTAGCATAACCCCTTGGGGCCTCTAAACGGGTCTTGAGGGGTTTTTTGCTGAAAGGAGGAACTATATCC
GGATTGGCGAATGGGACGCGCCCTGTAGCGGCGCATTAAGCGCGGCGGGTGTGGTGGTTACGCGCAGCGTGAC
CGCTACACTTGCCAGCGCCCTAGCGCCCGCTCCTTTCGCTTTCTT3'

Fig.4.17: Sequencing result of positive clone with LHE gene.

```
S1_T7.Forward    51  ATCATCATCACAGCAGCGGCCTGGTGCCGCGCGGCAGCCATATGGCTAGC   100
20275             1  ------------------------------ATGAAGGTGTCTCCGAT       17
                                                   ||||||||||||||||||
S1_T7.Forward   101  ATGACTGGTGGACAGCAAATGGGTCGCGGATCCATGAAGGTGTCTCCGAT   150

20275            18  CGACTCTAGTGATTTTAGCACAAATGCTTGGCTAACAGGTTTTAGTGAAG    67
                     ||||||||||||||||||||||||||||||||||||||||||||||||||
S1_T7.Forward   151  CGACTCTAGTGATTTTAGCACAAATGCTTGGCTAACAGGTTTTAGTGAAG   200

20275            68  CGGATAGTAATTTTTCTATTAGAATTACAGTTCGTAATAAAAAAACTGGT   117
                     ||||||||||||||||||||||||||||||||||||||||||||||||||
S1_T7.Forward   201  CGGATAGTAATTTTTCTATTAGAATTACAGTTCGTAATAAAAAAACTGGT   250

20275           118  AATATTCGAGTACAAACCACATATCGATTGGAAATTTCTACAAAAATAAA   167
                     ||||||||||||||||||||||||||||||||||||||||||||||||||
S1_T7.Forward   251  AATATTCGAGTACAAACCACATATCGATTGGAAATTTCTACAAAAATAAA   300

20275           168  CTTCAAACTAAATAGTTTTGATAATAATGTGTATCATACAAAAGAATTTC   217
                     ||||||||||||||||||||||||||||||||||||||||||||||||||
S1_T7.Forward   301  CTTCAAACTAAATAGTTTTGATAATAATGTGTATCATACAAAAGAATTTC   350

20275           218  TTACTAAAATTTGTAATTTTTTTTGGTAGAGCTTTTTATATTCGAGAACGT   267
                     |||||||||||||||||||||||||||||||||||||||||||||||||
S1_T7.Forward   351  TTACTAAAATTTGTAATTTTTTTTGGTAGAGCTTTTTATATTCGAGAACGT   400

20275           268  TTTAATAAGGATTGGGGTAAATCTTACACTTCCTGTATTGTAATAAGGTT   317
                     ||||||||||||||||||||||||||||||||||||||||||||||||||
S1_T7.Forward   401  TTTAATAAGGATTGGGGTAAATCTTACACTTCCTGTATTGTAATAAGGTT   450

20275           318  TAATCAAAGATCTGTACAAAAAGTTTATGATTACTTTCACAAATATCCAT   367
                     ||||||||||||||||||||||||||||||||||||||||||||||||||
S1_T7.Forward   451  TAATCAAAGATCTGTACAAAAAGTTTATGATTACTTTCACAAATATCCAT   500

20275           368  TTAAAGGCAGTAAATATTTGAATTTTATGGATTGGGCAAAGTGGTAGAA   417
                     |||||||||||||||||||||||||||||||||||||||||||||||||
S1_T7.Forward   501  TTAAAGGCAGTAAATATTTGAATTTTATGGATTGGGCAAAGTGGTAGAA   550

20275           418  ATGCCAAAGCCTTTGAGTGAAAGTAGGAAAAAACAGTGCGTTTCTATTCG   467
                     ||||||||||||||||||||||||||||||||||||||||||||||||||
S1_T7.Forward   551  ATGCCAAAGCCTTTGAGTGAAAGTAGGAAAAAACAGTGCGTTTCTATTCG   600

20275           468  TGAAAACTATAATAGCACACGTACTGTTTTTAGTTGGGAGCATCTGGATA   517
                     ||||||||||||||||||||||||||||||||||||||||||||||||||
S1_T7.Forward   601  TGAAAACTATAATAGCACACGTACTGTTTTTAGTTGGGAGCATCTGGATA   650

20275           518  GTCTGAATAACAAGAATTAA------------------------------   537
                     ||||||||||||||||||||
S1_T7.Forward   651  GTCTGAATAACAAGAATTAAAAAGCTTGCGGCCGCACTCGAGCACCACCAC   700
```

Fig.4.18: Sequence alignment of positive clone and LHE gene by CLUSTAL W2 pair wise alignment method.

Fig. 4.19: Over expression of LHE. Here lane 1: control (uninduced), lane 2-6: 1, 1.5, 2, 2.5 and 3 mM IPTG added 3hr induction.

4.4. Discussion

Mitochondria are the major players in the integration of Carbon and Nitrogen metabolism in plants (Pellny et al., 2008). Also mitochondria are involved in the process of programmed cell death and have a crucial role in plant defences during

stress conditions. However, mitochondria are a major source of cellular ROS, a property that is amplified by stress- induced inhibition and over-reduction of respiratory chain. In addition to that increased ROS governed enhanced expression of antioxidant enzymes led to increased tolerance towards biotic and abiotic stress (Van Aken et al., 2009). Thus accumulating evidences suggests that mitochondria may regulate the cellular stress response during abiotic stress condition (Arn-holdt-Schmitt et al., 2006; Clifton et al., 2006 and Van Aken et al., 2009).

Mitochondria are the organelles that possess their own genome and are involved in several functions. They are compartmentalized eukaryotic organelles and they evolved from an endosymbiotic α- proteobacterium (Lang and Burger, 2012). Mitochondrial genomes of microalgae are not extensively sequenced and studied. Currently a dozen mitochondrial genomes were deposited in the public domain and recently deposited genomes include *Chlorella heliozoae*, *Micractinium conductrix* and *Botryococcus braunii* (Blifernez- Klassen, et al., 2016). First time we are reporting the characteristics of mitochondrial genome sequence of *S. quadricauda* CASA CC202. One of the unique characteristic of mitochondrial genome of microalgae is that they are having coding regions of genes interrupted by introns. There are four types of introns based on their splicing mechanism as spliceosome, nuclear and archeal tRNA, group I and group II introns. Nedelcu et al., 2000 has sequenced mitochondrial genome of *Scenedesmus obliquus* and they have described peculiarities of *Scenedesmus* mitochondrial DNA. The genome size is of 42,919 bp and encodes 42 conserved genes, four additional open reading frames and an intronic reading frame with endonuclease/ maturase similarity. Also they revealed that there are no 5SrRNA or ribosomal protein coding genes in *Scenedesmus* mitochondrial DNA. In addition to that an important finding as a deviant genetic code was observed as UAG (stop codon) here it codes for leucine, along with that *Scenedesmus* mitochondrial DNA encodes another codon UCA (normally for serine) as a stop codon. Similarly in our study the *S. quadricauda* genome showed a size of about 30301 bp and other characteristics analogous to *S. obliquus*. Sevcikova et al., 2016 have sequenced three mitochondrial genome sequences of Eustigmatophyte lineages such as *Monodopsis sp.*, *Vischeria sp.* and *Trachydiscus minutes*, and compared with the *Nannochloropsis*. They found that they are highly collinear and similar in the coding gene content with extensive rearrangements in some of the lineages.

As discussed above mitochondria are crucial organelles with many characteristics. The stress associated mitochondrial protein identification was carried out by different research groups. The proteome analysis of microalgae was started by full characterization of of algal mitochondria (Van Lis et al., 2003). Higher carotenoid production was found in *Dunaliella* strain AL-1 under optimized condition they observed up regulation of the heat shock proteins, α and β subunit of mitochondrial ATP synthase (Ben Amor et al., 2017). Garibay-Hernandez et al., 2017 proposed that alternate electron pathways may be activated in nitrogen deprived *Ettlia oleoabundans* in order to satisfy varying energy demand as ATP/NADPH under abiotic stress conditions. Along with these additional mechanisms may be modulated in redox potential and ATP concentration of *E. oleoabundans* during nitrogen starvation (Cardol et al., 2003; Johnson and Alric, 2013; Erickson et al., 2015). Hernandez et al., 2017 suggests that they are able to identify proteins necessary for regulating ATP concentration within the chloroplast and mitochondria (adenylate kinase isoforms, mitochondrial and chloroplastic ADP/ATP carrier proteins and mitochondrial phosphate carrier protein. As described about the mitochondrial stress associated proteins, our present study also revealed a LAGLIDADG Homing Endonuclease associated with the nitrogen stress mediated lipid accumulation.

One of the nitrogen stress associated protein here described as LAGLIDADG Homing Endonuclease (LHE). Primarily Homing Endonucleases (HEs) are also known as meganucleases, are highly specific DNA cleaving enzymes that invade specific insertion sites by double- strand breaks on the target gene and insert the sequence by homologous recombination. They found in all forms of microbial life as well as in the eukaryotic mitochondria and chloroplasts, with genetic mobility and persistence (Stoddard 2014; Alvarez et al., 2012). LHE are the large protein families among the HEs and they comprise more than 200 members. They are termed as LAGLIDADG, DOD, dodeca peptide, dodecamer and decapeptide (Belfort and Roberts, 1997; Lambowitz and Belfort, 1993; Dalgaard et al., 1997; Stoddard, 2014; Belfort et al., 2002; Hausner et al., 2014). They are having either one or two copies of the LAGLIDADG motif, and they act as homo dimers such as I-Cre I (Thompson et al., 1992) and I-Ceu I (Marshall and Lemieux, 1992). The other groups which possess two copies of this motif separated by 80-150 residues, such as I-Dmo I (Dalgaard et al., 1993) and PI- Sce I (Gimble and Thorner, 1992) they act as heterodimers. Alvarez et

al., 2012 have identified a LHE in the chloroplast LSUrDNA of *Coccomyxa* algae. Also Lucas et al., 2001 have identified 28 new group I intron encoded proteins carrying a single LAGLIDADG motif from sequence analysis of chloroplast and mitochondria of about 75 green algae.

First time we are reporting the expression of LHE during nitrogen stress mediated lipid accumulation in *S. quadricauda*. Other reported role of LHE mainly relies in the following areas. OTP 51, pentatricopeptide with two LAGLIDADG motifs is required for the cis-splicing of plastid ycf3 intron 2 in *Arabidopsis thaliana* (De Longevialle et al., 2008). Lucas et al., 2001, have reported that some group I introns with LAGLIDADG motif encodes for maturases mainly in green algae, prokaryotes and Archaea. The De Longevialle et al., 2008 also evidenced that LHEs often have a dual function as DNA endonuclease and as a RNA splicing factor. In wheat (*Triticum aestivum* L.) the intron encoded LHE gene have been reported as a non-protein coding genes have critical role in the regulation of gene expression in abiotic stress. Also the intron- encoded DNA endonucleases aI5 alpha and aI4 in *Saccharomyces cereviciae* are involved in intron homing. It introduces a double strand break in the DNA of COX1 gene and thus mediates the insertion of introns into an intronless gene

4.5. Conclusion

Although *S. obliquus* and *S. quadricauda* belongs to the same clade there is a divergence in its sequence, thus mitochondrial genome sequencing of *S. quadricauda* CASA CC202 was performed. Out of 19 predicted proteins of *S. quadricauda* mitogenome, ORF 42 is having conserved motif as LAGLIDADG and it was identified as LAGLIDADG Endonuclease (LHE). During nitrogen starvation the LHE gene was found to be expressed about 4.2 fold than control. This class of LHE requires two LAGLIDADG motifs to exhibit its endonuclease function. The primary structure and the predicted tertiary structure of LHE reveal the conserved single LAGLIDADG motif. Therefore the LHE of *S. quadricauda* act as a homodimer. LHE being a homing endonuclease its biological relevance and its canonical homing site studies will lead to further mechanistic role of LHE during nitrogen stress mediated lipid accumulation.

CHAPTER

5

Sustaining biomass level during nitrogen stress- Role of Stress responsive hormone Abscisic acid (ABA)
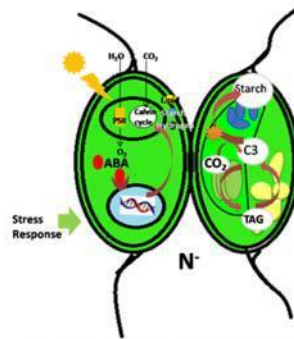
5.1. Introduction

When microalgae cultivated in environmental harsh condition it tends to accumulate neutral lipids. These unfavourable environmental conditions are nutrient starvation, pH, illumination, salinity, temperature etc. Among them, nutrient starvation-mediated lipid accumulation is the most feasible strategy in large scale. In *S. quadricauda* 2.27 fold increases in lipid yield with a drastic reduction in biomass were examined under nitrogen starvation (Anand and Arumugam et al., 2015). The sustained biomass with the increased lipid accumulation was the required feature when microalgae are to be cultivated in large scale. Nitrogen being an essential macro element, its level directly influences the cell and thus it becomes an integral part of the growth medium (Li et al., 2008; Arumugam et al., 2013). Nitrogen deprivation affects growth, development and metabolism of algae (Hockin, et al., 2012) and it is one of the extensively studied nutritional stresses. However, limiting this essential nutrient in the growth media, lead to enhanced TAG accumulation (Jiang, 2014: Anand and Arumugam, 2015). Even though the stress increases lipid but it drastically reduces the biomass yield (Anand and Arumugam, 2015). This limitation can be overcome by the supplementation of growth promoting agents to the stressed microalgae. The physiological relevance of stress hormone supplementation and its effects on growth and lipid metabolism are discussed in detail.

The phytohormones are essential for the growth and development of plants and they are active at very low concentration. Generally one of the phytohormone, Abscisic acid (ABA) regarded as a stress responsive hormone, which is present in all forms of life except Archaea. It is a sesquiterpenoid plant hormone involved in biotic and abiotic stresses in plants (Cutler et al., 2010). The ABA signalling, stress response and catabolism were well studied in higher plants particularly in *Arabidopsis thaliana* (Nagamune, et al., 2008; Hartung, 2010). Even though it is well understood in plants, the presence and physiological role of ABA in microalgae are poorly understood (Lu et al., 2014). However ABA will induce the protective measures against various environmental stresses such as desiccation, low temperature and osmotic shock (Yoshida, et al., 2003). But the real functions of ABA in microalgae is not fully established (Ludwig-Muller, 2011).

During abiotic stress, the endogenous level of ABA increases in plants and microalgae to cope-up with the stress. Hirsch, et al., 1989 reported the elevated levels of ABA in *Dunaliella* under salt stress. Also, an enhanced level of ABA was found in *Dunaliella sp.* and *Chlorella vulgaris* during nitrogen stress (Tominaga *et al.*, 1993) and heat stress (Bajguz, 2009) respectively. Evidence suggests the stimulation of ABA during osmotic stress in *Physcomitrella patens* helps them to tolerate the stress (Minami et al., 2005). The concentration of ABA present in algal cells vary between 7 and 34 nmol per Kg of fresh water biomass, this range is similar in liverwort as well (Hartung and Gimmler, 1994). But only limited data is available on the physiological effects of ABA during stress in microalga

External supplementation of ABA has revealed growth promotion and tolerance to the heavy metal induced stress in *Chlorella vulgaris* (Bajguz, 2011). In addition to photosynthetic microalgae, cyanobacteria *Nostoc* and *Anacystis* promoted their growth by supplemented ABA (Ahmad *et al*. 1978). ABA inhibits growth in *Coscinodiscus* were also reported by Kentzer and Mazur, 1991. In present study, for the first time, the elevated levels of ABA under nitrogen deficiency in *Scenedesmus quadricauda and* its role in sustaining the biomass and lipid yield were described. The interaction between ABA, nitrogen stress mediated lipid accumulation and its effect on FAME profile are discussed in the present chapter. Thus the role of ABA in sustaining biomass of nitrogen stress induced *S. quadricauda* was elucidated.

5.2. Materials and methods

5.2.1. Endogenous level of abscisic acid

Endogenous ABA level was quantified by phytodetect ELISA Kit as per manufactures instruction (Agdia). In brief, *S. quadricauda* pellets were collected at 0, 24, 48 and 72 hours from nitrogen-starved conditions and algal pellets were homogenized using a mortar and pestle under liquid nitrogen. The intracellular ABA was extracted after 24h at 4° C in the dark with a solution of 80 % methanol in 20 mM bicarbonate buffer (pH 8.0). Then the extract was then centrifuged at 5000 g for 15 min at 4 °C. The supernatant was vacuum dried at 30 °C and stored at -20 °C until use for ABA assay. An identical procedure was followed for quantification of ABA level in nitrogen rich condition as well.

5.2.2. External supplementation of ABA and effects on lipid metabolism of *S. quadricauda*

ABA were supplemented in various (1 μM- 5 μM) concentrations to the nitrogen deprived *S. quadricauda* (0-72 h). The cell growth, lipid, pigment and biomass were studied under this condition with respect to the control.

5.2.2.1. Cell growth and Biomass yield

The samples were periodically drawn after the treatment with ABA and the growth was determined spectrophotometrically at 530 nm. The cell number was enumerated by light microscopy (Leica) under a haemocytometer. The cell number was expressed in terms of 10^6 cells/ml. Dry biomass yield was calculated by gravimetrical analysis using cellulose nitrate filter membrane (Anand and Arumugam, 2015).

5.2.2.2. Total photosynthetic Pigment Analysis

Total photosynthetic pigments were quantified by Lichtenhaler method. Algal culture of 5 ml were taken and centrifuged at 8000 rpm for 10 minutes after the centrifugation pellets were collected. 5 ml of 100 % acetone was added and kept overnight in dark at room temperature. Then the sample was centrifuged at 8000 rpm for 10 minutes. The supernatant was collected and then optical density was measured at 644, 661 and 470 nm for chlorophyll *a*, chlorophyll *b*, and carotenoids respectively. The levels of pigments were quantified by using the following formula:

Chlorophyll *a* (mg L-1) = 11.24 × A 661.6 - 2.404 × A 644.8

Chlorophyll *b* (mg L-1) = 20.13 × A 644.8 - 4.19 × A 661.6

Total Chlorophyll (*a* + *b*) (mg L-1) = 7.05 × A 661.6 + 18.09 × A 644.8

Total carotenoids (mg L-1) = 1000 × A 470 – 1.9 × Chl*a* - 63.14 × Chl*b*/214

5.2.2.3. Total lipid analysis

The total lipid yield was quantified by Sulpho phosphor vanillin method. To estimate the total lipid yield 5 ml of algal culture was taken from the sample and the cells were centrifuged (8000 rpm) for 10 minutes. The pellet was suspended in 6 ml of Chloroform: Methanol (2:1). After 5 hours, 2 ml of 0.9 % saline was added, mixed vigorously and incubated for 12 h. The addition of saline creates a biphasic layer. The lower layer contained the lipid molecule. After the incubation, 0.5 ml of lower lipid

layer was taken and transferred to the fresh micro centrifuge tube and allowed for evaporation. After the evaporation, 0.5 ml of concentrated sulphuric acid was added into the sample and kept in a boiling water bath for 10 minutes. After cooling the tubes to room temperature, 0.2 ml of the sample was transferred into the fresh test tubes. 5 ml of vanillin reagent was added, mixed well and incubated for 20 minutes at room temperature. The pink colour developed was read at 520 nm.

5.2.2.4. TLC analysis of lipid

The extracted total lipid sample was spotted on to a TLC plate (10x 5 cm, Merck). The dried sample on TLC plate was then carefully dipped and allowed to stand in the TLC jar to solvent adsorption. The solvent system Hexane: Diethylether: Acetic acid (80:20:1) were prepared before sample spotting and allowed for saturation inside the TLC jar. The TLC plate was removed when the solvent system reached top of the TLC plate allowed to dry for 10 min at room temperature and visualized using iodine vapour.

5.2.2.5. FAME analysis by GC

The 400 ml culture of nitrogen deprived and ABA supplemented *S. quadricauda* cells were harvested by centrifugation at 10000 rpm for 15 minutes. Then the pellets were lyophilized and stored in -20 °C. Lipid was extracted from the pellet using chloroform: methanol (2:1) with the aid of sonication for 10 minutes. Then the crude solution was filtered through a Whatmann no.1 filter paper and the solvent from the sample was evaporated using rotary evaporator. The total lipid was then transesterified by 2 % methanolic H_2SO_4 at 95 °C for 6 hours in a water bath. The methyl esters of fatty acid were then purified by TLC and the samples were analysed by gas chromatography (Anand and Arumugam, 2015).

5.2.2.6. Nile red staining of lipid droplets

Nitrogen deprived and ABA supplemented algal cells of about 1 ml sample were withdrawn aseptically. Then the biomass was collected by centrifugation at 10000 rpm for 10 minutes. Further the steps were followed as described in the materials and methods of chapter 2 (2.2.2.5).

5.3. Results

5.3.1. Endogenous level of ABA in nitrogen depleted *S. quadricauda*

During nitrogen stress, in *S. quadricauda* Abscisic acid is immediately rising up during the onset of stress in order to cope-up with the stress and the level is falling down when the stress is sustained. The level of ABA shoots up within 24 hours and suddenly falls down after 24 hours. The ABA was quantified as described in materials and methods as 27.21 pmol/L in 24 hours and it was drastically reduced to 4 pmol/L during 48 hours (Fig. 5.2). The ABA level in nitrogen rich *S. quadricauda* is 6.77 pmol/L in 24 hours and it attains a constant level during the stress period. Thus intracellular ABA level was 4 fold increased during nitrogen deprived *S. quadricauda* during the onset of nitrogen starvation (24 hours). The concentration of ABA was calculated based on the standard curve (Fig. 5.1).
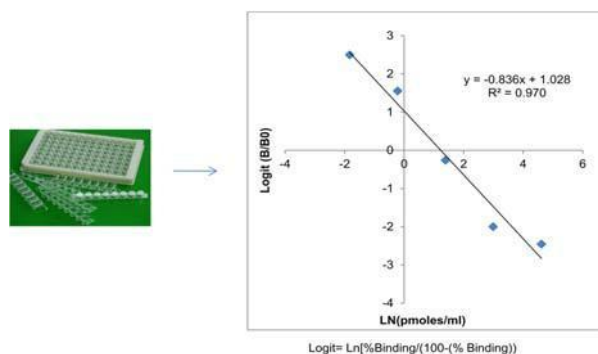
Fig. 5.1: Standard curve of Abscisic acid by quantitative competitive ELISA method.
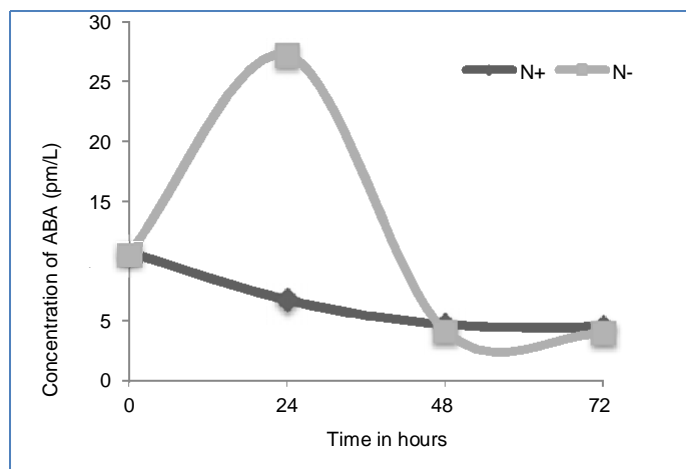
Fig.5.2: Endogenous levels of Abscisic acid in control (N$^+$) and nitrogen starved (N$^-$) conditions of *S. quadricauda* by phytodetect competitive ELISA method (Agdia). Control (N$^+$) samples drawn in corresponding days i.e., 12th -15th day. N$^-$ samples were drawn in 0-72 hour intervals.

5.3.2. External supplementation of ABA and its effects on growth

Phytohormones are signalling molecules that exhibit their effect at very low concentrations and have direct effects on growth of the organism. The ABA supplementation in nitrogen stressed cells had the effect of sustaining the growth up to 72 hours. The experiment shows that the addition of lower concentration of ABA (1 and 2 μM) is having effects on its cell density compared to other concentration. About 38×10^6 cells/ml of cells were enumerated in 2 μM ABA added cultures in 24 hours, which is a 1.4 fold increase when compared to nitrogen-starved *S. quadricauda* without external ABA supplementation (Fig. 5.3).
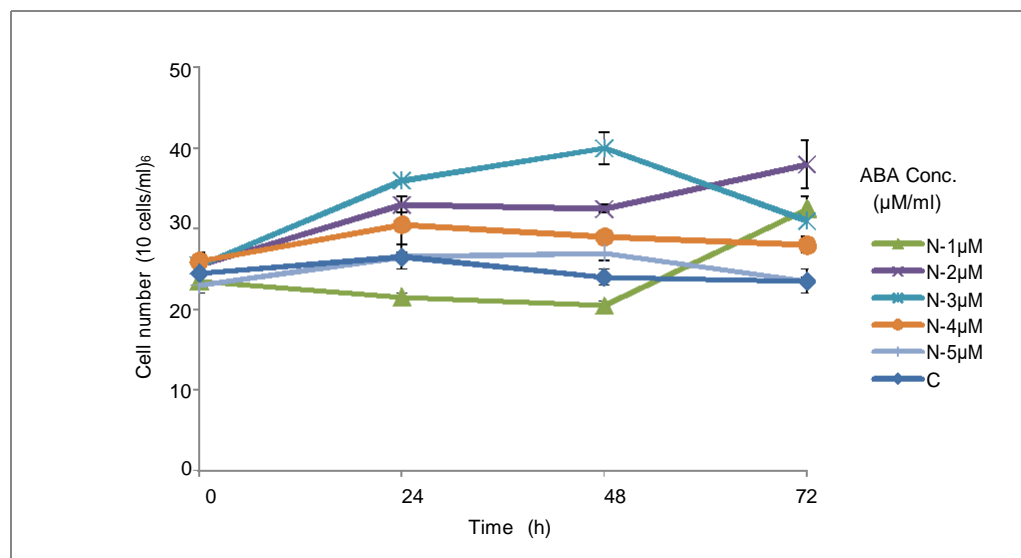
Fig. 5.3: Growth characteristics of *S. quadricauda* during ABA supplementation during nitrogen stress. Cell number of ABA treated and control (nitrogen starved) *S. quadricauda.*

5.3.3. External supplementation of ABA and effects on total lipid yield

Total lipid content in nitrogen deprived *S. quadricauda* is higher than that of nitrogen rich cells. The ABA supplementation leads to not much increment in lipid content rather the sustainability of lipid content were observed. Also the lipid content is higher at 48 hours compared to other time points. The lower concentration of ABA (1 and 2 μM) are only effective than the higher concentration of ABA (Fig. 5.4). The lipid yield in nitrogen-free *S. quadricauda* of about 389.99 mg/L was observed. The lipid yield showed after ABA supplementation was about 385.33 and 365.33 mg/L in 1 μM and 2 μM respectively (Fig. 5.4). The TLC profile of ABA supplemented

91

nitrogen stressed *S.quadricauda* revealed that the 2µM concentration of ABA has higher TAG accumulation, when compared to control (Fig. 5.5). The lipid yield was further confirmed by staining with lipophilic dye Nile red by fluorescence microscopy, showed a sustainable trend of lipid yield in nitrogen starved cells (Fig. 5.6). Similarly, the nitrogen starved *S. quadricauda* supplemented with ABA also maintains the lipid yield. Thus the ABA helps to sustain the lipid yield under nitrogen starvation as well as sustains the biomass yield.
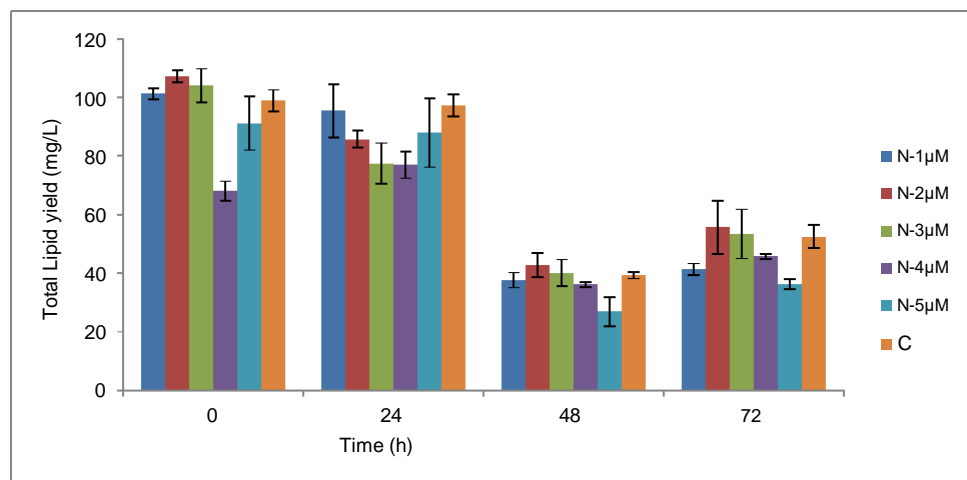
Fig. 5.4. Effect of ABA on lipid yield in treated and control (N-) *S. quadricauda.* The ABA supplemented cultures and nitrogen stressed *S. quadricauda* were depicted in the graph.
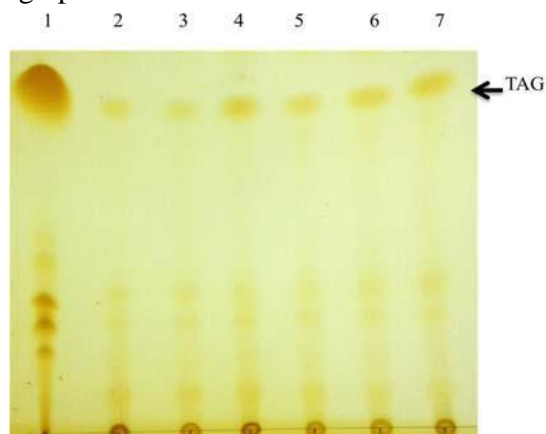
Fig. 5.5. Effect of ABA on lipid yield in treated and control (N-) *S. quadricauda.* The ABA supplemented cultures and nitrogen stressed *S. quadricauda* were depicted in the graph.
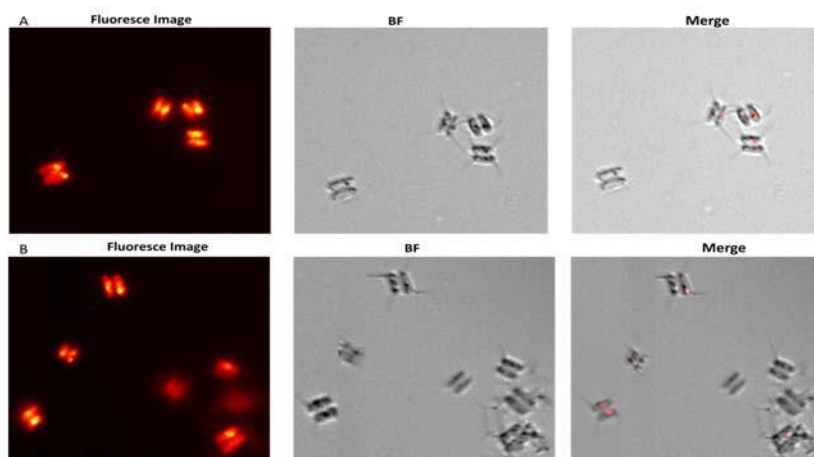
Fig. 5.6: Nile red image of (A) nitrogen starved (N⁻) and (B) ABA supplemented (2μM) *S. quadricauda.* The yellow golden colour represents the lipid droplets.

5.3.4. Influence of ABA supplementation on biomass yield

The major drawback of stress-induced lipid accumulation was the drastic reduction in biomass yield. ABA supplementation sustains the cell growth that eventually prevents the drastic reduction of biomass under nitrogen limitation. Here also, the lower concentrations of (1, 2 and 3 μM) have effects on biomass under nitrogen depletion. The maximum biomass was observed in 48 hours. After 48 hours there is not much increment in biomass yield. The dry biomass yield was 2.1 fold enhanced in ABA supplemented cultures compared to control (Table. 5.1).

ABA Conc.	Dry biomass yield (mg/L)			
	0 hr	24 hr	48 hr	72 hr
N+ (C1)	25	27.5	35	47.5
N- (C2)	15	20	25	22.5
N-1μM	15	22.5	32.5	43.5
N-2μM	15	27.5	52.5	45
N-3μM	20	25	45	35
N-4μM	15	20.5	33.5	30
N-5μM	12.5	22.5	35	42.5

Table. 5.1: Dry biomass yield of ABA supplemented nitrogen starved (N⁻) *S. quadricauda* and control.

5.3.5. Effect of ABA supplementation on pigments

Nitrogen starvation leads to degradation of chlorophyll and lipid accumulation in microalgae. Chlorophyll is a nitrogenous compound and its composition was influenced by nitrogen concentration under stress. During nitrogen stress, the photosynthetic pigments are drastically reduced and the culture becomes pale yellow. It was observed that total chlorophyll and carotenoids were reduced in nitrogen stress condition until 72 hours. After ABA supplementation, the pigment level has no further increment; rather it is protecting the stressed cells (Table. 5.2).

ABA conc.	Total Chlorophyll (mg/L)				Carotenoids (mg/L)			
	0 h	24 h	48 h	72 h	0 h	24 h	48 h	72 h
C1(N+)	2.967±0.20	3.023±0.58	2.989±0.38	1.580±0.29	0.1293±0.003	0.158±0.026	0.0916±0.02	0.049±0.01
C2(N-)	3.03±0.154	2.266±0.31	1.305±1.12	1.041±0.47	0.0983±0.010	0.1±0.009	0.0543±0.01	0.056±0.011
N-1µM	3.80±1.204	1.759±0.04	2.408±0.61	1.806±0.52	0.081±0.033	0.0746±0.011	0.0806±0.02	0.0393±0.017
N-2µM	2.664±0.04	4.037±1.39	1.225±0.00	1.646±0.99	0.1±0.004	0.1976±0.041	0.0366±0.00	0.0543±0.006
N-3µM	3.11±0.071	1.696±0.16	1.342±0.46	0.948±0.26	0.0866±0.004	0.0833±0.005	0.037±0.028	0.027±0.006
N-4µM	2.326±0.24	1.211±0.22	1.011±0.01	0.944±0.04	0.073±0.022	0.056±0.009	0.032±0.009	0.047±0.018
N-5µM	3.66±0.259	3.531±0.94	1.431±0.14	1.346±0.43	0.1006±0.005	0.1676±0.045	0.0583±0.00	0.0896±0.027

Table. 5.2. The effect of ABA supplementation in photosynthetic pigments of *S. quadricauda*. The photosynthetic pigments in ABA supplemented and nitrogen starved *S. quadricauda*

5.3.6. Fatty acid composition of ABA supplemented nitrogen starved *S. quadricauda*

Abscisic acid, the stress hormone had no rapid increment in saturated and unsaturated fatty acids in nitrogen deprived *S. quadricauda*. But ABA (5 μM) treated cultures showed 11.17 % increment in saturated fatty acid content and a decrease of 11.16 % of unsaturated fatty acid content. The lower concentrations are having fatty acid composition as similar to control. 1.4 % increment in monounsaturated fatty acid level in 1 μM ABA treated cultures was also observed under nitrogen deprivation (Fig. 5.7).
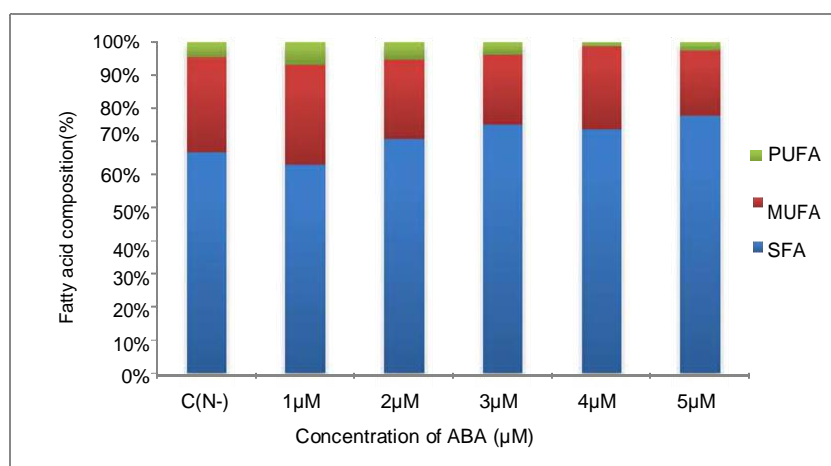
Table.5.7: The effect on fatty acid composition by ABA supplementation in *S. quadricauda*. Fatty acid composition of ABA supplemented and control (nitrogen starved) *S. quadricauda*.

5.4. Discussion

In our study for the first time we are reporting that the indigenous level of ABA was found to be 4 fold elevated than the control during nitrogen starvation in *S. quadricauda*. According to Kumari et al., 2013, intracellular ABA was increased up to 1.5 to 1. 7 fold under nutrient starvation in ASW-cultured thalli of *Ulva lactuca*. The ABA accumulation was also explained in chickpea roots under drought by De-Domenico et al. 2012 they reported it to be 20 % higher than the tolerant plants. They also observed a sharp increase in ABA within 24 h, after that the level was quantified as constant in tolerable variety but in stressed plant a decrease within 48 hours. The experiments

conducted by Lu et al. (2014) also suggested that the elevated level of intracellular ABA under nitrogen starvation in *Nannochloropsis oceanica*. Similarly, the same effect was observed by Tominaga et al., 1993 in green microalga *Dunaliella* species. Similarly the yet another abiotc stress, presence of heavy metals also leads to enhanced ABA level in microalgae (Lu, and Xu, 2015). During the abiotic stress, an endogenous level of ABA shoots up and is released across the plasma membrane of cyanobacteria and alga. Most often this enhancement was observed during onset of stress in order to cope-up with the stress by guarding the cells against photoinhibition in *Chlamydomonas reinhardtii* (Saradhi et al., 2000); overcoming the oxidative damage by reactive oxygen species and free radicals generated during stress in *Chlamydomonas reinhardtii* (Yoshida, 2005; Yasohida et al., 2003) and *Haematococcus pulvaris* (Kobayashi et al., 1997).

Nitrogen-limited TAP media with supplementation of phytohormone significantly increased the microalgal growth in *Chlamydomonas reinhardtii* thus it can be used in efficient microalgal cultivation for biofuel production (Park et al., 2013). The *Scenedesmus* sp. CCNM 1077 significantly reduces biomass under decreased nitrate concentration. It is due to decrease in metabolic activity and cell division of *Scenedesmus* sp. CCNM 1077 ;during nitrogen limitation (Pancha et al., 2014). Similar observations were also reported in *Chlorella* sp. (Illman et al., 2000). Phytohormone supplementation promotes growth that eventually leads to increase in biomass productivity from 54 to 69 % in *Chlamydomonas reinhardtii* (Park et al., 2013). Similarly in *S. quadricauda* there is an increased cell number in ABA treated cultures. Lipid droplets are reserved storage products which have been utilised during stress for survival of the cells (Courchesne et al., 2009). According to Pancha et al., 2014 the lipid content was increased from 18.87 to 27.93 % in nitrogen starved condition. Another report on enhanced lipid accumulation in *S. quadricauda* under nitrogen starvation explained that there was a 2.27 fold increment in total lipid yield (Anand and Arumugam, 2015).

Nitrogen is an essential major element involved in the biosynthesis of proteins, nucleic acids and photosynthetic pigments. Photosynthetic pigments

viz. Chl a, Chl b and total carotenoid were decreased during nitrogen limitation in microalgae which eventually affects the biomass yield (Berges et al., 1996; Kumar Saha et al., 2003; Li et al., 2008). The nutritional stress triggers the decrease in light harvesting complex and PSII activity and finally leads to photosynthesis inhibition (Anand and Arumugam, 2015). Current study also exhibits ABA supplementation is not having marked difference in pigment level in *S. quadricauda* during nitrogen starvation. A higher accumulation of carotenoids serves a protective function against oxidative stress during nitrogen deprivation (Zhang et al., 2013).

Nitrogen stress altered the fatty acid composition of *S. quadricauda* compared to nitrogen rich algal cells. The reported saturated fatty acid content of *S. quadricauda* is about 46 % by Anand and Arumugam et al., 2015. Treatments with ABA have altered the FAME yield of about more than 10 % in *Chlamydomonas reinhardtii* under nitrogen limitation (Park et al., 2013). Thus the ABA supplementation altered fatty acid composition towards a more suitable condition for biofuel application.

5.5. Conclusion

Biomass and lipid yield reduction during nitrogen starvation can be reduced by supplementing the stress responsible hormone ABA. In order to tolerate the stress the endogenous level of ABA also shoots up about 4 fold during nitrogen stress. The lower concentrations of ABA are promoting growth and biomass and sustains lipid yield. The fatty acid composition also showed a slight difference in saturated and unsaturated fatty acids. Thus, ABA plays a vital role in sustaining the biomass, lipid yield during nitrogen starved *S. quadricauda.*

CHAPTER

6

SUMMARY, CONCLUSION AND FUTURE PERSPECTIVES

6. Overall Summary and Conclusion

The biochemical and metabolic changes during nitrogen starvation was described here. The Nitrogen stress induces oxidative stress, eventually ROS generation which leads to lipid accumulation and lipid droplet maturation that causes enlargement in cell size. Also the increment in mitochondrial potential during initial hours of nitrogen stress which induces increased ROS generation. In order to suppress the generated ROS (H_2O_2 and OH^-) under nitrogen starvation the stress biomarkers such as peroxidase and catalase activity was increased. The integrated targeted metabolic analysis showed stress associated non proteinogenic amino acids and energy equivalents elevated during nitrogen starvation.

The molecular changes during nitrogen starvation were addressed in the aspect of differentially expressed proteins. The stress associated protein (SAP 1-4) were identified as mitochondrial orf151, ribosomal protein L23, envelope membrane protein (Chloroplast) and ATP synthase β-subunit of *Acutodesmus* (*Scenedesmus*) *obliquus* respectively. The differential expression analysis of RPL 23 (SAP 2) showed that there was about 2.6 fold expressions in nitrogen starved *S. quadricauda* after 6hr of incubation. The whole genome sequencing of mitochondrial DNA was performed and the phylogenetic tree showed divergence in sequence between *S. obliquus* and *S. quadricauda* even though they were in the same clade. SAP 1 was identified in ORF 42 of mitochondrial genome with similarity to LAGLIDADG Homing Endonuclease protein. LHE was differentially expressed about 4.2 fold during 48 hour of nitrogen stress induction in *S. quadricauda*. LAGLIDADG endonuclease of *S.quadricauda* acts as a homodimer and performs its endonuclease action. Thus the structure and DNA binding regions of LAGLIDADG endonuclease was predicted.

In order to sustain the biomass reduction during nitrogen starvation, ABA played a central role. ABA internal level is shooting up about 27.21pmol/l at 24 hour and then falling down within 48 hours of nitrogen stress induction. The ABA supplementation (2 μM) to the nitrogen starved *S.quadricauda* sustains the cell number and lipid yield with sustained biomass. The FAME profile of ABA treated cultures showed 11.17% increment in saturated fatty acid level and decrease of about 11.16% in unsaturated fatty acid content. The overall summary was postulated in the graphical scheme (Scheme. 6.1).
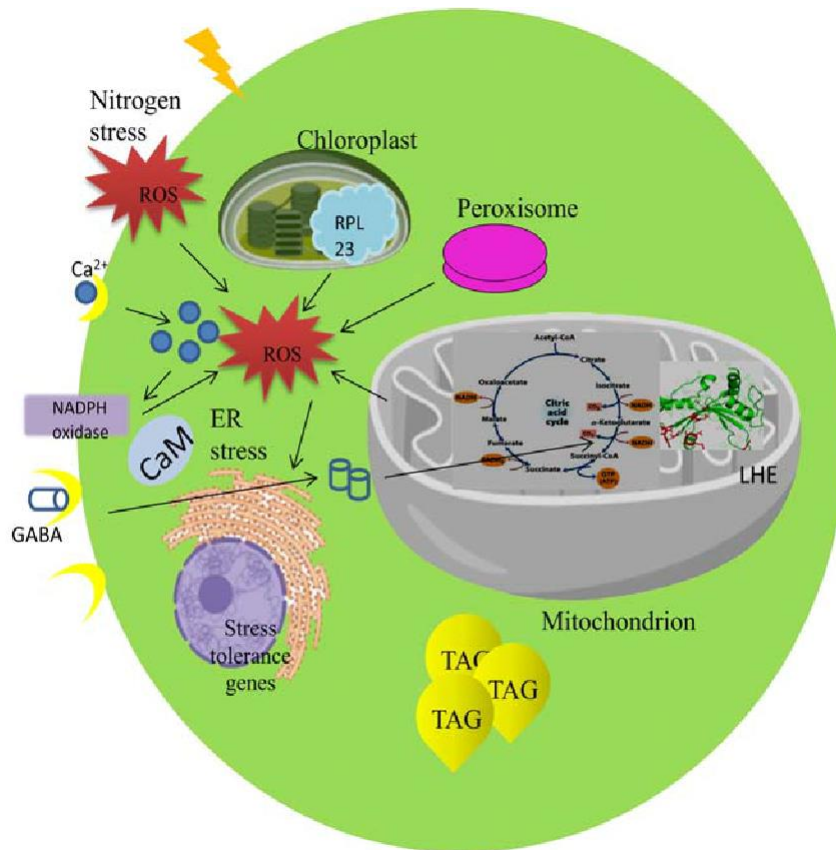
Scheme. 6.1: Schematic representation of selected biochemical, metabolic and molecular changes during nitrogen stress mediated lipid accumulation in *Scenedesmus quadricauda* CASA CC202.

6.1. Salient findings and future perspectives of the study

- Two SAPs were identified for the first time in nitrogen starvation –LAGLIDADG endonuclease and Ribosomal protein L23 – Its role in stress mediated lipid accumulation is interestingly explored.

- ABA shoots up during nitrogen stress. Study its relevance and ABA responsive factors during nitrogen stress shreds light on stress mediated lipid accumulation.

References

Abdallah, F., Salamini, F. and Leister, D., 2000. A prediction of the size and evolutionary origin of the proteome of chloroplasts of *Arabidopsis*. *Trends in Plant Science*, *5*(4), pp.141-142.

Adams, C., Godfrey, V., Wahlen, B., Seefeldt, L. and Bugbee, B., 2013. Understanding precision nitrogen stress to optimize the growth and lipid content trade off in oleaginous green microalgae. *Bioresource Technology*, *131*, pp.188-194.

Ahmad, M.R., Saxena, P.M., Amla, D.V. and Shyam, R., 1978. Effect of abscisic acid on the blue green algae *Anacystis nidulans* and *Nostoc muscorum. Beitrage zur Biologie der Pflanzen*, 54, pp.33–40.

Ali, M.B., Yu, K.W., Hahn, E.J. and Paek, K.Y., 2005. Differential responses of anti-oxidants enzymes, lipoxygenase activity, ascorbate content and the production of saponins in tissue cultured root of mountain Panax ginseng CA Mayer and *Panax quinquefolium L.* in bioreactor subjected to methyl jasmonate stress. *Plant Science*, *169*(1), pp.83-92.

Allen, A.E., Dupont, C.L., Oborník, M., Horak, A., Nunes-Nesi, A., McCrow, J.P., Zheng, H., Johnson, D.A., Hu, H., Fernie, A.R. and Bowler, C., 2011. Evolution and metabolic significance of the urea cycle in photosynthetic diatoms. *Nature*, *473*(7346), p.203.

Allen, J.W., DiRusso, C.C. and Black, P.N., 2015. Triacylglycerol synthesis during nitrogen stress involves the prokaryotic lipid synthesis pathway and acyl chain remodeling in the microalgae *Coccomyxa subellipsoidea*. *Algal research*, *10*, pp.110-120.

Alvarez, R., del Hoyo, A., Casano, L.M., Barreno, E. and del Campo, E.M., 2012. Newly identified LAGLIDADG homing endonucleases in the chloroplast LSU rDNA of *Coccomyxa* algae. In *Microbes In Applied Research: Current Advances and Challenges* (pp. 668-673).

Alvarez-Diaz, P.D., Ruiz, J., Arbib, Z., Barragan, J., Garrido-Perez, C. and Perales, J.A., 2014. Lipid production of microalga *Ankistrodesmus falcatus* increased by nutrient

and light starvation in a two-stage cultivation process. *Applied Biochemistry and Biotechnology*, *174*(4), pp.1471-1483.

Anand, J. and Arumugam, M., 2015. Enhanced lipid accumulation and biomass yield of *Scenedesmus quadricauda* under nitrogen starved condition. *Bioresource Technology*, *188*, pp.190-194.

Arnholdt-Schmitt, B., Costa, J.H. and de Melo, D.F., 2006. AOX–a functional marker for efficient cell reprogramming under stress?.*Trends in Plant Science*, *11*(6), pp.281-287.

Arumugam, M., Agarwal, A., Arya, M.C. and Ahmed, Z., 2013. Influence of nitrogen sources on biomass productivity of microalgae *Scenedesmus bijugatus*. *Bioresource Technology*, *131*, pp.246-249.

Asulabh, K.S., Supriya, G. and Ramachandra, T.V., 2012. Effect of salinity concentrations on growth rate and lipid concentration in *Microcystis* sp., *Chlorococcum* sp. and *Chaetoceros* sp. In *National Conference on Conservation and Management of Wetland Ecosystems. School of Environmental Sciences, Mahatma Gandhi University, Kottayam, Kerala*.

Babicki, S., Arndt, D., Marcu, A., Liang, Y., Grant, J.R., Maciejewski, A. and Wishart, D.S., 2016. Heatmapper: web-enabled heat mapping for all. *Nucleic acids research*, *44*(W1), pp.W147-W153.

Bajguz, A., 2009. Brassinosteroid enhanced the level of abscisic acid in *Chlorella vulgaris* subjected to short-term heat stress. *Journal of Plant Physiology*, *166*(8), pp.882-886.

Bajguz, A., 2011. Suppression of *Chlorella vulgaris* growth by cadmium, lead, and copper stress and its restoration by endogenous brassinolide. *Archives of Environmental Contamination and Toxicology*, *60*(3), pp.406-416.

Baracca, A., Sgarbi, G., Solaini, G. and Lenaz, G., 2003. Rhodamine 123 as a probe of mitochondrial membrane potential: evaluation of proton flux through F0 during ATP synthesis. *Biochimicaet Biophysica Acta (BBA)-Bioenergetics*, *1606*(1-3), pp.137-146.

Barbrook, A.C., Howe, C.J., Kurniawan, D.P. and Tarr, S.J., 2010. Organization and expression of organellar genomes. *Philosophical Transactions of the Royal Society B: Biological Sciences*, *365*(1541), pp.785-797.

Barnwal, B.K. and Sharma, M.P., 2005. Prospects of biodiesel production from vegetable oils in India. *Renewable and Sustainable Energy Reviews*, *9*(4), pp.363-378.

Battah, M., El-Ayoty, Y., Abomohra, A.E.F., El-Ghany, S.A. and Esmael, A., 2015. Effect of Mn $^{2+}$, Co $^{2+}$ and H_2O_2 on biomass and lipids of the green microalga *Chlorella vulgaris* as a potential candidate for biodiesel production. *Annals of Microbiology*, *65*(1), pp.155-162.

Belfort, M. and Roberts, R.J., 1997. Homing endonucleases: keeping the house in order. *Nucleic Acids Research*, *25*(17), pp.3379-3388.

Belfort, M., Derbyshire, V., Parker, M.M., Cousineau, B. and Lambowitz, A.M., 2002. Mobile introns: pathways and proteins. *Mobile DNA II* (pp. 761-783). American Society of Microbiology.

Ben Amor, F., Elleuch, F., Ben Hlima, H., Garnier, M., Saint-Jean, B., Barkallah, M., Pichon, C., Abdelkafi, S. and Fendri, I., 2017. Proteomic analysis of the Chlorophyta *Dunaliella* new strain AL-1 revealed global changes of metabolism during high carotenoid production. *Marine Drugs*, *15*(9), p.293.

Berges, J.A., Charlebois, D.O., Mauzerall, D.C. and Falkowski, P.G., 1996. Differential effects of nitrogen limitation on photosynthetic efficiency of photosystems I and II in microalgae. *Plant Physiology*, *110*(2), pp.689-696.

Bhaduri, A.M. and Fulekar, M.H., 2012. Antioxidant enzyme responses of plants to heavy metal stress. *Reviews in Environmental Science and BioTechnology*, *11*(1), pp.55-69.

Bhola, V., Desikan, R., Santosh, S.K., Subburamu, K., Sanniyasi, E. and Bux, F., 2011. Effects of parameters affecting biomass yield and thermal behaviour of *Chlorella vulgaris*. *Journal of Bioscience and Bioengineering*, *111*(3), pp.377-382.

Bishop, W.M. and Zubeck, H.M., 2012. Evaluation of microalgae for use as nutraceuticals and nutritional supplements. *Journal of Nutrition & Food Sciences, 2*(5), pp.1-6.

Blaby, I.K., Glaesener, A.G., Mettler, T., Fitz-Gibbon, S.T., Gallaher, S.D., Liu, B., Boyle, N.R., Kropat, J., Stitt, M., Johnson, S. and Benning, C., 2013. Systems-level analysis of nitrogen starvation–induced modifications of carbon metabolism in a *Chlamydomonas reinhardtii* starchless mutant. *The Plant Cell*, *25*(11), pp.4305-4323.

Blifernez-Klassen, O., Wibberg, D., Winkler, A., Blom, J., Goesmann, A., Kalinowski, J. and Kruse, O., 2016. Complete chloroplast and mitochondrial genome sequences of the hydrocarbon oil-producing green microalga *Botryococcus braunii* race B (Showa). *Genome Announc.*, *4*(3), pp.e00524-16.

Bobik, K. and Burch-Smith, T.M., 2015. Chloroplast signaling within, between and beyond cells. *Frontiers in Plant Science*, *6*, p.781.

Boyle, N.R., Page, M.D., Liu, B., Blaby, I.K., Casero, D., Kropat, J., Cokus, S.J., Hong-Hermesdorf, A., Shaw, J., Karpowicz, S.J. and Gallaher, S.D., 2012. Three acyltransferases and nitrogen-responsive regulator are implicated in nitrogen starvation-induced triacylglycerol accumulation in *Chlamydomonas*. *Journal of Biological Chemistry*, *287*(19), pp.15811-15825.

Bradford, M.M., 1976. A rapid and sensitive method for the quantitation of microgram quantities of protein utilizing the principle of protein-dye binding. *Analytical Biochemistry*, *72*(1-2), pp.248-254.

Branyikova, I., Marsalkova, B., Doucha, J., Branyik, T., Bisova, K., Zachleder, V. and Vítova, M., 2011. Microalgae novel highly efficient starch producers. *Biotechnology and Bioengineering*, *108*(4), pp.766-776.

Brennan, L. and Owende, P., 2010. Biofuels from microalgae- a review of technologies for production, processing, and extractions of biofuels and co-products. *Renewable and Sustainable Energy Reviews*, *14*(2), pp.557-577.

Breuer, G., Lamers, P.P., Martens, D.E., Draaisma, R.B. and Wijffels, R.H., 2012. The impact of nitrogen starvation on the dynamics of triacylglycerol accumulation in nine microalgae strains. *Bioresource Technology*, *124*, pp.217-226.

Buitenhuis, E.T. and Geider, R.J., 2010. A model of phytoplankton acclimation to iron-light colimitation. *Limnology and Oceanography*, *55*(2), pp.714-724.

Cakmak, T., Angun, P., Demiray, Y.E., Ozkan, A.D., Elibol, Z. and Tekinay, T., 2012. Differential effects of nitrogen and sulfur deprivation on growth and biodiesel feedstock production of *Chlamydomonas reinhardtii*. *Biotechnology and Bioengineering*, *109*(8), pp.1947-1957.

Campenni, L., Nobre, B.P., Santos, C.A., Oliveira, A.C., Aires-Barros, M.R., Palavra, A.M.F. and Gouveia, L., 2013. Carotenoid and lipid production by the autotrophic microalga *Chlorella protothecoides* under nutritional, salinity, and luminosity stress conditions. *Applied Microbiology and Biotechnology*, *97*(3), pp.1383-1393.

Cardol, P., Gloire, G., Havaux, M., Remacle, C., Matagne, R. and Franck, F., 2003. Photosynthesis and state transitions in mitochondrial mutants of *Chlamydomonas reinhardtii* affected in respiration. *Plant Physiology*, *133*(4), pp.2010-2020.

Carvalho, A.P. and Malcata, F.X., 2005. Optimization of ω-3 fatty acid production by microalgae: crossover effects of CO_2 and light intensity under batch and continuous cultivation modes. *Marine Biotechnology*, *7*(4), pp.381-388.

Castielli, O., De la Cerda, B., Navarro, J.A., Hervás, M. and De la Rosa, M.A., 2009. Proteomic analyses of the response of cyanobacteria to different stress conditions. *FEBS Letters*, *583*(11), pp.1753-1758.

Chan, K.X., Phua, S.Y., Crisp, P., Mc Quinn, R. and Pogson, B.J., 2016. Learning the languages of the chloroplast: Retrograde signaling and beyond. *Annual Review of Plant Biology*, *67*, p. 25–53.

Che, R., Huang, L., Xu, J.W., Zhao, P., Li, T., Ma, H. and Yu, X., 2017. Effect of fulvic acid induction on the physiology, metabolism, and lipid biosynthesis-related gene transcription of *Monoraphidium* sp. FXY-10. *Bioresource Technology*, *227*, pp.324-334.

Chen, G.Q. and Chen, F., 2006. Growing phototrophic cells without light. *Biotechnology Letters*, *28*(9), pp.607-616.

Chen, G.Q., Jiang, Y. and Chen, F., 2008. Salt-induced alterations in lipid composition of diatom *Nitzschia laevis* (Bacillariophyceae) under heterotrophic culture condition 1. *Journal of Phycology*, *44*(5), pp.1309-1314.

Chen, H., Zhang, Y., He, C. and Wang, Q., 2014. Ca^{2+} signal transduction related to neutral lipid synthesis in an oil-producing green alga *Chlorella* sp. C2. *Plant and Cell Physiology*, *55*(3), pp.634-644.

Chen, W., Provart, N.J., Glazebrook, J., Katagiri, F., Chang, H.S., Eulgem, T., Mauch, F., Luan, S., Zou, G., Whitham, S.A. and Budworth, P.R., 2002. Expression profile matrix of *Arabidopsis* transcription factor genes suggests their putative functions in response to environmental stresses. *The Plant Cell*, *14*(3), pp.559-574.

Cheng, D. and He, Q., 2014. Assessment of environmental stresses for enhanced microalgal biofuel production–an overview. *Frontiers in Energy Research*, *2*, p.26.

Cheng, J.S., Niu, Y.H., Lu, S.H. and Yuan, Y.J., 2012. Metabolome analysis reveals ethanolamine as potential marker for improving lipid accumulation of model photosynthetic organisms. *Journal of Chemical Technology & Biotechnology*, *87*(10), pp.1409-1418.

Chisti, Y., 2007. Biodiesel from microalgae. *Biotechnology Advances*, *25*(3), pp.294-306.

Chokshi, K., Pancha, I., Ghosh, A. and Mishra, S., 2017. Nitrogen starvation-induced cellular crosstalk of ROS-scavenging antioxidants and phytohormone enhanced the biofuel potential of green microalga *Acutodesmus dimorphus*. *Biotechnology for Biofuels*, *10*(1), p.60.

Choudhury, F.K., Rivero, R.M., Blumwald, E. and Mittler, R., 2017. Reactive oxygen species, abiotic stress and stress combination. *The Plant Journal*, *90*(5), pp.856-867.

Chu, F.F., Chu, P.N., Shen, X.F., Lam, P.K. and Zeng, R.J., 2014. Effect of phosphorus on biodiesel production from *Scenedesmus obliquus* under nitrogen-deficiency stress. *Bioresource Technology*, *152*, pp.241-246.

Chu, W.L., 2017. Strategies to enhance production of microalgal biomass and lipids for biofuel feedstock. *European Journal of Phycology*, *52*(4), pp.419-437.

Clifton, R., Millar, A.H. and Whelan, J., 2006. Alternative oxidases in *Arabidopsis*: a comparative analysis of differential expression in the gene family provides new insights into function of non-phosphorylating bypasses. *Biochimicaet Biophysica Acta (BBA)-Bioenergetics*, *1757*(7), pp.730-741.

Considine, M.J., MariaSandalio, L. and Helen Foyer, C., 2015. Unravelling how plants benefit from ROS and NO reactions, while resisting oxidative stress. *Annals of Botany*, *116*(4), pp.469-473.

Converti, A., Casazza, A.A., Ortiz, E.Y., Perego, P. and Del Borghi, M., 2009. Effect of temperature and nitrogen concentration on the growth and lipid content of *Nannochloropsis oculata* and *Chlorella vulgaris* for biodiesel production. *Chemical Engineering and Processing: Process Intensification*, *48*(6), pp.1146-1151.

Courchesne, N.M.D., Parisien, A., Wang, B. and Lan, C.Q., 2009. Enhancement of lipid production using biochemical, genetic and transcription factor engineering approaches. *Journal of Biotechnology*, *141*(1-2), pp.31-41.

Cui, S., Huang, F., Wang, J., Ma, X., Cheng, Y. and Liu, J., 2005. A proteomic analysis of cold stress responses in rice seedlings. *Proteomics*, *5*(12), pp.3162-3172.

Cutler, S.R., Rodriguez, P.L., Finkelstein, R.R. and Abrams, S.R., 2010. Abscisic acid: emergence of a core signaling network. *Annual Review of Plant Biology*, *61*, pp.651-679.

Dalgaard, J.Z., Garrett, R.A. and Belfort, M., 1993. A site-specific endonuclease encoded by a typical archaeal intron. *Proceedings of the National Academy of Sciences*, *90*(12), pp.5414-5417.

Dalgaard, J.Z., Klar, A.J., Moser, M.J., Holley, W.R., Chatterjee, A. and SairaMian, I., 1997. Statistical modeling and analysis of the LAGLIDADG family of site-specific endonucleases and identification of an intein that encodes a site-specific endonuclease of the HNH family. *Nucleic Acids Research*, *25*(22), pp.4626-4638.

Date, Y., Kojima, M., Hosoda, H., Sawaguchi, A., Mondal, M.S., Suganuma, T., Matsukura, S., Kangawa, K. and Nakazato, M., 2000. Ghrelin, a novel growth hormone-releasing acylated peptide, is synthesized in a distinct endocrine cell type in the gastrointestinal tracts of rats and humans. *Endocrinology*, *141*(11), pp.4255-4261.

De Clercq, I., Vermeirssen, V., Van Aken, O., Vandepoele, K., Murcha, M.W., Law, S.R., Inze, A., Ng, S., Ivanova, A., Rombaut, D. and Van De Cotte, B., 2013. The membrane-bound NAC transcription factor ANAC013 functions in mitochondrial retrograde regulation of the oxidative stress response in *Arabidopsis*. *The Plant Cell*, *25*(9), pp.3472-3490.

De Domenico, S., Bonsegna, S., Horres, R., Pastor, V., Taurino, M., Poltronieri, P., Imtiaz, M., Kahl, G., Flors, V., Winter, P. and Santino, A., 2012. Transcriptomic analysis of oxylipin biosynthesis genes and chemical profiling reveal an early induction of jasmonates in chickpea roots under drought stress. *Plant Physiology and Biochemistry*, *61*, pp.115-122.

de Lomana, A.L.G., Schauble, S., Valenzuela, J., Imam, S., Carter, W., Bilgin, D.D., Yohn, C.B., Turkarslan, S., Reiss, D.J., Orellana, M.V. and Price, N.D., 2015. Transcriptional program for nitrogen starvation-induced lipid accumulation in *Chlamydomonas reinhardtii*. *Biotechnology for Biofuels*, *8*(1), p.207.

De Longevialle, A.F., Hendrickson, L., Taylor, N.L., Delannoy, E., Lurin, C., Badger, M., Millar, A.H. and Small, I., 2008. The pentatricopeptide repeat gene OTP51 with two LAGLIDADG motifs is required for the cis-splicing of plastid ycf3 intron 2 in *Arabidopsis thaliana*. *The Plant Journal*, *56*(1), pp.157-168.

Dietz, K.J., 2015. Efficient high light acclimation involves rapid processes at multiple mechanistic levels. *Journal of Experimental Botany*, *66*(9), pp.2401-2414.

Ding, W., Zhao, Y., Xu, J.W., Zhao, P., Li, T., Ma, H., Reiter, R.J. and Yu, X., 2018. Melatonin: a multifunctional molecule that triggers defense responses against high light and nitrogen starvation stress in *Haematococcus pluvialis*. *Journal of Agricultural and Food Chemistry*, *66*(29), pp.7701-7711.

Dong, H.P., Williams, E., Wang, D.Z., Xie, Z.X., Hsia, R.C., Jenck, A., Halden, R., Li, J., Chen, F. and Place, A.R., 2013. Responses of *Nannochloropsis oceanica* IMET1 to long-term nitrogen starvation and recovery. *Plant Physiology*, *162*(2), pp.1110-1126.

Eckardt, N.A., 2011. Retrograde signaling: a new candidate signaling molecule. *Plant Cell, 23*, p. 3870-3870.

El-Kassas, H.Y., 2013. Growth and fatty acid profile of the marine microalga *Picochlorum* sp. grown under nutrient stress conditions. *The Egyptian Journal of Aquatic Research*, *39*(4), pp.233-239.

Erickson, E., Wakao, S. and Niyogi, K.K., 2015. Light stress and photoprotection in *Chlamydomonas reinhardtii*. *The Plant Journal*, *82*(3), pp.449-465.

Falkowski, P.G., Barber, R.T. and Smetacek, V., 1998. Biogeochemical controls and feedbacks on ocean primary production. *Science*, *281*(5374), pp.200-206.

Fan, J., Andre, C. and Xu, C., 2011. A chloroplast pathway for the de novo biosynthesis of triacylglycerol in *Chlamydomonas reinhardtii*. *FEBS Letters*, *585*(12), pp.1985-1991.

Fan, J., Cui, Y., Wan, M., Wang, W. and Li, Y., 2014. Lipid accumulation and biosynthesis genes response of the oleaginous *Chlorella pyrenoidosa* under three nutrition stressors. *Biotechnology for Biofuels*, *7*(1), p.17.

Fan, J., Yan, C., Andre, C., Shanklin, J., Schwender, J. and Xu, C., 2012. Oil accumulation is controlled by carbon precursor supply for fatty acid synthesis in *Chlamydomonas reinhardtii*. *Plant and Cell Physiology*, *53*(8), pp.1380-1390.

Fosse, H.K., 2016. Effect of nitrogen limitation on lipid and fatty acid composition of three marine microalgae (Master's thesis, NTNU).

Foyer, C.H. and Noctor, G., 2013. Redox signaling in plants. *Antioxidants & Redox Signaling. 18*, p. 2087–2090.

Fuentes-Grunewald, C., Garces, E., Alacid, E., Rossi, S. and Camp, J., 2013. Biomass and lipid production of dinoflagellates and raphidophytes in indoor and outdoor photobioreactors. *Marine Biotechnology*, *15*(1), pp.37-47.

Gao, C., Wang, Y., Shen, Y., Yan, D., He, X., Dai, J. and Wu, Q., 2014. Oil accumulation mechanisms of the oleaginous microalga *Chlorella protothecoides* revealed through its genome, transcriptomes, and proteomes. *BMC Genomics*, *15*(1), p.582.

Gao, K., 1998. Chinese studies on the edible blue-green alga, *Nostoc flagelliforme*: a review. *Journal of Applied Phycology*, *10*(1), pp.37-49.

Gao, Y., Yang, M. and Wang, C., 2013. Nutrient deprivation enhances lipid content in marine microalgae. *Bioresource Technology*, *147*, pp.484-491.

Gao, Z.Q. and Meng, C.X., 2007. Impact of extraneous ethylene concentrations to astaxanthin accumulation of *Haematoccus pluvialis. Food Science*, *10*, p.093.

Gargouri, M., Park, J.J., Holguin, F.O., Kim, M.J., Wang, H., Deshpande, R.R., Shachar-Hill, Y., Hicks, L.M. and Gang, D.R., 2015. Identification of regulatory network hubs that control lipid metabolism in *Chlamydomonas reinhardtii*. *Journal of Experimental Botany*, *66*(15), pp.4551-4566.

Garibay-Hernandez, A., Barkla, B.J., Vera-Estrella, R., Martinez, A. and Pantoja, O., 2017. Membrane proteomic insights into the physiology and taxonomy of an oleaginous green microalga. *Plant Physiology*, *173*(1), pp.390-416.

Ge, F., Huang, W., Chen, Z., Zhang, C., Xiong, Q., Bowler, C., Yang, J., Xu, J. and Hu, H., 2014. Methylcrotonyl-CoA carboxylase regulates triacylglycerol accumulation in the model diatom *Phaeodactylum tricornutum*. *The Plant Cell*, *26*(4), pp.1681-1697.

Gimble, F.S. and Thorner, J., 1992. Homing of a DNA endonuclease gene by meiotic gene conversion in *Saccharomyces cerevisiae*. *Nature*, *357*(6376), p.301.

Goncalves, A.M.M., Mesquita, A.F., Verdelhos, T., Coutinho, J.A.P., Marques, J.C. and Goncalves, F., 2016. Fatty acids' profiles as indicators of stress induced by of a common herbicide on two marine bivalves species: *Cerastoderma edule* (Linnaeus, 1758) and *Scrobicularia plana* (da Costa, 1778). *Ecological Indicators*, *63*, pp.209-218.

Goncalves, E.C., Johnson, J.V. and Rathinasabapathi, B., 2013. Conversion of membrane lipid acyl groups to triacylglycerol and formation of lipid bodies upon nitrogen starvation in biofuel green algae *Chlorella* UTEX29. *Planta*, *238*(5), pp.895-906.

Gray, M.W., Archibald, J.M., Bock, R. and Knoop, V., 2012. Genomics of chloroplasts and mitochondria.

Gray, M.W., Lang, B.F., Cedergren, R., Golding, G.B., Lemieux, C., Sankoff, D., Turmel, M., Brossard, N., Delage, E., Littlejohn, T.G. and Plante, I., 1998. Genome structure and gene content in protist mitochondrial DNAs. *Nucleic Acids Research*, *26*(4), pp.865-878.

Griffiths, M.J. and Harrison, S.T., 2009. Lipid productivity as a key characteristic for choosing algal species for biodiesel production. *Journal of Applied Phycology*, *21*(5), pp.493-507.

Guarnieri, M.T., Nag, A., Smolinski, S.L., Darzins, A., Seibert, M. and Pienkos, P.T., 2011. Examination of triacylglycerol biosynthetic pathways via de novo transcriptomic and proteomic analyses in an unsequenced microalga. *PLoS One*, *6*(10), p.e25851.

Guckert, J.B. and Cooksey, K.E., 1990. Triglyceride accumulation and fatty acid profile changes in *Chlorella* (Chlorophyta) during high Ph-induced cell cycle Inhibition 1. *Journal of Phycology*, *26*(1), pp.72-79.

Guerra, L.T., Levitan, O., Frada, M.J., Sun, J.S., Falkowski, P.G. and Dismukes, G.C., 2013. Regulatory branch points affecting protein and lipid biosynthesis in the diatom *Phaeodactylum tricornutum*. *Biomass and Bioenergy*, *59*, pp.306-315.

Guschina, I.A. and Harwood, J.L., 2006. Lipids and lipid metabolism in eukaryotic algae. *Progress in Lipid Research*, *45*(2), pp.160-186.

Hakalin, N.L., Paz, A.P., Aranda, D.A. and Moraes, L.M.P., 2014. Enhancement of cell growth and lipid content of a freshwater microalga *Scenedesmus* sp. by optimizing nitrogen, phosphorus and vitamin concentrations for biodiesel production. *Natural Science*, *6*(12), pp.1044-1054.

Halliwell, B., 2006. Reactive species and antioxidants. Redox biology is a fundamental theme of aerobic life. *Plant Physiology*, *141*(2), pp.312-322.

Han, X., Zeng, H., Bartocci, P., Fantozzi, F. and Yan, Y., 2018. Phytohormones and effects on growth and metabolites of microalgae: a review. *Fermentation*, *4*(2), p.25.

Hartung, W. and Gimmler, H., 1994. A stress physiological role for abscisic acid (ABA) in lower plants. In *Progress in Botany,* pp. 157-173. Springer, Berlin, Heidelberg.

Hartung, W., 2010. The evolution of abscisic acid (ABA) and ABA function in lower plants, fungi and lichen. *Functional Plant Biology*, *37*(9), pp.806-812.

Harwati, T.U., Willke, T. and Vorlop, K.D., 2012. Characterization of the lipid accumulation in a tropical freshwater microalgae *Chlorococcum* sp. *Bioresource Technology*, *121*, pp.54-60.

Hassan, F.M., Aljobory, I.F. and Al-Jumaily, E.F., 2013. Stimulation of biodiesel production from two algae: *Chlorella vulgaris* Berjerinck and Nitzschiapalea (Kutz) Smith, and study their some growth parameters under different light intensity. *Journal of Environmental Science, Toxicology and Food Technology,* *6*(2), pp.31-42.

Hausner, G., Hafez, M. and Edgell, D.R., 2014. Bacterial group I introns: mobile RNA catalysts. *Mobile DNA*, *5*(1), p.8.

He, J., Duan, Y., Hua, D., Fan, G., Wang, L., Liu, Y., Chen, Z., Han, L., Qu, L.J. and Gong, Z., 2012. DEXH box RNA helicase - mediated mitochondrial reactive oxygen species production in *Arabidopsis* mediates crosstalk between abscisic acid and auxin signaling. *The Plant Cell*, *24*(5), pp.1815-1833.

Hill, S. and Van Remmen, H., 2014. Mitochondrial stress signaling in longevity: a new role for mitochondrial function in aging. *Redox Biology*, *2*, pp.936-944.

Hirsch, R., Hartung, W. and Gimmler, H., 1989. Abscisic acid content of algae under stress. *Botanica Acta*, *102*(4), pp.326-334.

Ho, S.H., Chen, C.Y. and Chang, J.S., 2012. Effect of light intensity and nitrogen starvation on CO_2 fixation and lipid/carbohydrate production of an indigenous microalga *Scenedesmus obliquus* CNW-N. *Bioresource Technology*, *113*, pp.244-252.

Hockin, N.L., Mock, T., Mulholland, F., Kopriva, S. and Malin, G., 2012. The response of diatom central carbon metabolism to nitrogen starvation is different from that of green algae and higher plants. *Plant Physiology*, *158*(1), pp.299-312.

Hodges, D.M., De Long, J.M., Forney, C.F. and Prange, R.K., 1999. Improving the thiobarbituric acid-reactive-substances assay for estimating lipid peroxidation in plant tissues containing anthocyanin and other interfering compounds. *Planta*, *207*(4), pp.604-611.

Hu, Q., 2004. Environmental effects on cell composition. *Handbook of microalgal culture: Biotechnology and Applied Phycology*, *1*, pp.83-93.

Hu, Q., Sommerfeld, M., Jarvis, E., Ghirardi, M., Posewitz, M., Seibert, M. and Darzins, A., 2008. Microalgal triacylglycerols as feedstocks for biofuel production: perspectives and advances. *The Plant Journal*, *54*(4), pp.621-639.

Huang, J., Yang, J., Msangi, S., Rozelle, S. and Weersink, A., 2012. Biofuels and the poor: Global impact pathways of biofuels on agricultural markets. *Food Policy*, *37*(4), pp.439-451.

Huesemann, M.H., Hausmann, T.S., Bartha, R., Aksoy, M., Weissman, J.C. and Benemann, J.R., 2009. Biomass productivities in wild type and pigment mutant of *Cyclotella* sp.(Diatom). *Applied Biochemistry and Biotechnology*, *157*(3), pp.507-526.

Illman, A.M., Scragg, A.H. and Shales, S.W., 2000. Increase in *Chlorella* strains calorific values when grown in low nitrogen medium. *Enzyme and Microbial Technology*, *27*(8), pp.631-635.

Jiang, P.L., Pasaribu, B. and Chen, C.S., 2014. Nitrogen-deprivation elevates lipid levels in *Symbiodinium* spp. by lipid droplet accumulation: morphological and compositional analyses. *PloS One*, *9*(1), p.e87416.

Johnson, X. and Alric, J., 2013. Central carbon metabolism and electron transport in *Chlamydomonas reinhardtii*: metabolic constraints for carbon partitioning between oil and starch. *Eukaryotic Cell*, *12*(6), pp.776-793.

Jurica, M.S., Monnat Jr, R.J. and Stoddard, B.L., 1998. DNA recognition and cleavage by the LAGLIDADG homing endonuclease I-Cre I. *Molecular cell*, *2*(4), pp.469-476.

Keeling, P.J., 2010. The endosymbiotic origin, diversification and fate of plastids. *Philosophical Transactions of the Royal Society B: Biological Sciences*, *365*(1541), pp.729-748.

Kentzer, T. and Mazur, H., 1991. Abscisic acid as endogenous inhibitor of the marine diatom *Coscinodiscus granii*. *Acta Physiologiae Plantarum*, *13*, pp.153-157.

Kleine, T. and Leister, D., 2016. Retrograde signaling: organelles go networking. *Biochimica Et Biophysica Acta (BBA)-Bioenergetics*, *1857*(8), pp.1313-1325.

Kleine, T., Maier, U.G. and Leister, D., 2009a. DNA transfer from organelles to the nucleus: the idiosyncratic genetics of endosymbiosis. *Annual Review of Plant Biology*, *60*, pp.115-138.

Kleine, T., Voigt, C. and Leister, D., 2009b. Plastid signalling to the nucleus: messengers still lost in the mists?. *Trends in Genetics*, *25*(4), pp.185-192.

Kmiecik, P., Leonardelli, M. and Teige, M., 2016. Novel connections in plant organellar signalling link different stress responses and signalling pathways. *Journal of Experimental Botany*, *67*(13), pp.3793-3807.

Kovtun, A.N., Firsanov, V.B., Fominykh, V.I. and Isaakyan, G.A., 2000. Metrological parameters of the unified calibration whole-body phantom with gamma-emitting radionuclides. *Radiation Protection Dosimetry*, *89*(3-4), pp.239-242.

Kulkarni, M.G. and Dalai, A.K., 2006. Waste cooking oil an economical source for biodiesel: a review. *Industrial & Engineering Chemistry Research*, *45*(9), pp.2901-2913.

Kumar Saha, S., Uma, L. and Subramanian, G., 2003. Nitrogen stress induced changes in the marine cyanobacterium *Oscillatoria willei* BDU 130511. *FEMS Microbiology Ecology*, *45*(3), pp.263-272.

Kumari, P., Kumar, M., Reddy, C.R.K. and Jha, B., 2013. Nitrate and phosphate regimes induced lipidomic and biochemical changes in the intertidal macroalga *Ulva lactuca* (Ulvophyceae, Chlorophyta). *Plant and Cell Physiology*, *55*(1), pp.52-63.

Lambowitz, A.M. and Belfort, M., 1993. Introns as mobile genetic elements. *Annual Review of Biochemistry*, *62*(1), pp.587-622.

Lang, B.F. and Burger, G., 2012. Mitochondrial and eukaryotic origins: a critical review. In *Advances in Botanical Research* (Vol. 63, pp. 1-20). Academic Press.

Lauritano, C., De Luca, D., Amoroso, M., Benfatto, S., Maestri, S., Racioppi, C., Esposito, F. and Ianora, A., 2019. New molecular insights on the response of the green alga *Tetraselmis suecica* to nitrogen starvation. *Scientific Reports*, *9*(1), p.3336.

Lee, D.Y., Park, J.J., Barupal, D.K. and Fiehn, O., 2012. System response of metabolic networks in *Chlamydomonas reinhardtii* to total available ammonium. *Molecular & Cellular Proteomics*, *11*(10), pp.973-988.

Li, D., Zhao, Y., Ding, W., Zhao, P., Xu, J.W., Li, T., Ma, H. and Yu, X., 2017. A strategy for promoting lipid production in green microalgae *Monoraphidium* sp. QLY-1 by combined melatonin and photoinduction. *Bioresource Technology*, *235*, pp.104-112.

Li, Y., Horsman, M., Wang, B., Wu, N. and Lan, C.Q., 2008. Effects of nitrogen sources on cell growth and lipid accumulation of green alga *Neochloris oleoabundans*. *Applied Microbiology and Biotechnology*, *81*(4), pp.629-636.

Li, Z., Sun, M., Li, Q., Li, A. and Zhang, C., 2012. Profiling of carotenoids in six microalgae (Eustigmatophyceae) and assessment of their β-carotene productions in bubble column photobioreactor. *Biotechnology Letters*, *34*(11), pp.2049-2053.

Liang, K., Zhang, Q., Gu, M. and Cong, W., 2013. Effect of phosphorus on lipid accumulation in freshwater microalga *Chlorella* sp. *Journal of Applied Phycology*, *25*(1), pp.311-318.

Lichtenthaler, H.K., 1987. [34] Chlorophylls and carotenoids: pigments of photosynthetic biomembranes. In *Methods in Enzymology* (Vol. 148, pp. 350-382). Academic Press.

Lim, D.K., Garg, S., Timmins, M., Zhang, E.S., Thomas-Hall, S.R., Schuhmann, H., Li, Y. and Schenk, P.M., 2012. Isolation and evaluation of oil-producing microalgae from subtropical coastal and brackish waters. *PLoS One*, *7*(7), p.e40751.

Lima, J. F. De., Jose, A., Queiroz, D. M., Maria, R., Figueiredo, F. De., Herica, R., Rocha, C., Souza, W. R. De. And Agroenergy, E., 2018. Enhancement of Lipid Accumulation in *Chlorella* Sp . *Farming Culture Held in Open Photobioreactors,*p.88–99.

Liu, B. and Benning, C., 2013. Lipid metabolism in microalgae distinguishes itself. *Current opinion in biotechnology*, *24*(2), pp.300-309.

Liu, J., Yuan, C., Hu, G. and Li, F., 2012. Effects of light intensity on the growth and lipid accumulation of microalga *Scenedesmus* sp. 11-1 under nitrogen limitation. *Applied Biochemistry and Biotechnology*, *166*(8), pp.2127-2137.

Liu, Y., Jiang, H., Zhao, Z. and An, L., 2010. Nitric oxide synthase like activity-dependent nitric oxide production protects against chilling-induced oxidative damage in *Chorispora bungeana* suspension cultured cells. *Plant Physiology and Biochemistry*, *48*(12), pp.936-944.

Liu, Z.Y., Wang, G.C. and Zhou, B.C., 2008. Effect of iron on growth and lipid accumulation in *Chlorella vulgaris*. *Bioresource Technology*, *99*(11), pp.4717-4722.

Lu, Y. and Xu, J., 2015. Phytohormones in microalgae: a new opportunity for microalgal biotechnology?. *Trends in Plant Science*, *20*(5), pp.273-282.

Lu, Y., Tarkowska, D., Tureckova, V., Luo, T., Xin, Y., Li, J., Wang, Q., Jiao, N., Strnad, M. and Xu, J., 2014. Antagonistic roles of abscisic acid and cytokinin during response to nitrogen depletion in oleaginous microalga *Nannochloropsis oceanica* expand the evolutionary breadth of phytohormone function. *The Plant Journal*, *80*(1), pp.52-68.

Lucas, P., Otis, C., Mercier, J.P., Turmel, M. and Lemieux, C., 2001. Rapid evolution of the DNA-binding site in LAGLIDADG homing endonucleases. *Nucleic Acids Research*, *29*(4), pp.960-969.

Ludwig-Muller, J., 2011. Auxin conjugates: their role for plant development and in the evolution of land plants. *Journal of Experimental Botany*, *62*(6), pp.1757-1773.

Mandal, S. and Mallick, N., 2009. Microalga *Scenedesmus obliquus* as a potential source for biodiesel production. *Applied Microbiology and Biotechnology*, *84*(2), pp.281-291.

Mansour, M.P., Volkman, J.K., Jackson, A.E. and Blackburn, S.I., 1999. The fatty acid and sterol composition of five marine dinoflagellates. *Journal of Phycology*, *35*(4), pp.710-720.

Markou, G. and Nerantzis, E., 2013. Microalgae for high-value compounds and biofuels production: a review with focus on cultivation under stress conditions. *Biotechnology Advances*, *31*(8), pp.1532-1542.

Marshall, P. and Lemieux, C., 1992. The I-Ceu I endonuclease recognizes a sequence of 19 base pairs and preferentially cleaves the coding strand of the *Chlamydomonas moewusii* chloroplast large subunit rRNA gene. *Nucleic Acids Research*, *20*(23), pp.6401-6407.

Mata, T.M., Almeidab, R. and Caetanoa, N.S., 2013. Effect of the culture nutrients on the biomass and lipid productivities of microalgae *Dunaliella tertiolecta*. *Chemical Engineering*, *32*, p.973.

Matthew, T., Zhou, W., Rupprecht, J., Lim, L., Thomas-Hall, S.R., Doebbe, A., Kruse, O., Hankamer, B., Marx, U.C., Smith, S.M. and Schenk, P.M., 2009. The metabolome of *Chlamydomonas reinhardtii* following induction of anaerobic H_2 production by sulfur depletion. *Journal of Biological Chemistry*, *284*(35), pp.23415-23425.

Mignolet-Spruyt, L., Xu, E., Idänheimo, N., Hoeberichts, F.A., Muhlenbock, P., Brosche, M., Van Breusegem, F. and Kangasjärvi, J., 2016. Spreading the news: subcellular and organellar reactive oxygen species production and signalling. *Journal of Experimental Botany*, *67*(13), pp.3831-3844.

Millar, H., Considine, M.J., Day, D.A. and Whelan, J., 2001. Unraveling the role of mitochondria during oxidative stress in plants. *IUBMB Life*, *51*(4), pp.201-205.

Miller, R., Wu, G., Deshpande, R.R., Vieler, A., Gartner, K., Li, X., Moellering, E.R., Zauner, S., Cornish, A.J., Liu, B. and Bullard, B., 2010. Changes in transcript abundance in *Chlamydomonas reinhardtii* following nitrogen deprivation predict diversion of metabolism. *Plant Physiology*, *154*(4), pp.1737-1752.

Minami, A., Nagao, M., Ikegami, K., Koshiba, T., Arakawa, K., Fujikawa, S. and Takezawa, D., 2005. Cold acclimation in bryophytes: low-temperature-induced freezing tolerance in *Physcomitrella patens* is associated with increases in expression levels of stress-related genes but not with increase in level of endogenous abscisic acid. *Planta*, *220*(3), pp.414-423.

Minhas, A.K., Hodgson, P., Barrow, C.J. and Adholeya, A., 2016. A review on the assessment of stress conditions for simultaneous production of microalgal lipids and carotenoids. *Frontiers in Microbiology*, *7*, p.546.

Mittler, R., 2017. ROS are good. *Trends in Plant Science*, *22*(1), pp.11-19.

Moellering, E.R. and Benning, C., 2010. RNA interference silencing of a major lipid droplet protein affects lipid droplet size in *Chlamydomonas reinhardtii*. *Eukaryotic Cell*, *9*(1), pp.97-106.

Msanne, J., Xu, D., Konda, A.R., Casas-Mollano, J.A., Awada, T., Cahoon, E.B. and Cerutti, H., 2012. Metabolic and gene expression changes triggered by nitrogen

deprivation in the photoautotrophically grown microalgae *Chlamydomonas reinhardtii* and *Coccomyxa* sp. C-169. *Phytochemistry*, *75*, pp.50-59.

Nagamune, K., Xiong, L., Chini, E. and Sibley, L.D., 2008. Plants, endosymbionts and parasites: abscisic acid and calcium signaling. *Communicative & Integrative Biology*, *1*(1), pp.62-65.

Nedelcu, A.M., 1998. Contrasting mitochondrial genome organizations and sequence affiliations among green algae: potential factors, mechanisms, and evolutionary scenarios. *Journal of Phycology*, *34*(1), pp.16-28.

Nedelcu, A.M., Lee, R.W., Lemieux, C., Gray, M.W. and Burger, G., 2000. The complete mitochondrial DNA sequence of *Scenedesmus obliquus* reflects an intermediate stage in the evolution of the green algal mitochondrial genome. *Genome Research*, *10*(6), pp.819-831.

Negi, S., Barry, A.N., Friedland, N., Sudasinghe, N., Subramanian, S., Pieris, S., Holguin, F.O., Dungan, B., Schaub, T. and Sayre, R., 2016. Impact of nitrogen limitation on biomass, photosynthesis, and lipid accumulation in *Chlorella sorokiniana*. *Journal of Applied Phycology*, *28*(2), pp.803-812.

Ng, L.F., Gruber, J., Cheah, I.K., Goo, C.K., Cheong, W.F., Shui, G., Sit, K.P., Wenk, M.R. and Halliwell, B., 2014. The mitochondria-targeted antioxidant MitoQ extends lifespan and improves healthspan of a transgenic *Caenorhabditis elegans* model of Alzheimer disease. *Free Radical Biology and Medicine*, *71*, pp.390-401.

Ng, S., De Clercq, I., Van Aken, O., Law, S. R., Ivanova, A., Willems, P., Giraud, E., Van Breusegem, F. and Whelan, J., 2014. Antero grade and retrograde regulation of nuclear genes encoding mitochondrial proteins during growth, development, and stress. *Molecular Plant, 7*, p. 1075–1093.

Ng, S., Giraud, E., Duncan, O., Law, S.R., Wang, Y., Xu, L., Narsai, R., Carrie, C., Walker, H., Day, D.A. and Blanco, N.E., 2013. Cyclin-dependent kinase E1 (CDKE1) provides a cellular switch in plants between growth and stress responses. *Journal of Biological Chemistry*, *288*(5), pp.3449-3459.

Nguyen, H.M., Baudet, M., Cuine, S., Adriano, J.M., Barthe, D., Billon, E., Bruley, C., Beisson, F., Peltier, G., Ferro, M. and Li-Beisson, Y., 2011. Proteomic profiling of

oil bodies isolated from the unicellular green microalga *Chlamydomonas reinhardtii*: with focus on proteins involved in lipid metabolism. *Proteomics*, *11*(21), pp.4266-4273.

Pal, D., Khozin-Goldberg, I., Cohen, Z. and Boussiba, S., 2011. The effect of light, salinity, and nitrogen availability on lipid production by *Nannochloropsis* sp. *Applied Microbiology and Biotechnology*, *90*(4), pp.1429-1441.

Paliwal, C., Mitra, M., Bhayani, K., Bharadwaj, S.V., Ghosh, T., Dubey, S. and Mishra, S., 2017. Abiotic stresses as tools for metabolites in microalgae. *Bioresource Technology*, *244*, pp.1216-1226.

Pancha, I., Chokshi, K., George, B., Ghosh, T., Paliwal, C., Maurya, R. and Mishra, S., 2014. Nitrogen stress triggered biochemical and morphological changes in the microalgae *Scenedesmus* sp. CCNM 1077. *Bioresource Technology*, *156*, pp.146-154.

Park, J.J., Wang, H., Gargouri, M., Deshpande, R.R., Skepper, J.N., Holguin, F.O., Juergens, M.T., Shachar-Hill, Y., Hicks, L.M. and Gang, D.R., 2015. The response of *Chlamydomonas reinhardtii* to nitrogen deprivation: a systems biology analysis. *The Plant Journal*, *81*(4), pp.611-624.

Park, W.K., Yoo, G., Moon, M., Kim, C.W., Choi, Y.E. and Yang, J.W., 2013. Phytohormone supplementation significantly increases growth of *Chlamydomonas reinhardtii* cultivated for biodiesel production. *Applied Biochemistry and Biotechnology*, *171*(5), pp.1128-1142.

Parker, M.S., Mock, T. and Armbrust, E.V., 2008. Genomic insights into marine microalgae. *Annual Review of Genetics*, *42*, pp.619-645.

Pasaribu, B., Li, Y.S., Kuo, P.C., Lin, I.P., Tew, K.S., Tzen, J.T., Liao, Y.K., Chen, C.S. and Jiang, P.L., 2016. The effect of temperature and nitrogen deprivation on cell morphology and physiology of *Symbiodinium*. *Oceanologia*, *58*(4), pp.272-278.

Pasaribu, B., Weng, L.C., Lin, I.P., Camargo, E., Tzen, J.T., Tsai, C.H., Ho, S.L., Lin, M.R., Wang, L.H., Chen, C.S. and Jiang, P.L., 2015. Morphological variability and distinct protein profiles of cultured and endosymbiotic *Symbiodinium* cells isolated from *Exaiptasia pulchella*. *Scientific Reports*, *5*, p.15353.

Pastore, D., Trono, D., Laus, M.N., Di Fonzo, N. and Flagella, Z., 2007. Possible plant mitochondria involvement in cell adaptation to drought stress: a case study: durum wheat mitochondria. *Journal of Experimental Botany*, *58*(2), pp.195-210.

Pellny, T.K., Van Aken, O., Dutilleul, C., Wolff, T., Groten, K., Bor, M., De Paepe, R., Reyss, A., Van Breusegem, F., Noctor, G. and Foyer, C.H., 2008. Mitochondrial respiratory pathways modulate nitrate sensing and nitrogen-dependent regulation of plant architecture in *Nicotianasylvestris*. *The Plant Journal*, *54*(6), pp.976-992.

Piotrowska-Niczyporuk, A., Bajguz, A., Zambrzycka, E. and Godlewska-Zylkiewicz, B., 2012. Phytohormones as regulators of heavy metal biosorption and toxicity in green alga *Chlorella vulgaris* (Chlorophyceae). *Plant Physiology and Biochemistry*, *52*, pp.52-65.

Qi, H., Wang, J. and Wang, Z., 2013. A comparative study of maximal quantum yield of photosystem II to determine nitrogen and phosphorus limitation on two marine algae. *Journal of Sea Research*, *80*, pp.1-11.

Raghothama, K.G., 2000. Phosphate transport and signaling. *Current Opinion in Plant Biology*, *3*(3), pp.182-187.

Rao, A.R., Dayananda, C., Sarada, R., Shamala, T.R. and Ravishankar, G.A., 2007. Effect of salinity on growth of green alga *Botryococcus braunii* and its constituents. *Bioresource Technology*, *98*(3), pp.560-564.

Rawat, I., Kumar, R.R., Mutanda, T. and Bux, F., 2013. Biodiesel from microalgae: a critical evaluation from laboratory to large scale production. *Applied Energy*, *103*, pp.444-467.

Reitan, K.I., Rainuzzo, J.R. and Olsen, Y., 1994. Effect of nutrient limitation on fatty acid and lipid content of marine microalgae 1. *Journal of Phycology*, *30*(6), pp.972-979.

Renaud, S.M., Thinh, L.V., Lambrinidis, G. and Parry, D.L., 2002. Effect of temperature on growth, chemical composition and fatty acid composition of tropical Australian microalgae grown in batch cultures. *Aquaculture*, *211*(1-4), pp.195-214.

Rhoads, D.M., 2011. Plant mitochondrial retrograde regulation. In *Plant Mitochondria*, pp. 411-437. Springer, New York, NY.

Richmond, A., 1990. Handbook of micoalgal mass culture. *CRC Press, Boca Raton, FL, USA*.

Rodolfi, L., Chini Zittelli, G., Bassi, N., Padovani, G., Biondi, N., Bonini, G. and Tredici, M.R., 2009. Microalgae for oil: Strain selection, induction of lipid synthesis and outdoor mass cultivation in a low-cost photobioreactor. *Biotechnology and Bioengineering*, *102*(1), pp.100-112.

Rosa, M., Prado, C., Podazza, G., Interdonato, R., Gonzalez, J.A., Hilal, M. and Prado, F.E., 2009. Soluble sugars: Metabolism, sensing and abiotic stress: A complex network in the life of plants. *Plant Signaling & Behavior*, *4*(5), pp.388-393.

Ruiz-Dominguez, M.C., Vaquero, I., Obregón, V., de la Morena, B., Vílchez, C. and Vega, J.M., 2015. Lipid accumulation and antioxidant activity in the eukaryotic acidophilic microalga *Coccomyxa* sp. (strain onubensis) under nutrient starvation. *Journal of Applied Phycology*, *27*(3), pp.1099-1108.

Salama, E.S., Govindwar, S.P., Khandare, R.V., Roh, H.S., Jeon, B.H. and Li, X., 2019. Can omics approaches improve microalgal biofuels under abiotic stress?. *Trends in Plant Science*.

Salama, E.S., Kabra, A.N., Ji, M.K., Kim, J.R., Min, B. and Jeon, B.H., 2014. Enhancement of microalgae growth and fatty acid content under the influence of phytohormones. *Bioresource Technology*, *172*, pp.97-103.

Salbitani, G., Vona, V., Bottone, C., Petriccione, M. and Carfagna, S., 2015. Sulfur deprivation results in oxidative perturbation in *Chlorella sorokiniana* (211/8k). *Plant and Cell Physiology*, *56*(5), pp.897-905.

Sani, Y.M., Daud, W.M.A.W. and Aziz, A.A., 2013. Solid acid-catalyzed biodiesel production from microalgal oil- The dual advantage. *Journal of Environmental Chemical Engineering*, *1*(3), pp.113-121.

Saradhi, P.P., Suzuki, I., Katoh, A., Sakamoto, A., Sharmila, P., Shi, D.J. and Murata, N., 2000. Protection against the photo-induced inactivation of the photosystem II complex by abscisic acid. *Plant, Cell & Environment*, *23*(7), pp.711-718.

Sato, N., Hagio, M., Wada, H. and Tsuzuki, M., 2000. Environmental effects on acidic lipids of thylakoid membranes.

Schmollinger, S., Muhlhaus, T., Boyle, N.R., Blaby, I.K., Casero, D., Mettler, T., Moseley, J.L., Kropat, J., Sommer, F., Strenkert, D. and Hemme, D., 2014. Nitrogen-sparing mechanisms in *Chlamydomonas* affect the transcriptome, the proteome, and photosynthetic metabolism. *The Plant Cell*, *26*(4), pp.1410-1435.

Schwarzlander, M., Logan, D.C., Johnston, I.G., Jones, N.S., Meyer, A.J., Fricker, M.D. and Sweetlove, L.J., 2012. Pulsing of membrane potential in individual mitochondria: a stress-induced mechanism to regulate respiratory bioenergetics in *Arabidopsis*. *The Plant Cell*, *24*(3), pp.1188-1201.

Sevcikova, T., Klimes, V., Zbrankova, V., Strnad, H., Hroudova, M., Vlcek, C. and Elias, M., 2016. A comparative analysis of mitochondrial genomes in eustigmatophyte algae. *Genome biology and evolution*, *8*(3), pp.705-722.

Sheehan, J., Dunahay, T., Benemann, J. and Roessler, P., 1998. Look back at the US department of energy's aquatic species program: biodiesel from algae; close-out report (No. NREL/TP-580-24190). National Renewable Energy Lab., Golden, CO. (US).

Shi, F. and Collins, S., 2017. Second messenger signaling mechanisms of the brown adipocyte thermogenic program: an integrative perspective. *Hormone Molecular Biology and Clinical Investigation*.

Siaut, M., Cuine, S., Cagnon, C., Fessler, B., Nguyen, M., Carrier, P., Beyly, A., Beisson, F., Triantaphylides, C., Li-Beisson, Y. and Peltier, G., 2011. Oil accumulation in the model green alga *Chlamydomonas reinhardtii*: characterization, variability between common laboratory strains and relationship with starch reserves. *BMC Biotechnology*, *11*(1), p.7.

Sibi, G., Shetty, V. and Mokashi, K., 2016. Enhanced lipid productivity approaches in microalgae as an alternate for fossil fuels - A review. *Journal of the Energy Institute*, *89*(3), pp.330-334.

Simoons, M.L., Vos, J. and Martens, L.L., 1991. Cost-utility analysis of thrombolytic therapy. *European Heart Journal*, *12*(6), pp.694-699.

Singh, D.K. and Mallick, N., 2014. Accumulation potential of lipids and analysis of fatty acid profile of few microalgal species for biodiesel feedstock. *Journal of Microbiology & Biotechnology Research* , *4*, pp.37-44.

Singh, P., Kumari, S., Guldhe, A., Misra, R., Rawat, I. and Bux, F., 2016. Trends and novel strategies for enhancing lipid accumulation and quality in microalgae. *Renewable and Sustainable Energy Reviews*, *55*, pp.1-16.

Stoddard, B.L., 2014. Homing endonucleases from mobile group I introns: discovery to genome engineering. *Mobile DNA*, *5*(1), p.7.

Sulochana, S.B. and Arumugam, M., 2016. Influence of abscisic acid on growth, biomass and lipid yield of *Scenedesmus quadricauda* under nitrogen starved condition. *Bioresource Technology*, *213*, pp.198-203.

Sun, A.Z. and Guo, F.Q., 2016. Chloroplast retrograde regulation of heat stress responses in plants. *Frontiers in Plant Science*, *7*, p.398.

Suski, J.M., Lebiedzinska, M., Bonora, M., Pinton, P., Duszynski, J. and Wieckowski, M.R., 2012. Relation between mitochondrial membrane potential and ROS formation.In *Mitochondrial Bioenergetics* (pp. 183-205). Humana Press.

Sweetlove, L.J., Beard, K.F., Nunes-Nesi, A., Fernie, A.R. and Ratcliffe, R.G., 2010. Not just a circle: flux modes in the plant TCA cycle. *Trends in Plant Science*, *15*(8), pp.462-470.

Takagi, M. and Yoshida, T., 2006. Effect of salt concentration on intracellular accumulation of lipids and triacylglyceride in marine microalgae *Dunaliella* cells. *Journal of Bioscience and Bioengineering*, *101*(3), pp.223-226.

Takagi, M., Watanabe, K., Yamaberi, K. and Yoshida, T., 2000. Limited feeding of potassium nitrate for intracellular lipid and triglyceride accumulation of *Nannochloris* sp. UTEX LB1999. *Applied Microbiology and Biotechnology*, *54*(1), pp.112-117.

Takahashi, S. and Murata, N., 2008. How do environmental stresses accelerate photoinhibition?. *Trends in Plant Science*, *13*(4), pp.178-182.

Tang, H., Chen, M., Garcia, M.E.D., Abunasser, N., Ng, K.S. and Salley, S.O., 2011. Culture of microalgae *Chlorella minutissima* for biodiesel feedstock production. *Biotechnology and Bioengineering*, *108*(10), pp.2280-2287.

Taylor, N.L., Tan, Y.F., Jacoby, R.P. and Millar, A.H., 2009. Abiotic environmental stress induced changes in the *Arabidopsis thaliana* chloroplast, mitochondria and peroxisome proteomes. *Journal of Proteomics*, *72*(3), pp.367-378.

Thompson, A.J., Yuan, X., Kudlicki, W. and Herrin, D.L., 1992. Cleavage and recognition pattern of a double-strand-specific endonuclease (I-CreI) encoded by the chloroplast 23S rRNA intron of *Chlamydomonas reinhardtii*. *Gene*, *119*(2), pp.247-251.

Tominaga, N., Takahata, M. and Tominaga, H., 1993. Effects of NaCl and KNO_3 concentrations on the abscisic acid content of *Dunaliella* sp. (Chlorophyta). In *Saline Lakes V* (pp. 163-168). Springer, Dordrecht.

Tredici, M.R., 2010. Photobiology of microalgae mass cultures: understanding the tools for the next green revolution. *Biofuels*, *1*(1), pp.143-162.

Tsai, C.H., Warakanont, J., Takeuchi, T., Sears, B.B., Moellering, E.R. and Benning, C., 2014. The protein Compromised Hydrolysis of Triacylglycerols 7 (CHT7) acts as a repressor of cellular quiescence in *Chlamydomonas*. *Proceedings of the National Academy of Sciences*, *111*(44), pp.15833-15838.

Turmel, M., Otis, C. and Lemieux, C., 1999. The complete chloroplast DNA sequence of the green alga *Nephroselmisolivacea*: insights into the architecture of ancestral chloroplast genomes. *Proceedings of the National Academy of Sciences*, *96*(18), pp.10248-10253.

Udayan, A. and Arumugam, M., 2017. Selective enrichment of Eicosapentaenoic acid (20: 5n-3) in *N. oceanica* CASA CC201 by natural auxin supplementation. *Bioresource Technology*, *242*, pp.329-333.

Vaahtera, L., Brosche, M., Wrzaczek, M. and Kangasjarvi, J., 2014.Specificity in ROS signaling and transcript signatures. *Antioxidants & Redox Signaling*, *21*(9), pp.1422-1441.

Van Aken, O., Zhang, B., Carrie, C., Uggalla, V., Paynter, E., Giraud, E. and Whelan, J., 2009. Defining the mitochondrial stress response in *Arabidopsis thaliana*. *Molecular Plant*, *2*(6), pp.1310-1324.

Van Breusegem, F., Vranova, E., Dat, J.F. and Inze, D., 2001. The role of active oxygen species in plant signal transduction. *Plant Science*, *161*(3), pp.405-414.

Van Lis, R., Atteia, A., Mendoza-Hernandez, G. and Gonzalez-Halphen, D., 2003. Identification of Novel Mitochondrial Protein Components of *Chlamydomonas reinhardtii*. A Proteomic Approach. *Plant Physiology*, *132*(1), pp.318-330.

van Oijen, T., van Leeuwe, M.A., Gieskes, W.W. and de Baar, H.J., 2004. Effects of iron limitation on photosynthesis and carbohydrate metabolism in the Antarctic diatom *Chaetoceros brevis* (Bacillariophyceae). *European Journal of Phycology*, *39*(2), pp.161-171.

Velikova, V., Yordanov, I. and Edreva, A., 2000. Oxidative stress and some antioxidant systems in acid rain-treated bean plants: protective role of exogenous polyamines. *Plant Science*, *151*(1), pp.59-66.

Vranova, E., Inze, D. and Van Breusegem, F., 2002. Signal transduction during oxidative stress. *Journal of Experimental Botany*, *53*(372), pp.1227-1236.

Wase, N., Black, P.N., Stanley, B.A. and Di Russo, C.C., 2014. Integrated quantitative analysis of nitrogen stress response in *Chlamydomonas reinhardtii* using metabolite and protein profiling. *Journal of Proteome Research*, *13*(3), pp.1373-1396.

Wase, N., Tu, B., Black, P.N. and DiRusso, C.C., 2015. Phenotypic screening identifies Brefeldin A/Ascotoxin as an inducer of lipid storage in the algae *Chlamydomonas reinhardtii*. *Algal Research*, *11*, pp.74-84.

Woodson, J.D. and Chory, J., 2008. Coordination of gene expression between organellar and nuclear genomes. *Nature Reviews Genetics*, *9*(5), p.383.

Wu, G., Gao, Z., Du, H., Lin, B., Yan, Y., Li, G., Guo, Y., Fu, S., Wei, G., Wang, M. and Cui, M., 2018. The effects of abscisic acid, salicylic acid and jasmonic acid on

lipid accumulation in two freshwater *Chlorella* strains. *The Journal of General and Applied Microbiology*, *64*(1), pp.42-49.

Wu, L.F., Chen, P.C. and Lee, C.M., 2013. The effects of nitrogen sources and temperature on cell growth and lipid accumulation of microalgae. *International Biodeterioration & Biodegradation*, *85*, pp.506-510.

Xin, L., Hong-Ying, H. and Yu-Ping, Z., 2011. Growth and lipid accumulation properties of a freshwater microalga *Scenedesmus* sp. under different cultivation temperature. *Bioresource Technology*, *102*(3), pp.3098-3102.

Xin, L., Hong-Ying, H., Ke, G. and Ying-Xue, S., 2010. Effects of different nitrogen and phosphorus concentrations on the growth, nutrient uptake, and lipid accumulation of a freshwater microalga *Scenedesmus* sp. *Bioresource Technology*, *101*(14), pp.5494-5500.

Xu, D., Marino, G., Klingl, A., Enderle, B., Monte, E., Kurth, J., Hiltbrunner, A., Leister, D. and Kleine, T., 2019. Extrachloroplastic PP7L Functions in Chloroplast Development and Abiotic Stress Tolerance. *Plant physiology*, *180*(1), pp. 323–341.

Xupeng, C., Song, X. and Xuran, F., 2017. Amino Acid Changes during Energy Storage Compounds Accumulation of Microalgae under the Nitrogen Depletion. *Amino Acid: New Insights and Roles in Plant and Animal*, p.197.

Yeh, K.L. and Chang, J.S., 2012. Effects of cultivation conditions and media composition on cell growth and lipid productivity of indigenous microalga *Chlorella vulgaris* ESP-31. *Bioresource Technology*, *105*, pp.120-127.

Yilancioglu, K., Cokol, M., Pastirmaci, I., Erman, B. and Cetiner, S., 2014. Oxidative stress is a mediator for increased lipid accumulation in a newly isolated *Dunaliella salina* strain. *PLoS One*, *9*(3), p.e91957.

Yokotani, N., Higuchi, M., Kondou, Y., Ichikawa, T., Iwabuchi, M., Hirochika, H., Matsui, M. and Oda, K., 2010. A novel chloroplast protein, CEST induces tolerance to multiple environmental stresses and reduces photo oxidative damage in transgenic *Arabidopsis*. *Journal of Experimental Botany*, *62*(2), pp.557-569.

Yoshida, K., 2005. Evolutionary process of stress response systems controlled by abscisic acid in photosynthetic organisms. *Yakugaku zasshi: Journal of the Pharmaceutical Society of Japan*, *125*(12), pp.927-936.

Yoshida, K., Igarashi, E., Mukai, M., Hirata, K. and Miyamoto, K., 2003. Induction of tolerance to oxidative stress in the green alga, *Chlamydomonas reinhardtii*, by abscisic acid. *Plant, Cell & Environment*, *26*(3), pp.451-457.

Yu, F., Liu, X., Alsheikh, M., Park, S. and Rodermel, S., 2008. Mutations in SUPPRESSOR OF VARIEGATION1, a factor required for normal chloroplast translation, suppress var2-mediated leaf variegation in *Arabidopsis*. *The Plant Cell*, *20*(7), pp.1786-1804.

Yu, W.L., Ansari, W., Schoepp, N.G., Hannon, M.J., Mayfield, S.P. and Burkart, M.D., 2011. Modifications of the metabolic pathways of lipid and triacylglycerol production in microalgae. *Microbial Cell Factories*, *10*(1), p.91.

Zhang, B. and Singh, K.B., 1994. ocs element promoter sequences are activated by auxin and salicylic acid in *Arabidopsis*. *Proceedings of the National Academy of Sciences*, *91*(7), pp.2507-2511.

Zhang, Y., and Lu, H. (2009). Signaling to p53: ribosomal proteins find their way. Cancer Cell 16, 369–377.

Zhang, Y., Liu, Y., Cao, X., Gao, P., Liu, X., Wang, X., Zhang, J., Zhou, J., Xue, S., Xu, G. and Tian, J., 2016. Free amino acids and small molecular acids profiling of marine microalga *Isochrysis zhangjiangensis* under nitrogen deficiency. *Algal Research*, *13*, pp.207-217.

Zhang, Y.M., Chen, H., He, C.L. and Wang, Q., 2013. Nitrogen starvation induced oxidative stress in an oil-producing green alga *Chlorella sorokiniana* C3. *PloS One*, *8*(7), p.e69225.

Zhao, Y., Hou, Y., Liu, Z., Che, S. and Che, F., 2016. Identification of $NaHCO_3$ stress responsive proteins in *Dunaliella salina* HTBS using iTRAQ-based analysis. *Journal of Proteomics & Bioinformatics*, *9*, pp.137-143.

Zhao, Y., Li, D., Ding, K., Che, R., Xu, J.W., Zhao, P., Li, T., Ma, H. and Yu, X., 2016. Production of biomass and lipids by the oleaginous microalgae *Monoraphidium* sp. QLY-1 through heterotrophic cultivation and photo-chemical modulator induction. *Bioresource Technology*, *211*, pp.669-676.

Zhao, Y., Li, D., Xu, J.W., Zhao, P., Li, T., Ma, H. and Yu, X., 2018. Melatonin enhances lipid production in *Monoraphidium* sp. QLY-1 under nitrogen deficiency conditions via a multi-level mechanism. *Bioresource Technology*, *259*, pp.46-53.

Zhila, N.O., Kalacheva, G.S. and Volova, T.G., 2011. Effect of salinity on the biochemical composition of the alga *Botryococcus braunii* Kutz IPPAS H-252. *Journal of Applied Phycology*, *23*(1), pp.47-52.

Zhou, X., Liao, J.M., Liao, W.J. and Lu, H., 2012. Scission of the p53-MDM2 loop by ribosomal proteins. *Genes & Cancer*, *3*(3-4), pp.298-310.

Zhou, X., Liao, W.J., Liao, J.M., Liao, P. and Lu, H., 2015. Ribosomal proteins: functions beyond the ribosome. *Journal of Molecular Cell Biology*, *7*(2), pp.92-104.

Zhu, L.D., Li, Z.H. and Hiltunen, E., 2016. Strategies for lipid production improvement in microalgae as a biodiesel feedstock. *BioMed Research International*, *2016*.

Agrawal, G. K., Jwa, N. and Rakwal, R., 2009. Rice proteomics: ending phase I and the beginning of phase II. *Proteomics* 9, pp.935–963.

Kobayashi, M., Hirai, N., Kurimura, Y., Ohigashi, H., Tsuji, Y., 1997. Abscisic acid-dependent algal morphogenesis in the unicellular green alga *Haematococcus pluvialis*. *Plant growth Regulation*, 22, pp.79-85.

Jurica, M.S., Monnat, R.J and Stoddard, B.L., 1998. DNA recognition and cleavage by the LAGLIDADG homing endonuclease I-Cre I. *Mol. Cell*, 2(4), pp.469-76.

List of Publications

- **Sujitha, BS** and Arumugam, M. (2016). Influence of abscisic acid on growth, biomass and lipid yield of *Scenedesmus quadricauda* under nitrogen starved condition. *Bioresource Technology*. 213: 198-203.
- Anand, J, **Sujitha, BS,** Steffi James, P and Arumugam, M. (2016). Major Lipid Body Protein: A conserved structural component of lipid body accumulated during abiotic stress in *S. quadricauda* CASA-CC202. Front. Energy Res. 4:37. doi:10.3389/fenrg.2016.
- Anusree, VM, **Sujitha, BS,** Anand, J and Arumugam, M (2017) Dissolved inorganic carbonate sustain the growth, lipid and biomass yield of *Scenedesmus quadricauda* under nitrogen starved condition. Indian Journal of Experimental Biology.55:702-710.
- Ramya, AN, Ambily, PS, **Sujitha, BS**, Arumugam, M and Maiti, KK. (2017). Single cell lipid profiling of *Scenedesmus quadricauda* CASA-CC202 nitrogen starved condition by surface enhanced Raman scattering (SERS) finger printing. Algal Research. 25: 200–206. doi: 10.1016/j.algal.2017.05.011.
- Sujitha BS and Arumugam. Molecular Characterisation of Stress associated proteins in nitrogen stress mediated lipid accumulation in *S. quadricauda* (under preparation)*.
- Sujitha BS and Arumugam. Targeted metabolomic and biochemical changes during nitrogen stress mediated lipid accumulation in *Scenedesmus quadricauda* CASA CC202 (Communicated).

Popular article

- **Sujitha, B S**., Arumugam, M. (2016): Stress hormone level shoots up during abiotic stress to sustains the stress in *Scenedesmus quadricauda*. Atlas of Science. May 14, 2016.

Book Chapters

1. **Sujitha, B S**, Anand J and Arumugam, M. (2019). Biochemical and molecular insight of the abiotic stress mediated lipid accumulation in *Scenedesmus quadricauda* CASA CC202. In Algae. Center for Advanced Studies in Botany, University of Madras, Chennai, pp 218-234. [ISBN: 978-93-88680-21-9].

Conference Proceedings

- **Sujitha B S** and M Arumugam: "Biochemical and metabolic changes in *Scenedesmus quadricauda* CASA CC202 during nitrogen stress mediated lipid accumulation." Page no. 227-228, Session BEB-35. NHBT-2019, Trivandrum, 20-24 Nov 2019.

- Hariharan, S, **Sujitha, B.S** and M. Arumugam, "Essential omega-3 fatty acids production in edible marine microalgae *Nannochloropsis oceanica CASA CC201* using plant growth regulators" at 8th Annual Meeting of Biomedical Sciences conference on "Deliberation on translation of basic scientific insights into affordable healthcare products" on February 25-27, 2019 at CSIR-National Institute for Interdisciplinary Science and Technology, Thiruvananthapuram, Kerala, India. NPP-6, pp-154.

- **Sujitha B S** and M Arumugam: "Influence of Abscisic acid on growth, biomass and lipid yield of *Scenedesmus quadricauda* under nitrogen starved condition. Page no.356, Session BR-11. NHBT-2015, Trivandrum, 22-25 Nov 2015.

GenBAnk Gene Submissions

1. Sujitha, B S. and Arumugam, M. (2019) *Scenedesmus quadricauda* CASA CC202, LAGLIDADG Homing Endonuclease <u>GenBank accession No. MN648648</u>

2. Prasad, S., **Balakrishnan Sulochana, S**., Jebakumar, S. and Arumugam, M.(2018) *Scenedesmus sp. I1* internal transcribed spacer 1, partial sequence; 5.8S ribosomal RNA gene and internal transcribed spacer 2, complete sequence; and large subunit ribosomal RNA gene, partial sequence. <u>GenBank accession No. MH068685</u>

3. Prasad, S., **Balakrishnan Sulochana, S**., Jebakumar, S. and Arumugam, M.(2018) *Chlamydomonasdebaryana* strain I2 internal transcribed spacer 1,partial sequence; 5.8S ribosomal RNA gene and internal transcribed spacer 2, complete sequence; and large subunit ribosomal RNA gene,partial sequence. <u>GenBank accession No. MH068686.</u>

4. Prasad, S., **Balakrishnan Sulochana, S**., Jebakumar, S. and Arumugam, M.(2018) *Chlorella sp. I3* internal transcribed spacer 1, partial sequence; 5.8S ribosomal RNA gene and internal transcribed spacer 2, complete sequence; and large subunit ribosomal RNA gene, partial sequence. <u>GenBank accession No. MH068687.</u>

5. Prasad, S., **Balakrishnan Sulochana, S**., Jebakumar, S. and Arumugam, M.(2018) *Chlamydomonas sp. I4* internal transcribed spacer 1, partial sequence; 5.8S ribosomal RNA gene and internal transcribed spacer 2, complete sequence; and large subunit ribosomal RNA gene, partial sequence. <u>GenBank accession No. MH068688.</u>

6. Prasad, S., **Balakrishnan Sulochana, S**., Jebakumar, S. and Arumugam, M.(2018) *Scenedesmus sp. I5* internal transcribed spacer 1, partial sequence; 5.8S ribosomal RNA gene and internal transcribed spacer 2, complete sequence; and large subunit ribosomal RNA gene, partial sequence. GenBank accession No. MH068689

7. Prasad, S., **Balakrishnan Sulochana, S**., Jebakumar, S. and Arumugam, M.(2018) *Balticola sp. I6* internal transcribed spacer 1, partial sequence; 5.8S ribosomal RNA gene and internal transcribed spacer 2, complete sequence; and large subunit ribosomal RNA gene, partial sequence. GenBank accession No. MH068690

8. Prasad, S., **Balakrishnan Sulochana, S**., Jebakumar, S. and Arumugam, M.(2018) *Chlorella sp.* S1 internal transcribed spacer 1, partial sequence; 5.8S ribosomal RNA

gene and internal transcribed spacer 2, complete sequence; and large subunit ribosomal RNA gene, partial sequence. <u>GenBank accession No. MH068691.</u>

9. Prasad, S., **Balakrishnan Sulochana, S**., Jebakumar, S. and Arumugam, M.(2018) *Tetradesmusdimorphus* strain S2 internal transcribed spacer 1, partial sequence; 5.8S ribosomal RNA gene and internal transcribed spacer 2, complete sequence; and large subunit ribosomal RNA gene, partial sequence. <u>GenBank accession No. MH068692.</u>

10. Prasad, S., **Balakrishnan Sulochana, S**., Jebakumar, S. and Arumugam, M.(2018) *Chlamydomonas sp. S4* internal transcribed spacer 1, partial sequence; 5.8S ribosomal RNA gene and internal transcribed spacer 2, complete sequence; and large subunit ribosomal RNA gene, partial sequence. <u>GenBank accession No. MH068693.</u>

11. Prasad, S., **Balakrishnan Sulochana, S**., Jebakumar, S. and Arumugam, M.(2018) *Tetradesmusdimorphus* strain S6 internal transcribed spacer 1, partial sequence; 5.8S ribosomal RNA gene and internal transcribed spacer 2, complete sequence; and large subunit ribosomal RNA gene, partial sequence. <u>GenBank accession No. MH068694.</u>

12. Prasad, S., **Balakrishnan Sulochana, S**., Jebakumar, S. and Arumugam, M.(2018) *Chlorella sp*. S8 internal transcribed spacer 1, partial sequence; 5.8S ribosomal RNA gene and internal transcribed spacer 2, complete sequence; and large subunit ribosomal RNA gene, partial sequence. <u>GenBank accession No. MH068695.</u>

13. Prasad, S., **Balakrishnan Sulochana, S**., Jebakumar, S. and Arumugam, M.(2018) *Tetradesmusdimorphus* strain S10 internal transcribed spacer 1, partial sequence; 5.8S ribosomal RNA gene and internal transcribed spacer 2, complete sequence; and large subunit ribosomal RNA gene, partial sequence. <u>GenBank accession No. MH068696.</u>

14. Prasad, S., **Balakrishnan Sulochana, S.**, Jebakumar, S. and Arumugam, 11M.(2018) *Coelastrellavacuolata* strain S12 internal transcribed spacer 1, partial sequence; 5.8S ribosomal RNA gene and internal transcribed spacer 2, complete sequence; and large subunit ribosomal RNA gene, partial sequence. <u>GenBank accession No. MH068697.</u>

AcSIR Course Work

Sl No.	Level 100	Course No. and Title	Status
1.	BIO-101	Biostatistics	Completed
2.	BIO-102	Bioinformatics	Completed
3.	BIO-103	Basic Chemistry	Completed
4.	BIO-104	Research Methodology, communication/ ethics/ safety	Completed
	Level 200		
1.	BIO-NIIST-201	Biotechnology and Instrumentation	Completed
2.	BIO-NIIST-206	Protein Sciences and Proteomics	Completed
3.	BIO-NIIST-239	Basic Molecular Biology	Completed
	Level 300		
1.	BIO-NIIST-301	Seminar Course	Completed
2.	BIO-NIIST-337	Bioprocess Technology	Completed
3.	BIO-NIIST-369	Enzymology and Enzyme Technology	Completed
	Level 400		
1.	BIO-NIIST-4-001	Review writing	Completed
2.	BIO-NIIST-4-002	Project proposal	Completed
		CSIR-800	Completed